University of Huddersfield Logo

# University of Huddersfield Repository

Stroe, Octavian

Complete Overview and Analysis of an Electro-Luminescent Based Optical Cell

## Original Citation

Stroe, Octavian (2018) Complete Overview and Analysis of an Electro-Luminescent Based Optical Cell. Masters thesis, University of Huddersfield.

This version is available at http://eprints.hud.ac.uk/id/eprint/34532/

http://eprints.hud.ac.uk/

# Complete Overview and Analysis
# of an Electro-Luminescent Based Optical Cell

**Octavian Tudor Stroe**

A thesis submitted to the University of Huddersfield in partial fulfilment
of the requirements for the degree of Master by Research

**-** The University of Huddersfield -

- September 2017 –

# Abstract

Electro-luminescent optical cells form the first layer in the unique sound of an optical compressor and are the main element in achieving gain reduction. This research was carried out in order to identify key low-level parameters within the optical cell assembly that relate to the colouration added to the musical signal. Variations of an optical cells were built, each with a modification to the identified parameter (electro-luminescent panel, light dependent resistor, exposure area, etc.). Objective analysis was performed, and multiple tests were carried out to determine the performance characteristics of each modified cell. Various stimuli were utilised which included broadband pink noise, band-limited pink noise (63 Hz band and 1 kHz band) and sine wave bursts. Further to the individual cell testing, audio measurements and analysis of the resultant signal utilising the cells within an audio compressor were undertaken.

Key findings of the report conclude that the optical cells do exhibit a 'memory effect' determined by the amount of compression applied. They also have a two-staged attack characteristic that is independent from the audio stimuli and a different timing response based on the combination of the two elements inside the optical cell (the Light Dependent Resistor and the Electro-Luminescent panel). Further to this, it was determined that the attack/release characteristics of the optical compressor and the Total Harmonic Distortion (THD) levels of the compressed audio stimuli changed as a direct result of the optical cell's modified parameters. Moreover, it was proved that some electro-luminescent panels do exhibit a colour-shift phenomenon and a frequency-dependent brightness that affect the cell's compression characteristics with different audio stimuli. Further to the findings, additional attack and release characteristics are proposed based on parameter modifications.

# Table of Contents

# Table of Figures

# 1 Introduction

Opto-Electrical compressors are compressors that utilise some form of optical cell to control the audio compression. They have been used since the first one was invented (LA-2A, 1960) and every single model built has its own unique timbre and sonic characteristic. This is a direct result of circuit implementation and components used in the optical cell. These compressors are usually preferred for vocals or sustained bass instruments due to their unique characteristics, creating a 'fatter and bigger' sound (Scott, 2006) which are a direct result of the optical cell assembly. The changing characteristics are a possible result of the driving signal properties (amplitude variations and signal length) have fascinated engineers around the world and raised numerous discussions that revolved around the relationship of the driving circuit and the optical assembly, but no in-depth investigations were made solely on the cell.

## 1.1 Aims and objectives

The key objectives of this study are to review different methods of optical cell implementation with a view to ascertaining the effect of low-level parameters on the overall sound of the compressor. The analysis will be looking at the colour of the lighting element inside the optical cell and its relation to the light dependent resistor (LDR) used and how they interact. Key research questions are how does the time versus brightness influence the response of the LDR and is there any difference in compression if using a totally different LDR and light source? The aims are to investigate the low-level parameters of an optical cell (EL panel and LDR) and investigate the relationship between the parameter and its effect on the audio signal. Once the low-level

parameters have been identified, circuits will be designed with different modified versions of the same parameters and tests will be conducted to determine the effects.

## 1.2 Fundamentals of Compressors

This chapter will be looking into what a compressor is and its theory of operation. Different compressor types and the associated side-chain circuits (feed-forward, feedback, peak or root-mean-square (RMS) detection) will be analysed to give an overall look at the different types of compressors. Attack and release will be discussed together with some factors that influence the performance of compressors.

## 1.3 Theory of operation

Before delving into the compressor topologies and different controls, it is first important to describe what dynamic range is in the context of this report. As specified by Bohn (2000) this represents the difference in dB between the quietest sound (lowest amplitude waveform) and the loudest sound (largest amplitude waveform). Compressors are used in music production and broadcasting to reduce this dynamic range to make all instruments/sources "sit together", prevent overloading of the recording devices and sometimes to impose a specific sonic character to the sound (Moore, Till and Wakefield, 2016). Professional grade compressors will output approximately +26 dBu with a noise floor of about -94 dBu, giving a total of 120 dB of dynamic range, matching that of the human hearing system as noted by Bohn (2000).

All compressors have a gain element and a sidechain element as noted by Kadis (2012). The gain element controls gain reduction (the compression) based on control voltage information provided by the sidechain (Johnsen, 1998). The sidechain circuit has a threshold control that allows

the users to control the level (in dB) over which the compressor starts to work, defining that point as the knee of the compressor, as described by Droney and Massey (2001). Simply put, the threshold controls a value (dB, volts), which if exceeded by the input signal the compressor applies gain reduction. Kadis (2012) states that any incoming signal that will be detected as being over that threshold will trigger automatic level reduction. This theory is also backed-up by Bohn (2000) which points out that dynamic range compressors will compress the peaks that exceed the threshold. The amount of level reduction is applied according to the ratio control which is defined by Giannoulis, Massberg, and Reiss (2012) as input-to-output ratio for signals that overshoot the threshold. For example, a compressor with a X:1 compression ratio, the output will increase by 1 dB for each X dBs of input that exceed the threshold, therefore a compressor with 20:1 or more is generally considered a limiter. Floru (1998) also defines compression ratio as the ratio between the rate of input change over the rate of output change. The compression curves one might be interested in to see how the compressors react to different inputs at certain thresholds and ratios are called static compression curves. Berners (2006) defines them as the relationship of the input level to the final output level, achieved for steady state signals, usually tested with sinewaves. An example of such curves can be seen in Figure 1.1.
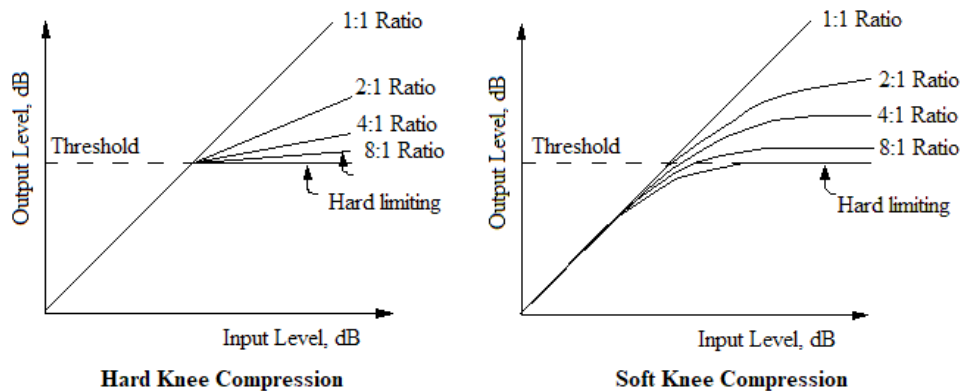


**Figure 1.1: Hard-Knee vs. Soft-Knee Compression (Lerner, n.d.)**

It is to be noted that dynamic range compression is not only achieved by compressing the peaks, but as showed by Kadis (2012), compressors also boost the low signals. In other words, dynamic range reduction is obtained by lowering the peaks and boosting the quiet sounds.

## 1.4 Topologies

According to Kadis (2012) and Abel and Berners (2003) compressors fall into two topologies:

- Feedforward - where the input signal is fed to the sidechain circuit and is used to generate the control voltage for the gain reduction (Figure 1.2)

- Feedback – where the output signal is fed to the sidechain element and a control voltage is generated controlling the input signal level (Figure 1.3)
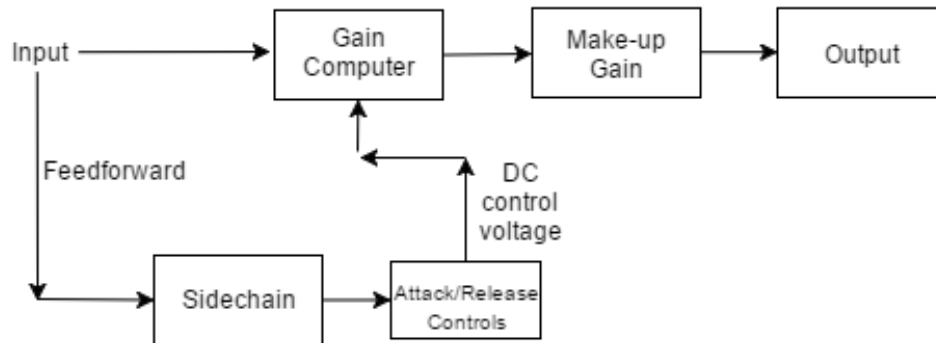
**Figure 1.2: Feedforward Topology**
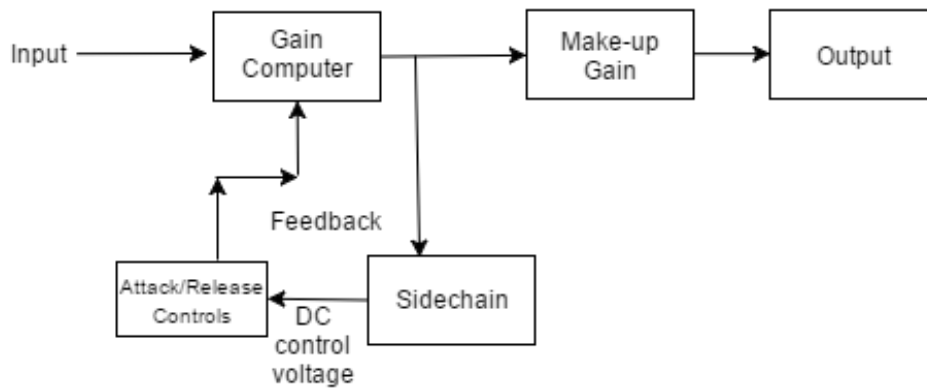
**Figure 1.3: Feedback Topology**

Abel and Berners (2003) suggest that only feedforward compressors can achieve true limiting as the sidechain circuit generates the control voltage based on the input, thus no matter how much the input increases, the circuit will be able to provide infinite gain reduction. This cannot be the case for a feedback compressor, as the control voltage is generated based on the output signal which needs to change in order for the sidechain to detect when to apply gain reduction, so therefore it cannot stay constant. The theory is also backed-up by Floru (1998) which states that feedback designs cannot achieve limiting.

It is also to be noted that, as stated by Giannoulis, Massberg and Reiss (2012) and Kleczkowski (2001), feedback compressors need to work with lower dynamic ranges as the input in the sidechain is already compressed as opposed to feedforward compressors which need to be able to deal with higher dynamic ranges. This statement is also supported by Abel and Berners (2003).

It has also been claimed that there is a difference in THD between the two topologies, but the testing results obtained by Floru (1998) show that distortion level is equal at low frequencies, while higher frequencies exhibit higher distortion figures. Simmer, Schmidt and Bitzer (2006) noted that feedback compressors also produce higher non-linear distortions for higher compression ratios. Moreover, as Floru (1998) states, another source of distortion in both the feedforward and feedback topologies is the ripple factor (high frequency noise superimposed on the audio signal) that modulates the compressor's gain.

## 1.5 Sidechain circuit

The sidechain, most commonly referred to as the heart of the compressor, takes an audio input and generates a control voltage also known as the control envelope (Kadis, 2012). Bohn (2000) describes that there are 4 main parameters that govern the sidechain activity: Threshold, Ratio, Attack and Release.

The way the sidechain generates the control voltage and how it identifies the peaks or the average level of the music, to know when to apply compression, is the job of the detector circuit. First of all, as stated by Ciletti and Hill (2008), its main function is to convert the audio signal into a DC control voltage that matches, as closely as possible, the signal's changing amplitude (Just like the capacitor charges up with the applied voltage). Kadis (2012) describes that the detector uses a rectifier that is configured to either detect the peaks in the signals (Figure 1.4) or a dedicated circuit that can calculate the RMS value of these signals. As a result of different detection circuits, the compressor reacts differently depending on the audio source, as stated by Berners (2006). Johnsen (1998) also describes that the timbre characteristic depends mostly on how the sidechain handles the control voltage. Droney and Massey (2001) suggest that peak detection is better to be used for limiters (where no transients are allowed to pass), whereas RMS detection is better suited for compressors. Johnsen (1998) further backs-up this idea by stating that compressors based on peak detection are more prone to introduce distortions and unnatural signal dynamics.
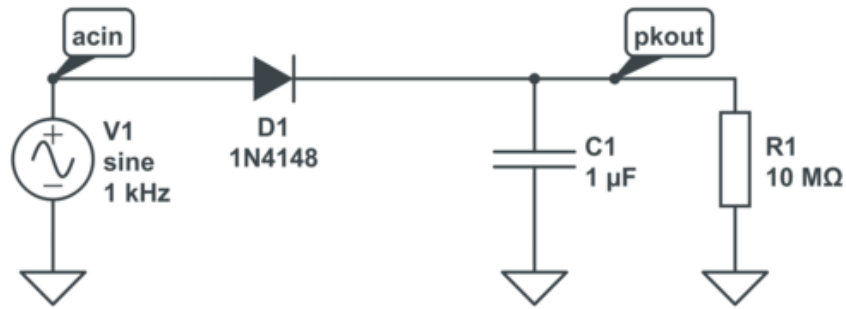
**Figure 1.4: Improved peak detector circuit (Signality, 2012)**
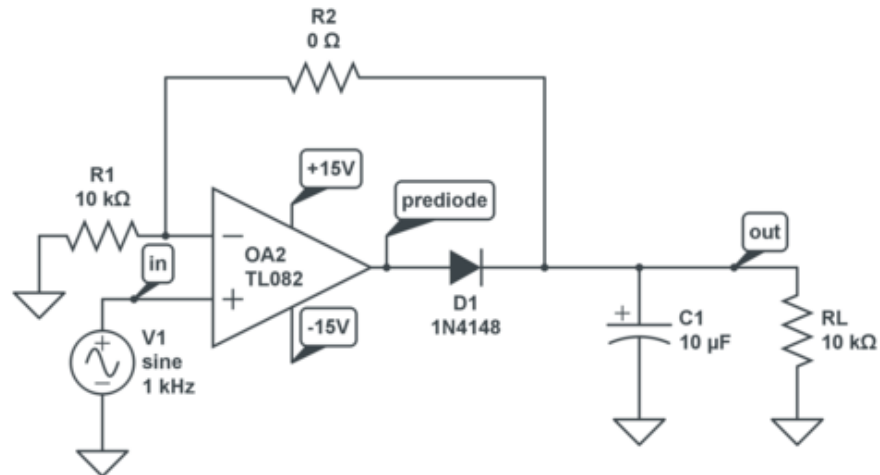


**Figure 1.5: Decoupled peak detector circuit (Khauser, 2012)**

Floru (1998) reports that another type of detection can be used, which is a trade-off between peak and RMS, called average detection. According to Johnsen's (1998) statements, it can be partially achieved with RC circuits which create an approximation average power with some waveforms. The same author suggests that RMS is the only circuit that can relate to a signal's power level and is independent on the signal waveform, whereas the average detector only computes the mean level. Moreover, same author mentions that RMS value of an AC is the equivalent to the DC voltage that generates the same real power in a resistive load. Considering

that human hearing system responds to the average power of a signal, as described by Johnson (1998), it is safe to suggest that RMS detection would work best for compressors that deal with steady state energy levels like bass sounds, guitars and vocals. RMS detection circuits are complex and usually they come packaged as integrated chips.

## 1.6 Controls – Attack and Release

As previously discussed, the four main controls of the detector circuit are the Threshold, Ratio, Attack and Release. Threshold and Ratio were discussed in the theory of operation and are important controls that contribute to the overall sound of the compressor. Other important controls for sculpting the sound are the attack and release which are vital for an engineer for shaping the envelope of the control signal. According to Berners (2006), attack and release controls typically characterize the behaviour of the compressor. Kadis (2012) describes the attack time as the time needed for the level to reduce to the intended gain reduction once the signal hits the threshold, whereas the release is defined as the time needed to get back to the original level after the signal drops below threshold. Kicks (2009) defines the attack as the amount of time from the point where the signal hits the threshold to the point where full gain reduction has been achieved. On the other hand, Bohn (2000) defines the attack time a bit different, as the time needed for the compression to reduce the gain to about 86% to 95% of the final value. Release is defined in the same way as the previous authors did. Other companies and engineers measure the attack interval as the time needed for the signal to reach 63% of final gain reduction and release as the time needed to recover 63% of the initial value (Just like the time constant of a capacitor).

In most cases, attack and release time constants are implemented in the form of an RC circuit. Floru (1998) notes that attack and release controls change the time constants of the detector

circuit thus changing the envelope of the control voltage. Kleczkowski (2001) specifies that part of the distortion in the compressors is due to the difference in spectra between the original signal and the spectra of the attack/release phase, resulting in distortion.

Fast attack times could be used to tame the transients and slower attack times to let the transients unchanged and control the body of the instruments. Slower release is usually used more on steady state signals like voice, bass and guitars where a fast release could result in a "pumping" effect (Kadis, 2012). It is to be noted, that according to Floru (1998), a higher time constant (faster attack) could result in more distortion, idea also described by Kleczkowski (2001).

It is worth mentioning that even though some compressors may have the same topology, same parameters (threshold, ratio and input, release) thus resulting in the same static compression curve among them, they might not work in the same way as Berners (2006) describes. A good example is presented in Figure 1.6, where the same author presents the release characteristic of 3 compressors, each having the same input signal, same static compression curves and same release time, yet they exhibit a different behaviour. Investigations have been conducted to further research the presence of this phenomenon with different optical cells and the results are presented in Discussion of Results.
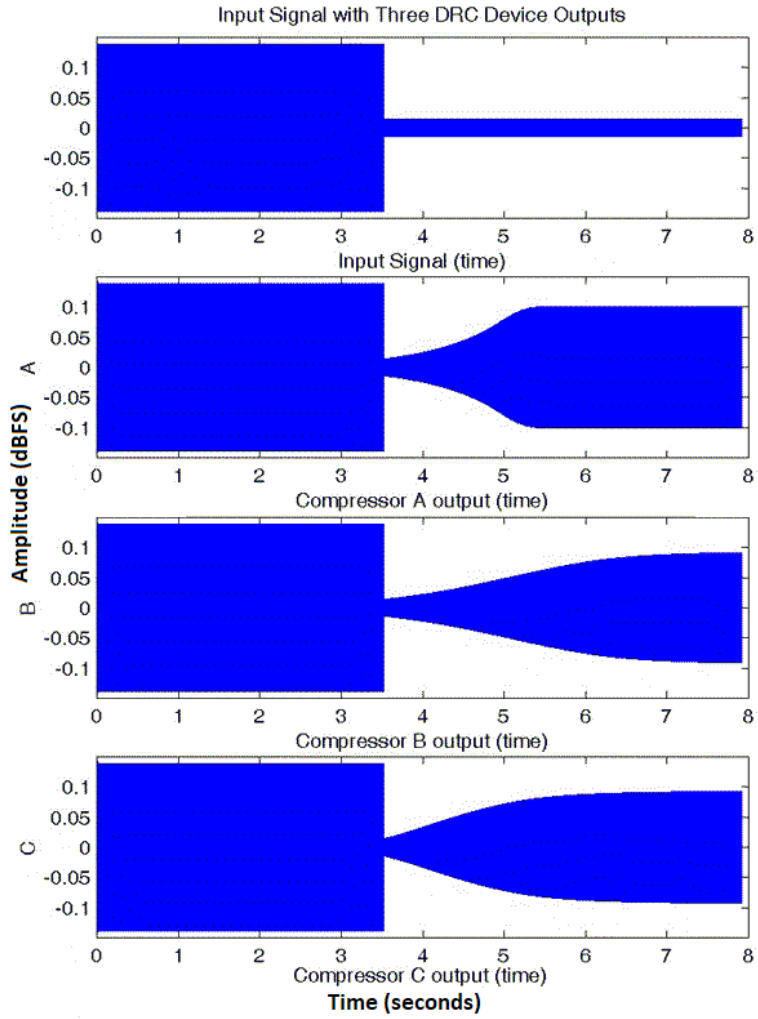
**Figure 1.6: Release characteristics of different compressors (Berners, 2006)**

## 1.7 Factors that influence performance

Floru (1998) identified some factors that influence the performance of the compressors:

- If the rectifier circuit is not 100% symmetrical the RMS detector circuit could add unwanted harmonics.

- The equivalent series resistance (ESR) of the capacitors in the timing circuits (attack and release controls) will produce a different transient response than it can be predicted by theory. Moreover, other effects of ESR include a rise in ripple resulting in a higher distortion. The rise in ripple phenomenon was also described by Horowitz and Hill (2016). Aging process of the LDRs described by Moore, Till and Wakefield (2016) is also applicable to capacitors, whose ESR increases with time and use. A possible proposed solution mentioned by Floru (1998) could be the addition of a resistor in series with the timing capacitor.

## 1.8 Types of compressors

There are different types of compressors developed over the past decades, whose names are given by the element that controls the gain. "The big four" as mentioned by Hicks (2009) are:

- **Tube** compressors also known as **Vari-Mu** – regarded as the oldest types of compressors and tend to have a slower response (slower attack and release) as noted by Hicks (2009) and Lisa (2013).

- **Optical** compressors – which, as Hicks (2009) specifies, control the dynamics of the signal using a light element and an LDR. Lisa (2013) notes that even though an optical compressor is somehow crude in design, inefficient and depends on a lagging lighting element, they are incredibly musical. An example of a such compressor is the LA-2A.

- **FET** (Field Effect Transistor) compressors – have been developed to emulate the tube sound as described by Hicks (2009). Moore, Till and Wakefield (2016) note that the FET works as a voltage-controlled resistor, whose resistance can be changed by the control voltage applied to its gate. To achieve this, Horowitz and Hill (2016) mention that the FET has to be configured to work in the ohmic region. Lisa (2013) describes the FET compressors as having very fast attack and release times making them more suitable for peak-style compression. An example of a such compressor is the 1176.

- **VCA** (Voltage Controlled Amplifiers) compressors – represent the pinnacle in both technical and sonic development (Lisa.2013). Hicks (2009) describes them as having less coloration (change of the original timbre, compromising the fidelity by introducing musical artefacts) than any other compressors. An example of such a compressor is the dbx 160.

The aim of the research is to do an in-depth investigation into the optical cells and identify key low-level parameters that can be changed in order to modify the behaviour of the optical cell, which would ultimately change the effect it has over a musical signal. Individual testing of the optical cells will provide an insight into the LDR's resistance curve change with input levels, frequencies and Electroluminescent panel (EL panel) colour. The research will describe the fundamentals of compression, the basic functionality of an optical cell, identified parameters of the optical cells that can be exploited to change the characteristics, the testing methodology and proposed testing circuits. In order to provide an understanding of such devices a brief description of optical compression will be given and exemplified with electronic circuits.

# 2 Optical Compression

## 2.1 Theory of operation

As mentioned earlier, optical compressors achieve gain reduction by using a combination of a light source and a light dependent resistor (LDR). As Lisa (2013) notes, the input of an optical compressor is fed to a light source that will output more or less light in response to the signal level of the incoming audio. Figure 2.1 describes a functional block diagram of such a compressor. There are different block diagrams as two different light sources have been used throughout the years inside the optical assembly: Electro-Luminescent Panel (EL Panel) and Light Emitting Diode (LED).
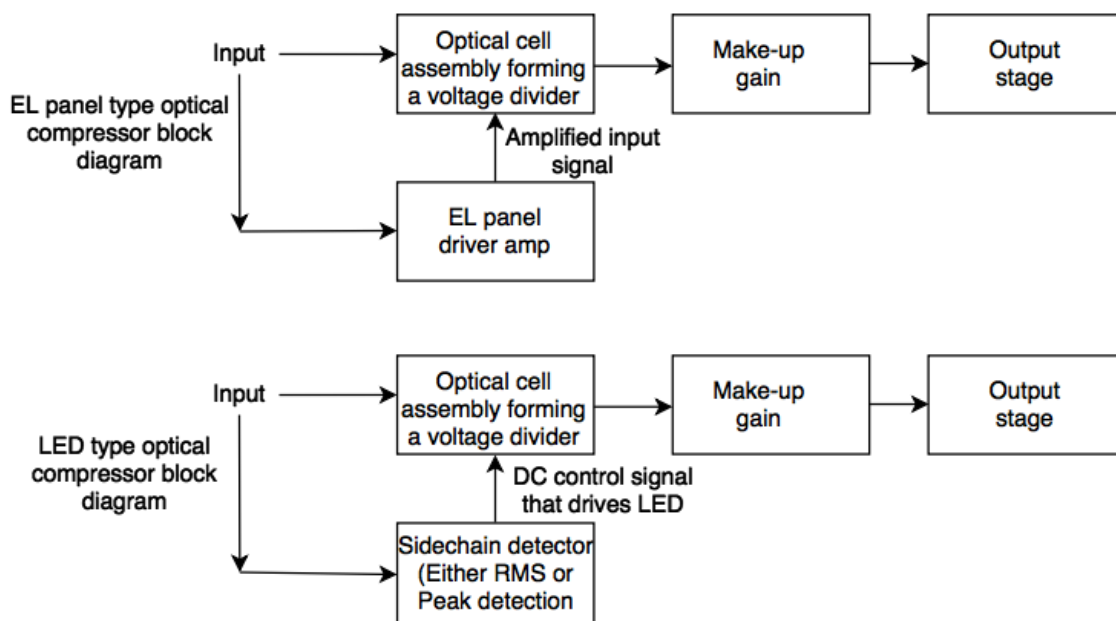


**Figure 2.1: Optical Compressors block diagram**

The optical cell employed in such compressors is also referred to as an optical attenuator which is basically a light dependent volume control (Ciletti, 1998). The photo-resistor, also called an LDR, changes its resistance dynamically with light levels as stated by the same author. Such

optical cells act as light-variable resistors that either shunt the signal to ground or pass it to the next stage. Figure 2.2 and Figure 2.3 show how the optical cells are arranged in the circuit allowing for gain reduction based on the LDR's value. Looking at Figure 2.2, the input signal from the secondary of the audio transformer is split into two different paths. First path takes the signal to the grid of the gain make-up valve and the second path takes the audio signal to the pentode drive amplifier. The amplified signal coming from the pentode is applied to the EL panel which glows according to the change in amplified voltage (based on the change in input voltage). Depending on the light level, the LDR varies its resistance allowing more or less signal to pass to the valve. A low resistance creates a low impedance path, shunting most of the signal to ground, while a higher resistance value allows more signal to pass to the next stage via the gain potentiometer. The pentode amplifier is necessary as the EL panel is a high impedance, low current device, needing a high AC voltage to light up.
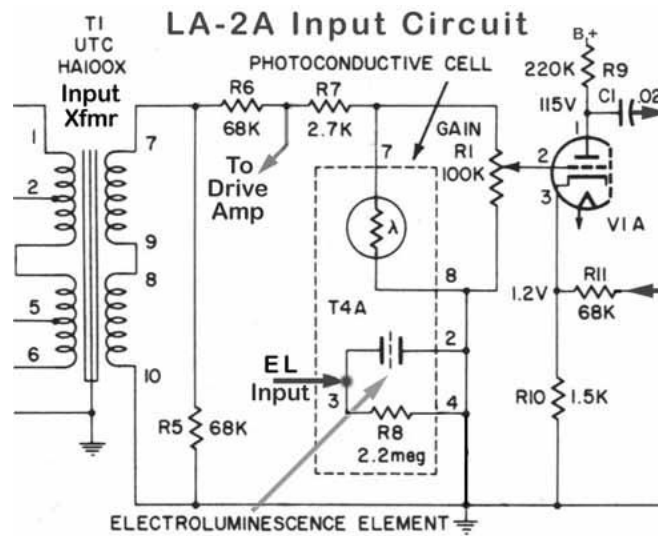


**Figure 2.2: LA-2A Input Circuit (Ciletti, 1998)**

The circuit in Figure 2.3 works almost in the exact same manner, but instead of an EL panel it is using an LED. The signal is split into two paths. First path is the signal that is meant to be controlled and goes to the voltage divider section and the second path sends the signal through a

rectifying circuit which creates a control voltage from it. This DC control voltage is used to drive the LED. Same as for the EL panel, when the LED's brightness increases the LDR's resistance drops, therefore more of the signal is shunting to ground instead of passing through the operational amplifier.
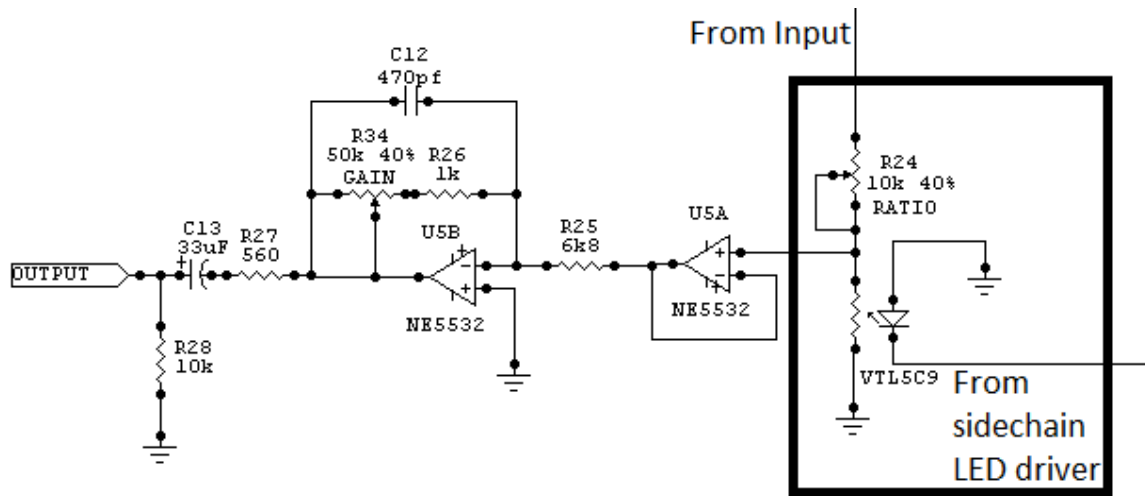


**Figure 2.3: Modern implementation of optical cell (Mnats, 2003)**

Older optical compressor circuits were using EL panels, whereas nowadays, for speed, LEDs are used (Ciletti, 1998). White (2003) also mentions the usage of LEDs for modern optical compressors, which are mostly integrated within one package, together with the detector circuit and use of feedback to increase the response time.

EL panels are built somewhat like a capacitor (Lawrence, 1964), with two conductive plates separated by a small gap filled with phosphor which reacts to AC voltage. Such compressors that employ an EL panel use a special driver/amplifier that boosts voltage to be able to drive the panel that has a very high impedance according to Ciletti (1998).

One of the many components that have been held responsible for the sound of the optical compressor is the optical attenuator itself. Moore, Till and Wakefield (2016) report that these cells

exhibit program dependent time constants which vary with the audio material. The same authors note that aging of the cell also determines changes in the time constants. Ciletti (1998) describes the LDR inside the optical cell as having a variable response, non-linear, which contributes to the attack/release time constants of the compressor. The non-linear response of the LDR together with the program dependent time constant will be further investigated and tested in order to determine the effect on the audio signal.

## 2.2 Difference in Optical Cells

Many companies have reproduced the LA-2A compressor from the same schematic. Even though the schematics are identical, it has been reported that none sound the same and all have a different type of coloration (changing the original timbre and compromising the fidelity by introducing musical artefacts e.g. distortion). What is different in such copies, apart from the input/output transformer, is the actual optical attenuator, more specifically the LDR and light source. All copies use different EL panels and LDRs. A list of these differences can be found in the table below:

| Company | EL panel | Photocell (LDR) |
|---|---|---|
| Universal Audio | GSI EL panel | Silonex NSL-02-042 |
| UREI | No-name El panel | Clairex CL-505L |
| IGS | No-name El panel | Silonex NSL5910 |

**Table 2.1: El panels and LDRs used by different companies**
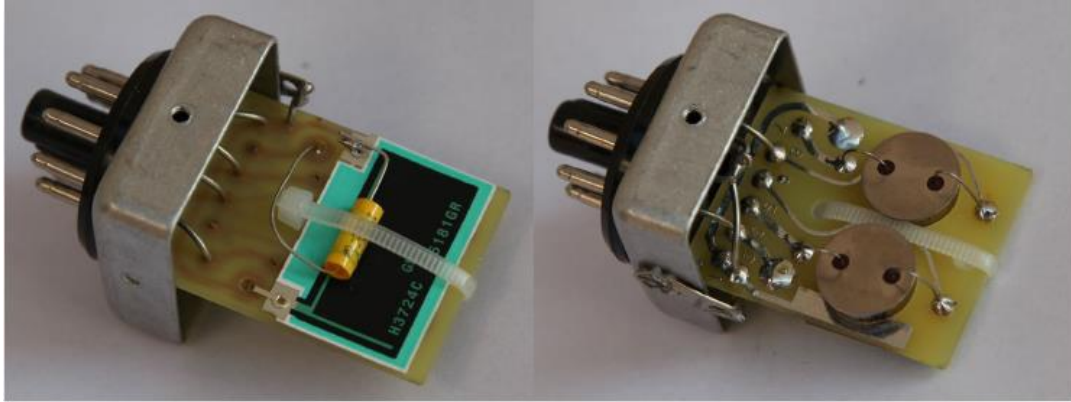
**Figure 2.4: Universal Audio Optical Cell (Sobczyk, n.d.)**



**Figure 2.5: UREI Optical Cell (Sobczyk, n.d.)**
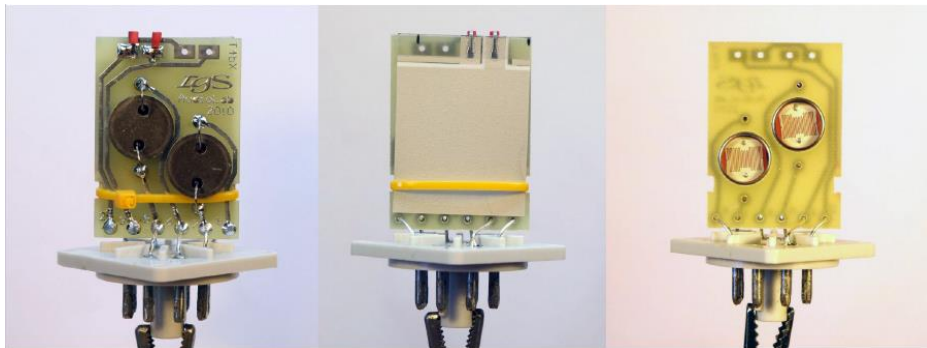


**Figure 2.6: IGS Audio Optical Cell (Sobczyk, n.d.)**

Figure 2.7 illustrates the difference in attack/release times for the same type of optical compressor, but from different manufacturers. The difference is assumed to be due to the change of LDR/light source inside the optical assembly. Due to missing measurements of these results, a more thorough study is required which will investigate the relationship between LDRs, light sources and attack/release times.

The image clearly shows more ripple modulation (change in the behaviour of the time constant, resistance fluctuation) for the IGS Audio version of the LA-2A. This ripple element will also be researched to determine its cause.
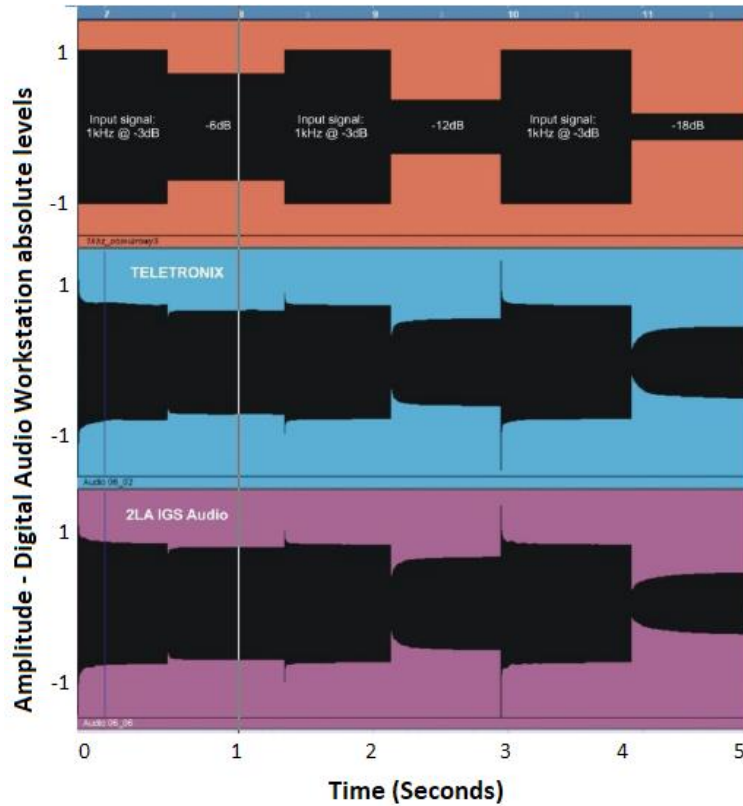


**Figure 2.7: Compression characteristics of two LA-2A implementations (Sobczyk, n.d.)**

# 3 Optical Cells

In this chapter, a detailed analysis of optical cells assembly will be presented and the two components that make up the cell will be investigated. Different material composites that form the photoconductive element in the LDRs will be included and low-level parameters will be examined in close relationship with the influence different light sources may have over them. Therefore, the interaction between LDRs and different light sources will be noted and will help identify key low-level parameters that can be exploited for sound timbre modifications. It will also establish links between certain parameters and the result over the dynamic range reduction behaviour. The reported memory effect and aging process that affect the cells will also be discussed and analysed.

## 3.1 Light Dependent Resistors (LDRs)

The LDR (or photoresistor, photoconductor) is a light sensitive device that reacts and varies its resistance depending on the light changes and it is based on the photoconductivity effect (Ciletti, 1998; Horowitz and Hill, 2016). Its resistance falls with increasing light intensity, as noted by RS (1997). The photoresistors are made using a thin film of light sensitive polycrystalline semiconductor that has a very high gain of electrons per photons as described in an engineering report from PerkinElmer Optoelectronics (n/a). Such semiconductor material can either be Cadmium Sulphide (CdS) or Cadmium Selenide (CdSe). A cutaway view of a photoresistor can be seen in Figure 3.1.

Fig. 1 -- Cutaway view of a photocell or light dependent resistor (LDR).
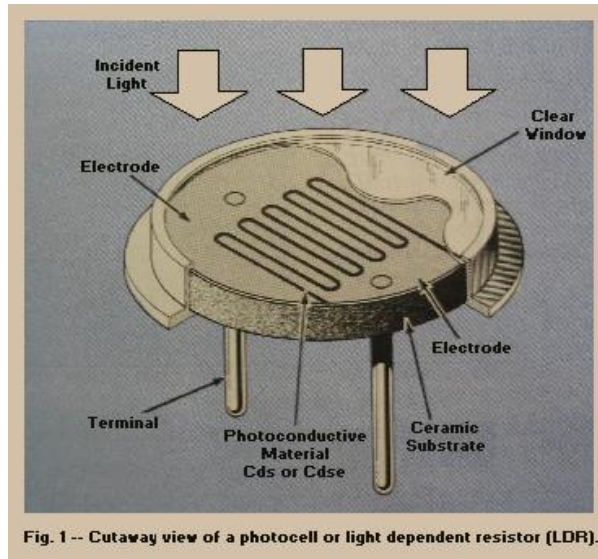
**Figure 3.1: Cutaway view of a photoresistor**

**(Marston & van Roon, 2011)**
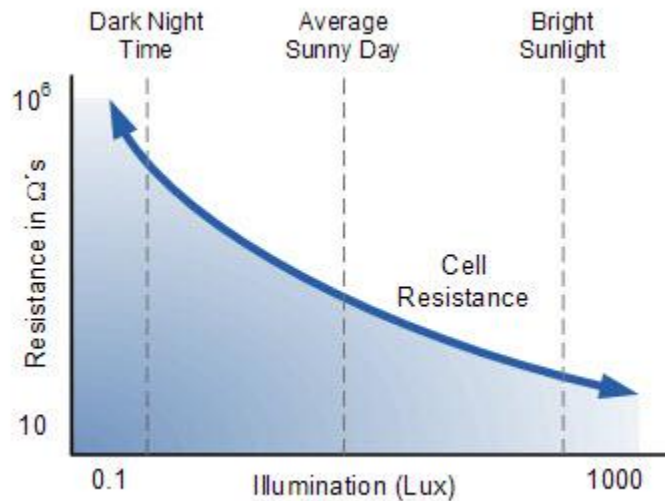


**Figure 3.2: LDR Resistance Curve vs. Light Intensity (Safwan, 2012)**

Figure 3.2 shows a typical resistance curve versus light intensity for a commercial LDR. An example of photocell used in a volume control circuit can be seen in Figure 3.3. As Ballou (2008) describes, when the light source becomes brighter, the LDR drops in resistance and therefore most of the signal will be appearing across R, causing less signal to appear on the output.
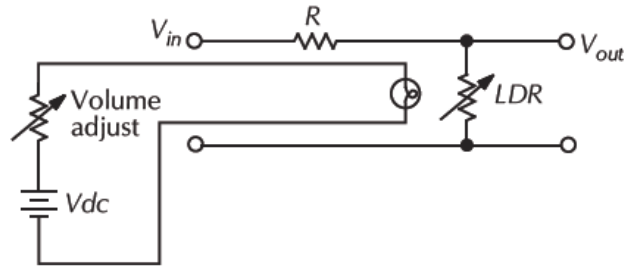
**Figure 3.3: LDR used as a volume control (Ballou, 2008)**

An advantage of using such optical attenuators as automated volume controls, as Ballou (2008) notes, is the lack of potentiometer's wiper noise that could get injected in the signal.

3.1.1 LDR Aging

The LDR aging process discussed by Moore, Till and Wakefield (2016) affects the cell's time constant and causes ripple modulation of the signal's amplitude. Shanks (2003) describes that the aging process affects the release time, making the curve to be less smooth, thus introducing ripple and possibly higher distortion. Ballou (2008) also supports the idea of photocell aging

with respect to the release curve.

Figure 3.4 shows two typical curves for the rise and fall resistances versus time when exposed to a certain amount of light.

As it can be noted from the image, both light and dark conditions produce a non-linear behaviour, where the resistance curves for the two states are not the same. When the LDR is exposed to light it produces a very fast resistance drop, whereas the dark condition produces a slow gradual increase in resistance. PerkinElmer Optoelectronics (n/a) explains this aging process that takes place in a photocell. It is stated in the paper covering optical isolators, that as the LDRs age, they exhibit

an increased output resistance. In the paper, it is reported that an estimate of 10% increase in resistance will develop each year. Intermittent operation of the cell slows down the aging process. Figure 3.5 shows the resistance change against time of a commercially available optical-isolator (VTL5C3).
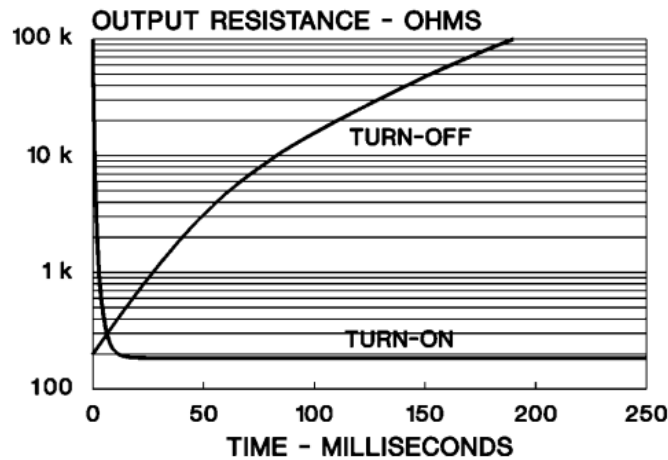


**Figure 3.4: Resistance Rise and Fall times (PerkinElmer, n.d.)**

This modification of resistance curve could therefore affect the release time described by Shanks (2003), by making the curve more abrupt. Zhao (2007) describes that the aging of the CdS thin film (material used for an LDR) can also be attributed to impurities. As constant operation of the cell increases the aging process, taking into consideration that the operating conditions can vary greatly, PerkinElmer Optoelectronics (n/a) shows that the response time of the LDR also changes with temperature. It is described that a low temperature increases the response time, becoming more pronounced depending on the photoconductive material. The same paper defines that elevated temperature rises the resistance of the photocell during the turn-on period.
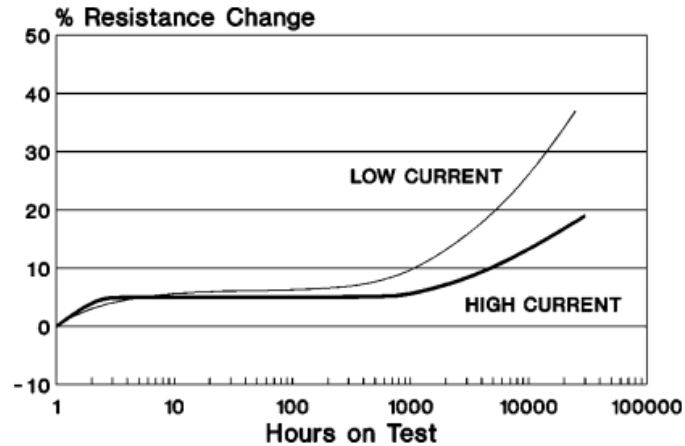
**Figure 3.5: Resistance change with time and current (PerkinElmer, n.d.)**

### 3.1.2 Memory effect

Memory effect of an optical cell refers to the LDR component and as described by Ciletti and Hill (1999) it represents the photocell's non-linear recovery from a transient signal, exhibiting a fast resistance recovery followed by a much slower one. Same authors describe that, when under constant compression (constant light over LDR), the release time increases giving rise to the so called "memory effect" which determines the release characteristic to be "program dependent". When analysing the optical cell of the LA-2A, Moore, Till and Wakefield (2016) described it as exhibiting a program dependant timing with a fast release for transient material and a slower release time for steady state material. In an article published on the Sweetwater website (2002) it is stated that the photocell exhibits a two-stage type of release, with an initial fast release followed by a slower release (as Ciletti and Hill described) that can take several seconds. In the article, the memory effect phenomenon is described as arising from the duration and intensity of the light to which the LDR is exposed. The two-stage release is also described by PerkinElmer Optoelectronics (n/a) in an application note stating that after removing the light, the cell's

resistance increases exponentially, tripling in a couple of milliseconds and then increasing linearly with time. Same type of two-stage release was proved in the conducted experiments.

For a particular photocell, Lawrence (1964) specifies that the LDR provides a faster resistance reduction (attack time) if any gain reduction has occurred within the last 20 or 30 seconds. Moreover, for a particular LDR, he shows that attack time is around 10 µs for a 50 % of the total gain reduction if the cell had previously been active. An approximate of 50 to 100 µs of attack time has been shown if no previous gain reduction occurred.

In the application note from PerkinElmer Optoelectronics (n/a) it is stated that dark storage causes the photoresistor to adapt to dark conditions, which increases the photocell's sensitivity to when it is exposed to light. Sensitivity is described by Horowitz and Hill (2016) as the relationship between the amount of light and the resulting output resistance. It is described in the paper that a cell which has experienced a dark adaption period will be able to reach a lower minimum resistance when is exposed to light. As the LDR can achieve a lower resistance after dark adaption, this can lead to a slower attack time. An LDR datasheet from RS (1997) also describes that the photocells remember the light condition in which they have been stored and this memory effect can be minimised by storing the cells in light before use. In the application note from PerkinElmer Optoelectronics it is also described that dark adaption of the cells begins immediately after removing the input drive (light source). High light levels allow the photocell to adapt to light condition within minutes as stated in the same paper. In a guide published by the same company, which covers the criteria on how to choose a photocell, the hysteresis of the LDR is compared, as an analogy, to the way the human eye adapts to light variation. The eye's sensitivity depends on the level of light to which was previously exposed, taking a longer time to recover full eyesight

after a long time of dark condition. The given recommendation on how to minimize this effect is to store the LDR in a low light level.

Lawrence (1964) states that return to dark condition approximates a log function if ohms are plotted against time, release time being dependent on the amount of gain reduction that took place before, thus sustaining the idea described by Ciletti and Hill.

Figure 3.6 shows the variation of resistance with light history expressed as the ratio $R_{LH}$ and $R_{DH}$ at various test light levels. $R_{LH}$ represents the infinite light history resistance and $R_{DH}$ represents the infinite dark history. $R_{DH}$ is achieved by keeping the LDR for 24 hours in dark while $R_{LH}$ in achieved by 24 hours' exposure at 30 fc (foot candles). After the LDR was stored in dark for the 24h period it's illuminated with a fixed amount of light (0.01, 0.1, 1, 10, 100 fc) and the resistance is measured. Then it is stored in low light for 24h and then exposed to the same previous amount of light and the resistance is measured. After the two measurements, a ratio between the two is calculated. The procedure is repeated for different illumination levels as shown in the table. What the table shows is that at low exposure levels the ratio between the two measurements is higher compared to the ratio at higher exposure levels. Therefore, memory effect is higher at low exposure levels, whereas at high levels of light the ratio remains unaffected.

| | Illumination | | | | |
|---|---|---|---|---|---|
| $R_{LH}/R_{DH}$ Ratio | 0.01 fc | 0.1 fc | 1.0 fc | 10 fc | 100 fc |
| | 1.55 | 1.35 | 1.20 | 1.10 | 1.10 |

**Figure 3.6: Light History (PerkinElmer, 2001)**

As stated in the photocell guide from PerkinElmer Optoelectronics, the figure showed that a photocell which has been stored under light condition for a long period will have higher light

resistance than the cells stored for a long period in the dark and that there is a certain threshold of light level, above which, the storage conditions should not matter. During testing it was found that at high light levels, the differences in output resistance between different LDRs are very small compared to low light levels.

It is to be noted that most manufacturers of photocells quote the rise and fall times associated to the cells as the time needed to reach 63% (1-1/e conductance) of the final value, identical to the way capacitor's time-constant is measured.

The noise performances are measured just like for any other resistor, the most important being the thermal/Johnson's noise calculated according to the formula described by Horowitz and Hill (2016):

$$\mathbf{I_{NJ}} = \sqrt{(4kTBW)/R}$$

**Equation 3.1: Noise Calculation**

where $I_{NJ}$ is the noise current in amps RMS, k is Boltzmann's constant, T is temperature measured in Kelvins, R is photocell's resistance and BW represents the bandwidth of interest in Hertz.

The memory effect could also be linked to the photoelectric fatigue which is specific to semiconductors and will be described in the following subchapters.

3.1.3    Photoconductivity, Energy Bands and Spectral Sensitivity

**Photoconductivity**

As stated at the beginning of the chapter, photocells work on the principle of photoconductivity. As mentioned by Rouse (2005), photoconductivity is a substance's tendency to conduct electricity depending on the intensity of the light-radiant energy that is absorbed by the

material. Perkowitz (n/s) notes that photoconductivity in such materials serves as a tool to understand the internal processes and it is widely used to detect the presence of light. Cadmium sulphide and cadmium selenide used in photocells are both semiconductors that exhibit this photoconductive effect, as described by Silonex (2007). The resistance value and the power rating for each cell is determined by the material, its thickness and deposition width. (Marston,1992). Perkowitz (n/s) defines the cadmium sulphide as a crystalline semiconductor and the selenium as a semimetal. Rouse (2005) describes that in order to create a photoelectric device the photoconductive substances are doped with impurities.

**Semiconductor Doping**

It has been described above that both CdS and CdSe are semiconductor devices. Semiconductors are defined by Rouse (2015) as solid or compound chemical elements that have the ability to conduct electricity under specific conditions. Conductance is dependent on the current or voltage applied or on other stimulating factors such as irradiation by infrared, visible light or ultraviolet light. Neamen (2003) describes semiconductors as having conductivity properties between metals and insulators, elemental materials occupying group IV in the periodic table, while compound semiconductor materials are a combination of group III and group V. To alter conducting properties, the semiconductor has to be doped with impurities, whose purpose are to provide free carriers in the semiconductor material (Zeghbroeck, 1997). Same author describes that semiconductors which are doped with ionized impurities will contain free carriers, therefore the ionized donors create free electrons and the semiconductor is called n-type, while ionized acceptors create holes referred to as a p-type conductor. The process can be seen in Figure 3.7.
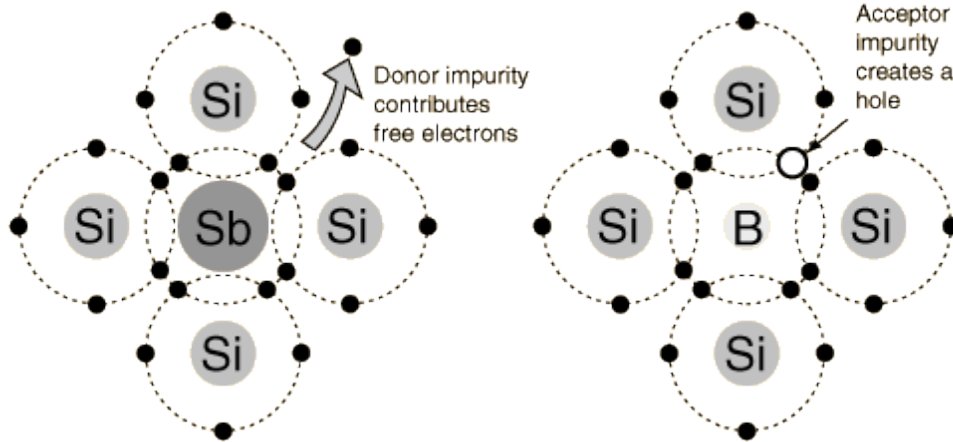
**Figure 3.7: N-type and P-type Semiconductors (Nave, n.d.)**

Physics-Assignment (2013) further advances this idea, describing that impurities and imperfections in the photoconductive material contribute towards photoconductivity, and such impurities allow photons with lower energies to be able to produce mobile electrons and holes. For cadmium sulphide, Grovenor (1998) shows that the dopant elements can either be Gallium, Iodine or Fluorine for n-type and Lithium or Sodium for p-type. Table 3.1 describes the dopants and with the atomic position. Atomic position shows which atom does the dopant substitute.

| Cadmium Sulphide | Dopant | Atomic position | Doping character |
|---|---|---|---|
| | Gallium | Cd | n-type |
| | Iodine | S | n-type |
| | Fluorine | S | n-type |
| | Lithium | Cd | p-type |
| | Sodium | Cd | p-type |

**Table 3.1: Dopants for CdS**

Therefore, incident light over the cadmium sulphide creates an electron-hole pair, as stated by Schiavello (1985).

$$CdS + h\nu \rightarrow e^- + hole^+$$ **Equation 3.2: Electron - Hole pair creation in CdS**
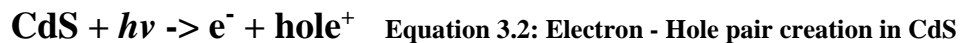
where $h\nu$ is the energy of the light (photon).

Cadmium selenide (CdSe) is described by Grovenor (1998) as being an anion compound of the CdS.

Moreover, another important aspect of semiconductors is the presence of traps. Traps are impurities or imperfections in the material which are capable to capture an electron or a hole (Physics-Assignment, 2013). Traps can either be recombination traps that help electrons and holes recombine or traps that restrict the motion of holes and electrons, thus affecting the photoconductivity of the material. Photons that create electrons and holes in the CdS create a nonequilibrium condition (Schiavello, 1985).

**Energy bands**

Simply put, as described by Harrison (1998), there are three energy bands in semiconductors:

- Band gap (also known as forbidden band)
- Valence band
- Conduction band

The same author describes that the valence band and the conduction bands determine the electrical conductivity of the material, where the valence band contains the highest range of electron energies (electrons), while the conduction band has the lowest range of vacant electronic states (holes). The band gap, as noted by Neamen (2003), is an energy range that contains no electron states, and it usually refers to the energy difference that exists between the conduction band and the valence band. This energy difference is measured in electron-volts (eV). Grovenor (1998) describes the energy of the band gap as the required energy for a valence electron bond to an atom to become conductive, thus becoming free to move within the semiconductor, serving as a charge carrier. In the case of a photocell, which depends on the energy of the light, the energy of photons has to be

at least at the same magnitude as that of the band gap (Entner, 2007), thus the electron's energy becomes:

$$E_c = E_v + h\nu$$

**Equation 3.3: Electron Energy**

(MIT online course, 2013),

where **Ec** is the energy of the electron in the conduction band, **Ev** is the energy of the electron in the valence band and **hv** is the energy received (in our case photon's energy)
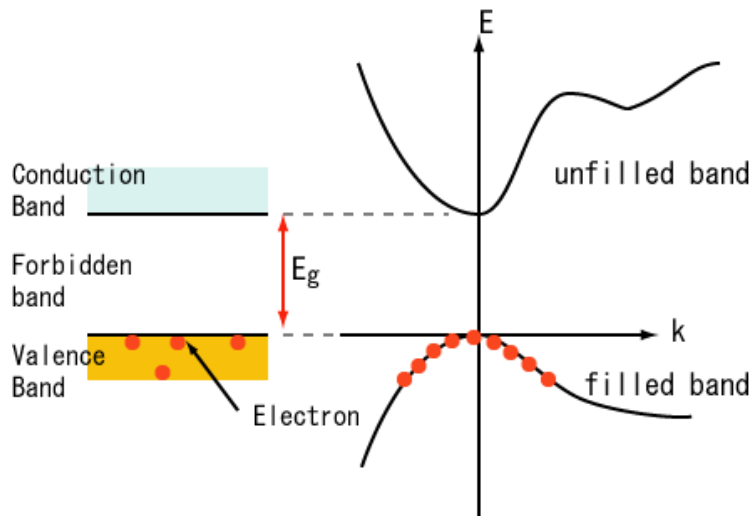


**Figure 3.8: Energy Bands (S-kei, 2006)**

In Figure 3.9 it can be seen how different material types have the energy bands closer together or how different types of semiconductors exhibit a closer distance between gap band and any of the valence or conduction bands. It is described by Neamen (2013) that lower energies for the gap band dictates that the material gets closer to a conductor, while high energies for the gap band describes an insulator. This fact can be observed in the figure below.
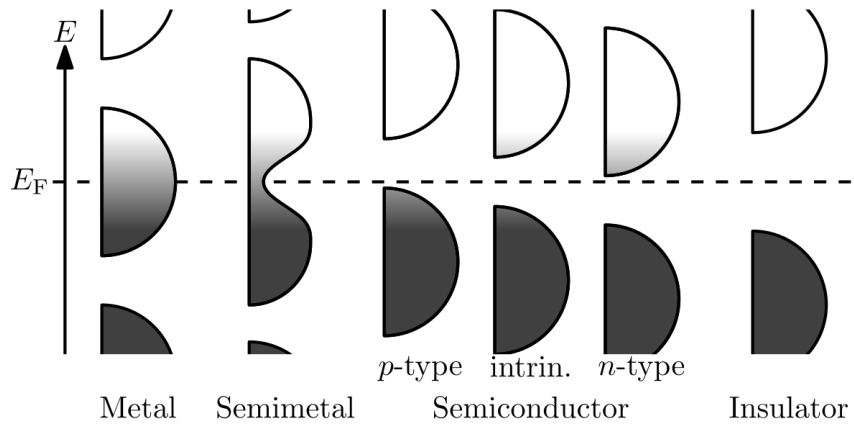
**Figure 3.9: Different material energy bands (Nanite, 2013)**

In this case, the semiconductors that of interest (CdS and CdSe) are direct band-gap semiconductors, which have a band gap of 2.42 eV (CdS) and 1.74 eV (CdSe) (Perkowitz (n/s), Potter and Schalla, 1967). It is described in an article published by University of Cambridge (2007), that in a direct band-gap semiconductor, the energy difference between the valence band and band-gap and the conduction band and band-gap are equal. This is exemplified in Figure 3.10.
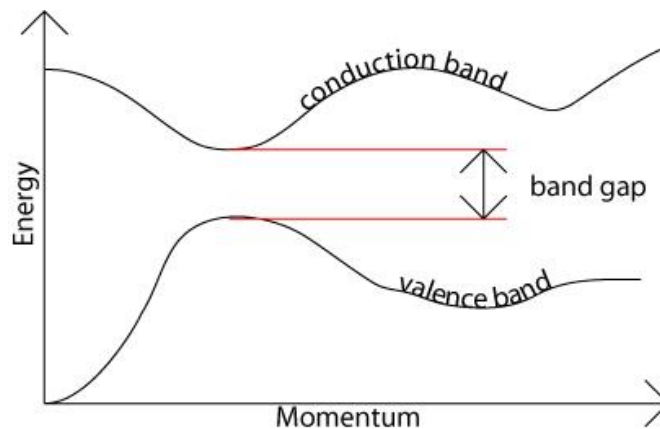


**Figure 3.10: Direct band semiconductor energy (University of Cambridge, 2015)**

It is worth mentioning that according to Zeghbroeck (1997), energy band gap is temperature dependent, tending to decrease as the temperature goes up. The author explains this phenomenon by relating to the increased thermal energy which translates into higher amplitudes of the atomic

vibrations. If the atomic vibrations increase, they give rise to an increase in interatomic spacing, thus decreasing the potential seen by the electrons in the material. This results in a decreased band-gap. The temperature dependence of the band gap can be calculated using the following formula:

$$\mathbf{E_g(T) = E_g\,(0)\,-\,\frac{\alpha * T * T}{T + \beta}},$$ **Equation 3.4: Temperature dependence of band gap**

α is measured in eV/K and *β* is measured in K.

Lawrence (1964) describes the effect the light and its intensity have over the resistance of the photocell, stating that the energy of the light reduces the adherence of outer orbit electrons in the cadmium sulphide crystal atoms. The author states the cause of this to be that detached electrons become free, participating in the conduction process. Therefore, the conductivity of the photocell depends on the amount of light. Lawrence also suggests that resistance decrease (light condition) is much faster than return to high resistance (dark condition), as after light is removed, the electrons take more time to recombine. Entner (2007) defines this process as carrier generation and recombination, where in carrier generation, electron-hole pairs are being created after an electron is excited from the valence band to the conduction band resulting in the creation of a hole in the valence band (University of Toledo, 2012). The recombination is the reverse process, where the electrons and holes are combined and thus annihilated. Thus, the recombination process in the case of the photocell is the return to high resistance (dark condition). Kraftmakher (2006) describes that for an intrinsic photoconductor (the photocell in our case) the concentration of electrons and holes is equal. But because of the higher diffusion rate of the electrons, as stated by Mehrotra and Klimeck (2010), when light intensity increases, more electron-hole pairs are generated and because the electrons have higher rates of diffusion, this results in fewer electrons remaining to take part in recombination, by diffusing away faster in comparison to holes. This only happens at the centre

of the semiconductor though. Entner (2007) provides an equation for recombination rate that takes into account the density of electrons and holes:

$$\boldsymbol{R_{np} = \ C_c * n * p,} \text{ Equation 3.5: Recombination rate}$$

where **n** and **p** are the density of electrons and holes.

According to the equation and how more light means more electron-hole pairs generation, this explains the reason why the release curve of a photoresistor depends on the previous light condition. Moreover, if more holes are created in the middle of the semiconductor than electrons, as Mehrotra and Klimeck (2010) stated, it may result in a slower recombination process, thus slower increase of resistance.

**Spectral Response**

As discussed above, the photocells react to the energy received through photons (light), becoming more and more conductive. It was also mentioned the band gap energies for the two photoconductive materials used in LDRs:

- 2.42 eV for CdS
- 1.74 eV for CdSe

In order to excite the electrons, the energy received through photons has to be at least as the same energy as that of the band-gap, and as noted by Perkowitz (2016), that corresponds to a photon of a wavelength of 512 nanometres (for CdS). Same value is calculated by using the table published by Halas Nanophotonics Group from Rice University (n/s). Perkowitz (2016) also notices that a wavelength of 512 corresponds to the visible green light. Therefore, spectrum response is defined as the photon's minimum required energy to excite an electron across the band (Armed Services Technical Information Agency, 1961).

In the photocell selection guide published by PerkinElmer Optoelectronics () it is described that the relative spectral sensitivity of a photocell depends on the light's wavelength, thus on the colour of the light. It is not to be confused with the sensitivity, which, as discussed above refers to the relationship between light intensity and the output resistance. A typical spectrum response of the photocell is comparable to that of the human eye, as it can be seen in Figure 3.11.
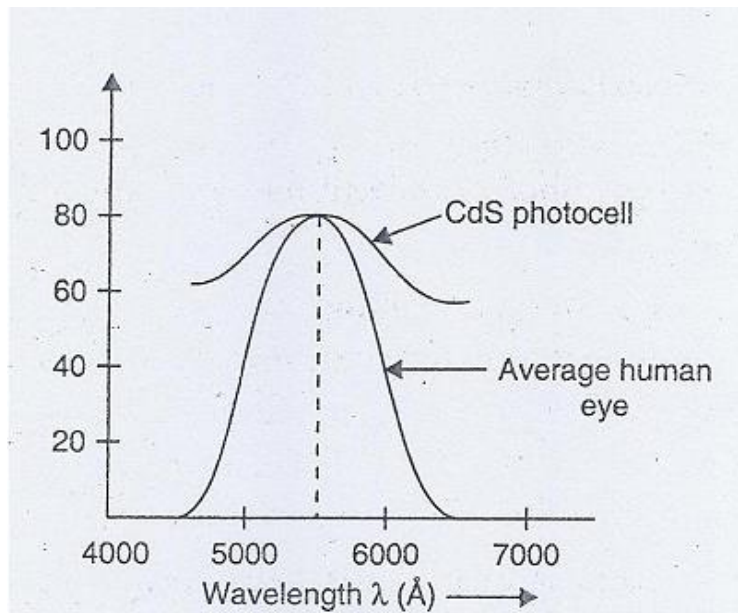


**Figure 3.11: Photocell spectrum response (no longer online)**

The X-axis is the wavelength, which is measured in angstroms ($1*10^{-10}$ cm) and on the Y-axis it is measured the efficiency of the photocell.
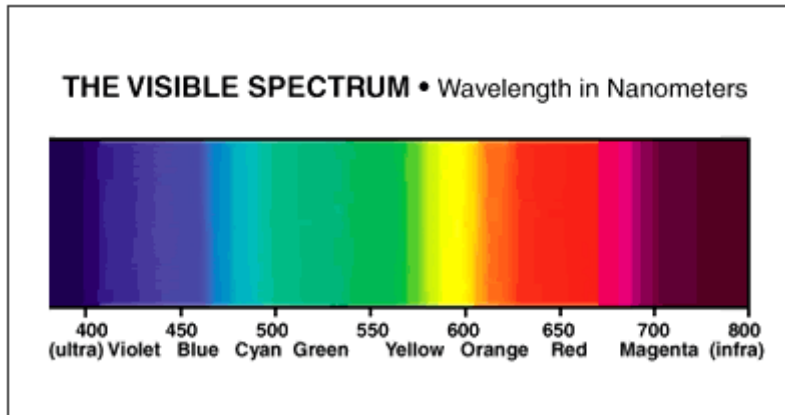
**Figure 3.12: Visible Spectrum Wavelengths (Newt, 2004)**

It is worth mentioning that Figure 3.11 represents an ideal case and is based on an ideal photocell, but, as previously discussed, the photocell has imperfections and impurities which create a deviation from the perfect-world theory.

In the two figures below (Figure 3.13 and Figure 3.14), taken from an LDR's datasheet from RS electronics, it is clearly visible the difference in spectral response between two photocells made out of the same semiconductor, but having different sizes
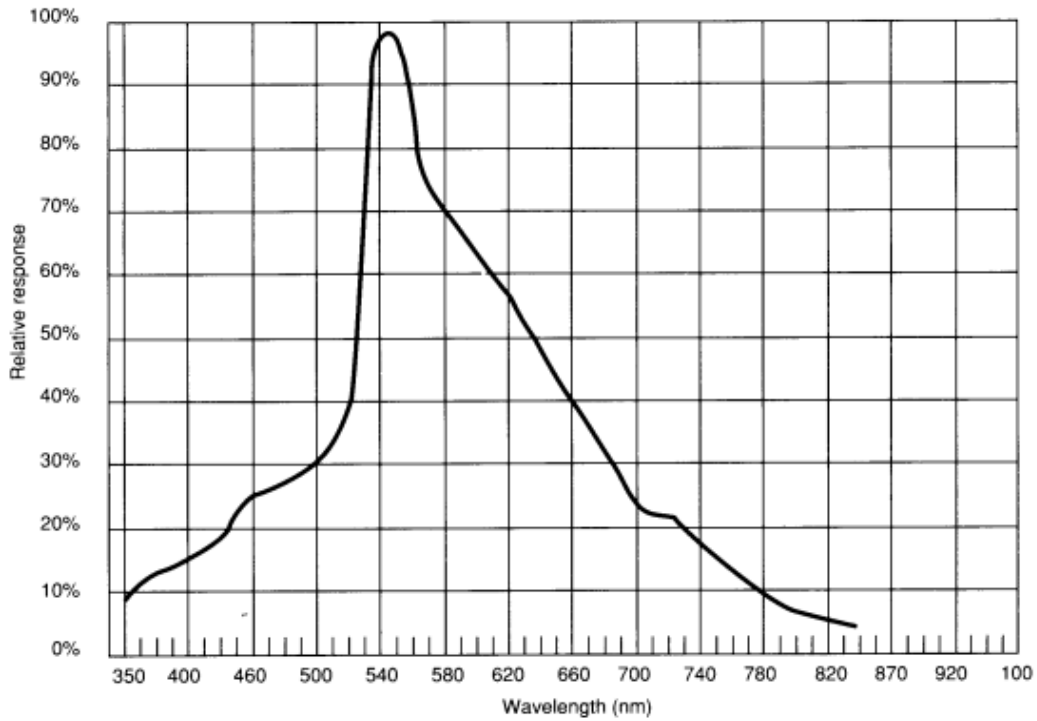
**Figure 3.13: A CdS cell spectral response (RS Components, 1997)**

As it can be seen, the spectrum response is different. Figure 3.13 presents a relative response of 20 at 450 nm, 100 at 550 nm, 60 at 650 nm, 40 at 700. Figure 3.14 shows a relative response of 20 at 450 nm, approximately 100 at 550 nm, 60 at 600 nm and 40 at 660 nm. As a general rule, it can be remarked that all LDRs (CdS material) exhibit a peak response around 550 nm (darker shade of green according to Figure 3.12).
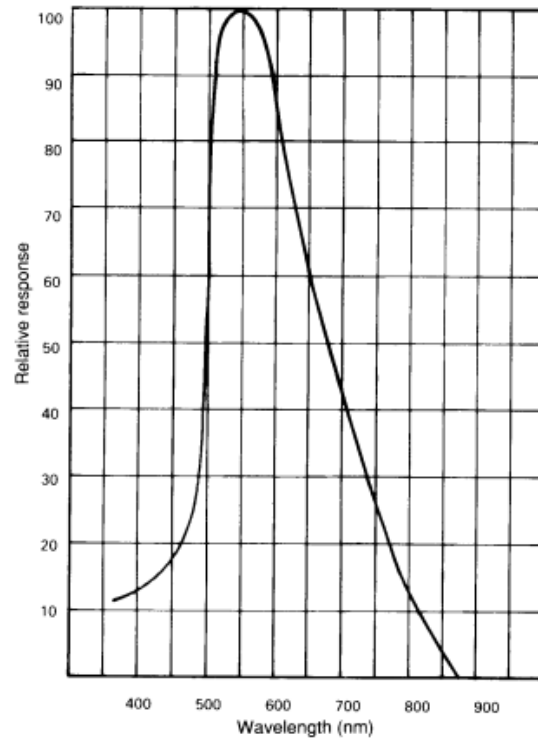
**Figure 3.14: A different CdS cell spectral response**

(RS Components, 1997)

Figure 3.15 shows how efficient is the absorption of photons by the CdS at different wavelengths and it is also compared to other photoconductive materials. The efficiency is measured using an absorption coefficient that is a measure of the light absorption strength for a given photon energy (University of Toledo, 2012)
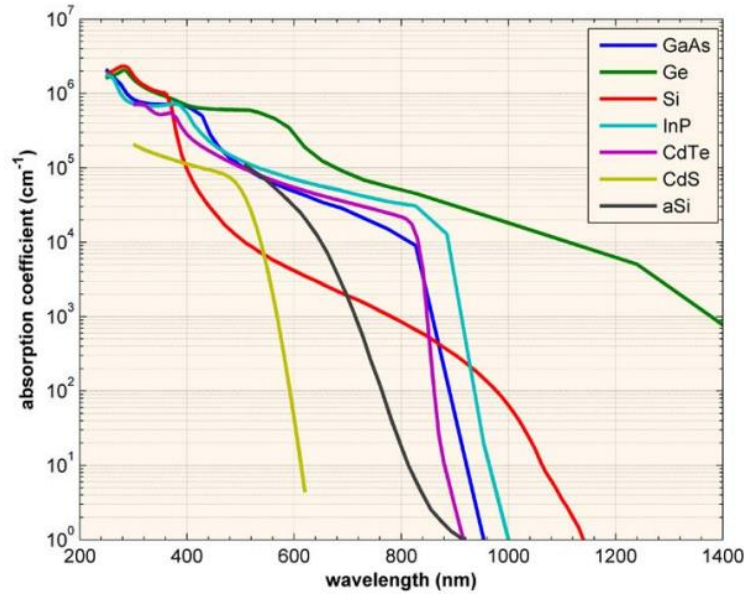
**Figure 3.15: Photon absorption efficiency (Gowdham, n.d.)**

3.1.4    Photoelectric Fatigue

The phenomenon called 'photoelectric fatigue' was mentioned in **Memory effect** subchapter and was referred to as a possible cause of the memory effect. This phenomenon is an aspect of the semiconductor photoconductivity in which the sensitivity decreases considerably in magnitude with time (Joshi, 1990). This effect can be seen in Figure 29.
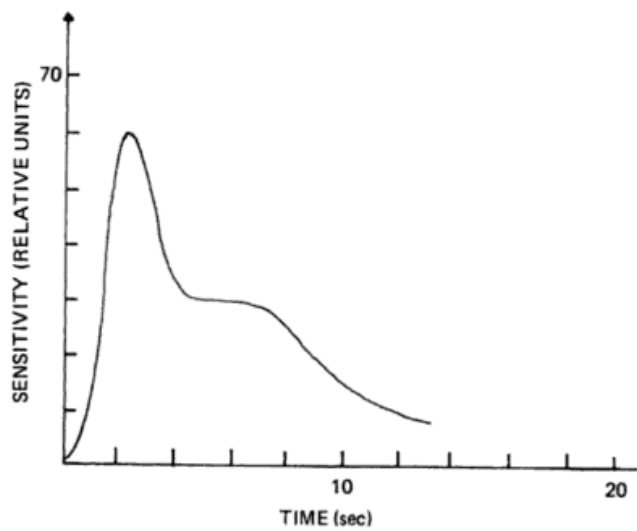


**Figure 3.16: Photoelectric fatigue (Joshi, 1990)**

The image shows how the photo-response reaches a maximum value of sensitivity as soon as light falls on it and then starts decreasing with time.

Photoelectric fatigue (PEF) is also called optical obsolescence or photoconductivity relaxation of the 2$^{nd}$ kind (Petrosjan, Shik, Vul' & Sheinkman, 1977). Same authors suggest that PEF appears in a sample exposed for a long time to any kind of photonic radiation under the form of decreased conductivity. Relating to the previously discussed increase in sensitivity of photocells that have been extensively stored in dark condition, the authors suggest that in some cases the initial value of the sensitivity can be restored under dark exposure, and this fatigue can sometimes be removed by infrared illumination.

Korsunskaya et all. (1973) suggest that PEF happens apparently because of photochemical reactions, which are impossible to externally control or reduce. Throughout study, Petrosjan, Shik, Vul' & Sheinkman (1977) showed that PEF affects CdS, but in-depth mathematical demonstrations are outside the scope of this research.

## 3.2 Light Sources

For an optical compressor to work properly, a suitable light source is needed. As discussed earlier, the photocell's resistive properties change depending on the light spectrum, thus its sensitivity relates directly to light's colour and intensity. The following chapter will describe Electroluminescent Panels that are used in the optical cells, studying the advantages and disadvantages of using them. There are other possible light sources, but due to the identified disadvantages of the working principle, they are not suitable to be used in audio circuits. The electroluminescent principle will be detailed and a comprehensive explanation of light intensity/brightness and measuring techniques will be provided, which will help understand the

optical cell's testing procedures that will follow. Based on different properties of light sources, key parameters will be identified, which will be the main focus of the testing procedures that will follow.

3.2.1   Electroluminescence Phenomenon

Electroluminescence (EL) is an electrical and optical phenomenon that takes place in certain semiconductors and refers to their ability of emitting light when current is passed through them, as described by Mohankumar (2012). Honsberg and Bowden (n/a) define that electroluminescence is generated by the radiative recombination of carriers. These carriers, which are also described by Mohankumar (2012), are the electrons and holes in the semiconductor. Bani, Abdul-Malek and Ahman (2015) also note that EL occurs when a material is put under a high electrical field, associated with charge carrier generation in that material. Radiative recombination is the inverse process of photoconductivity, in which an electron goes back to its equilibrium energy band radiating a photon (Goetzberger, Knobloch and Voss, 1998). Same authors state that the energy of the emitted photon is equal or less to that of the semiconductor's band-gap, which has been described in the previous subchapter. It is also described that radiative recombination is specific for direct band semiconductors.

The recombination rate is defined by the following formula (Green, 2003):

$$R = B * n * p,$$ **Equation 3.6: Radiative recombination**

 where **B** is a constant for a given semiconductor, **n** is the concentration of electrons and **p** is the concentration of holes. Figure 3.17 illustrates the generation of photons.
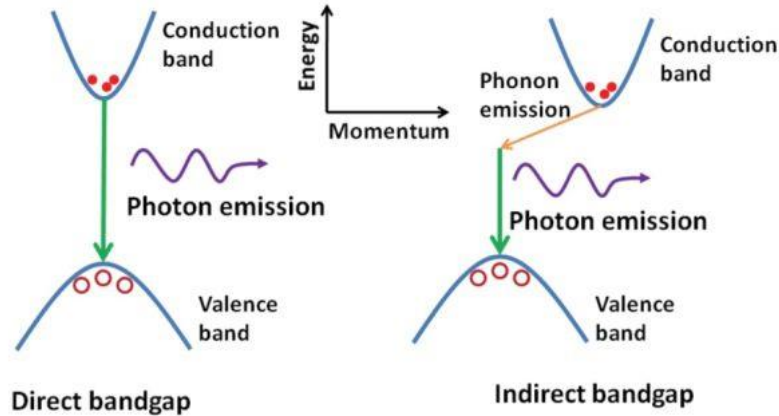
**Figure 3.17: Electroluminescence phenomenon (Sun, 2010)**

It is to be noted the fact that, according to Goetzberger, Knobloch and Voss (1998), the energy of

the emitted photon may not always be equal to the that of the band-gap because some energy may

be lost due to defects in the semiconductor and the lost energy is radiated as phonons (mechanical

thermal vibrations).

3.2.2    EL Panels

Electroluminescent panels are built somewhat like a capacitor, as stated by Lawrence

(1964), with two conductive plates separated by a small gap filled with phosphor that reacts to AC

voltage or a very strong electric field. As noted by Mohankumar (2012), the light emitting material

is sandwiched between two electrodes, one of which has to be transparent to allow light to pass

through. The transparent surface is usually coated with Indium Oxide or Tin Oxide and the back

electrode is coated with a reflective metal. Same author mentions that EL light is not directional,

thus it cannot be compared against any other light sources, which are usually measured in lumens.

Moreover, it is mentioned that the brightness of an EL device appears to be uniform, thus having

almost the same brightness from all viewing angles.

The phosphor used in the El panel is a solid material that emits light when it is exposed to

radiation or to an electron beam, as described by Stark (n/a).  Phosphors are transition metal

compounds that are used commonly in cathodic ray tube (CRT) displays, backlit displays or fluorescent lights. According to King (2012), phosphors consist of a host material which is doped with an activating substance that is used as the light emission centre. According to the same author, to be a phosphor host, the material must have a large band gap (>3.0 eV) so that it can emit visible light without absorption. It is described by Strock (2014) that currently only II-VI materials like Zinc Sulphide (ZnS) and Strontium Sulphide (SrS) are used in commercial products.

The light colour of the El panels comes from the activator material used and the host material (usually) or due to a certain colour filter used in the processing, as it can be seen in Figure 3.18.
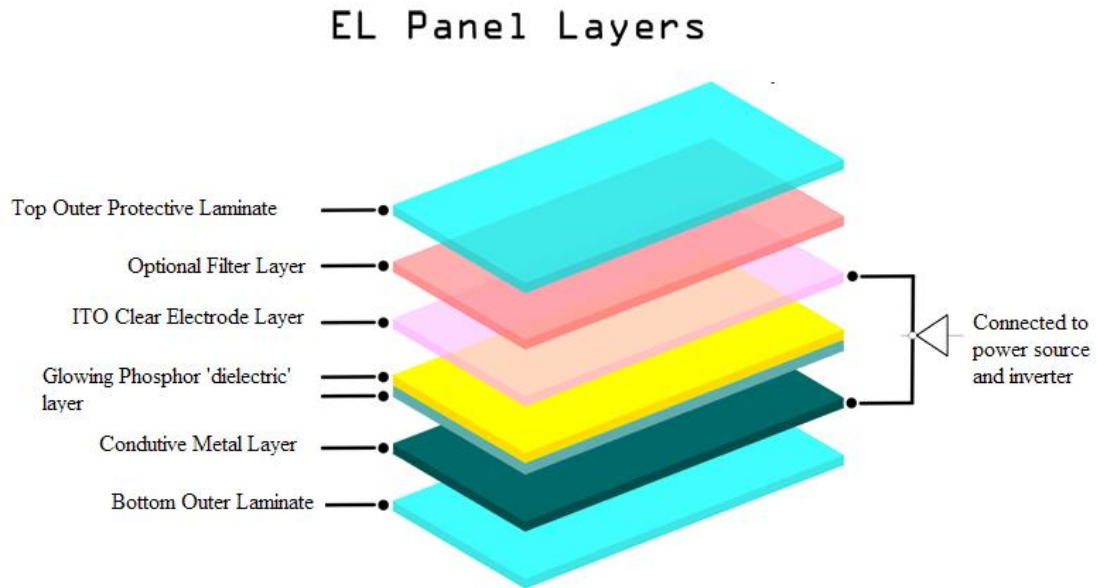


**Figure 3.18: EL Panel construction (EL Panel tape, n.d.)**

Table 3.2 shows the phosphor material and the output colour achieved. The CIE (International Commission of Illumination) characterizes colours by a luminance parameter and a two-colour coordinate (X and Y), which specify the point on the chromaticity diagram for a more

precision colour measurement (Nave, 2017). An example of such a chromaticity diagram can be seen in Figure 3.19.

| Emission Colour | Phosphor Material | CIE X | CIE Y |
|---|---|---|---|
| Yellow | ZnS:Mn | 0.50 | 0.50 |
| Red | ZnS:Mn/Filtered | 0.65 | 0.35 |
| | CaSSe:Eu | 0.66 | 0.33 |
| Green | ZnS:TbOF | 0.30 | 0.60 |
| | ZnS:Mn/Filtered | 0.47 | 0.53 |
| Blue | SrS:Ce | 0.19 | 0.36 |
| | SrS:Cu | 0.17 | 0.16 |

**Table 3.2: Emission colour based on the phosphor material**
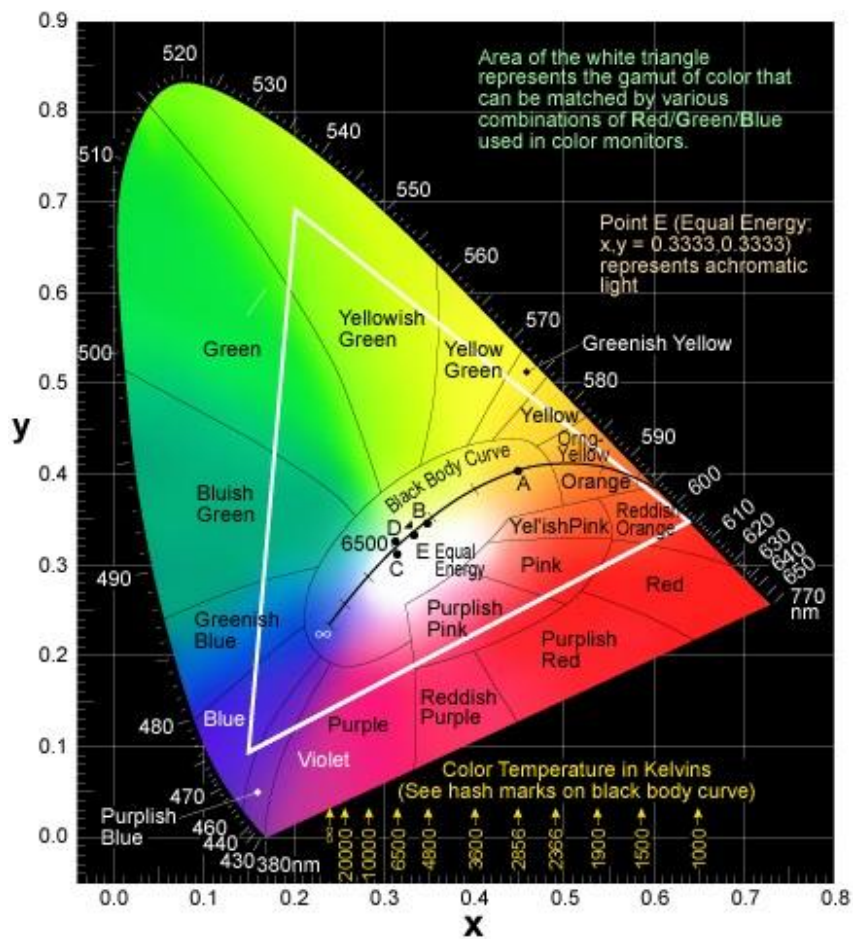


**Figure 3.19: Chromaticity diagram in CIE (Rainbow Light, 2017)**

In the case of the EL panel used in optical compressors, this is made out of flexible plastic. According to Strock (2014), this EL panel has almost the same construction as discussed before, where one electrode is a white thin aluminium foil coated with a high-dielectric material and then coated with a phosphor in a high-dielectric organic material which hardens into a tough plastic once baked. The other electrode is made out of a thin conductive glass paper cemented to a phosphor layer. These two electrodes are then sandwiched together and enclosed into a sealed electrical and moisture protective material.

Strock (2014) also mentions that the EL panel is made to be operated between 50 and 500 V, at frequencies between 60 to 6000 Hz. It is yet unknown if panels used in compressors such as LA-2A were modified to suit a higher bandwidth.

Figure 3.20 shows the relationship between brightness, voltage and frequency. The Y-axis represents the brightness measured in arbitrary units. Cycles per seconds (CPS) are used here instead of Hz, but they are equivalent. It is also reported by Strock (2014), that at high frequencies, the EL panel can manifest a shift towards the blue colour (Figure 3.21), behaviour that has not been reported yet in any optical compressor, which may be worth investigating, as a shift in colour can contribute to a decrease in LDR efficiency.
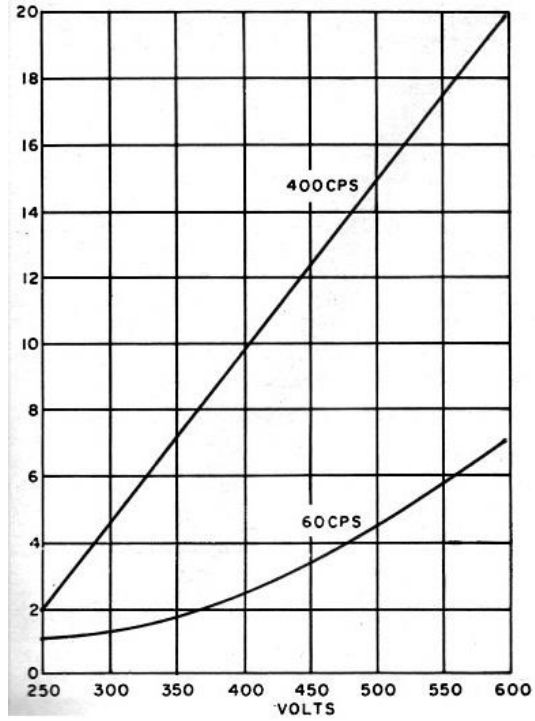
**Figure 3.20: Brightness vs. Voltage and Frequency (Strock, 2014)**
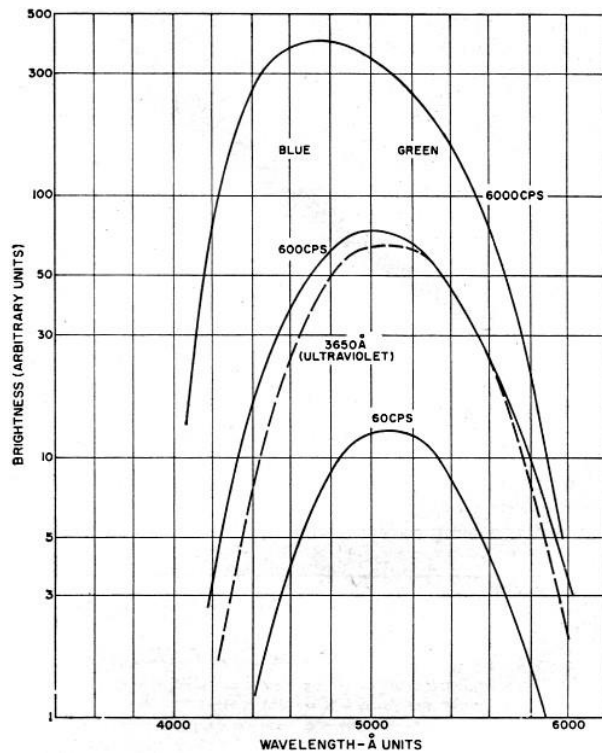


**Figure 3.21: Colour shift with frequency (Strock, 2014)**

One disadvantage noted by Whelan (2013) with EL panels is the reduced light intensity output over time, which may explain why some optical compressor's gain reduction indicator has to be tweaked from time to time. An example of this can be seen in Figure 3.22 taken from an EL panel brochure by Surelight (n/a).
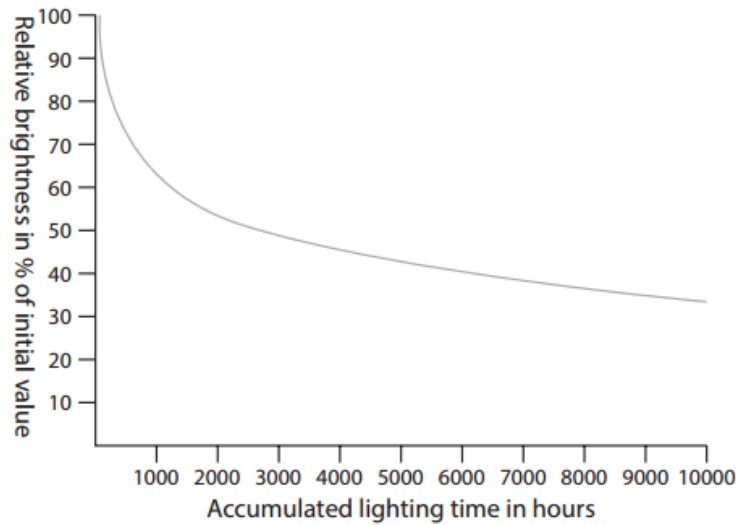


**Figure 3.22: EL Panel brightness decrease over time (Surelight, n.d.)**

Another aspect that may affect the performance of the EL panel, in terms of response speed, is that different phosphor materials used for different colours have different chemical or physical properties that affect the response speed or the afterglow, as described by Yano and Nagano (2001). Afterglow refers to the prolonged decay time of emission after voltage application ceased and it is a function of the activator material.

Afterglow of the EL panel could relate to the smooth release curves often associated with optical-compressors and can cause a smoother resistance decay characteristic of the LDR.

## 3.3 Identified Parameters and Attributes

Following an extensive literature review on light dependent resistors, on light sources and the impact on the characteristics of the LDR and the analysis of circuits used in optical cells assembly, certain parameters were identified that may be exploited and modified to see if they produce any changes in the attributes of the optical cell.

The following parameters and attributes have been identified and tests will be carried out to establish the effect on the underlying audio signal. Table 3.3 describes the parameters that will be changed in the optical cell and what attribute will be measured and investigated. A more detailed analysis of how each attribute will be measured, testing stimuli used and testing circuits are described in the following chapters.

| Parameter | Attribute Measured | Testing Stimuli |
|---|---|---|
| CdS LDR + EL Panel (Red, Green, Old Modelled) -With one panel at a time | - Resistance curve versus input level stimuli (using pink noise) <br> - Resistance curve versus frequency (using sine waves) <br> - LDR resistance oscillations (may relate to ripple modulation) <br> - Distortion characteristics at different amounts of compression <br> - Distortion during attack time frame <br> - Attack and Release characteristics + Memory effect <br> - El Panel colour shift with frequency <br> - El Panel frequency dependent brightness | -Broadband pink noise <br> -Band-limited pink noise (63 Hz Band and 1 kHz band) <br> -Sine waves with different frequencies <br> -Sine wave bursts with different mark/space ratios |
| CdSe LDR + EL Panel (Red, Green, Old Modelled) -With one panel at a time | | |
| CdS LDR + CdSe LDR in parallel + EL Panel -With one panel at a time | | |
| CdS LDR + CdSe LDR in series + EL Panel (Red and Green) -With one panel at a time | | |
| CdS LDR with reduced exposure area + EL Panel -Only with green panel | | |

**Table 3.3: Identified parameters and measurable attributes**

# 4   Testing Methodology

This chapter describes the proposed methodologies to test the optical cell parameters described above. In order to obtain useful data that can be identified as key information for a certain parameter, extensive testing has to be carried out which involves testing the different optical cells both in isolation and in conjunction with the rest of the circuit (forming a complete compressor). The testing strategy will focus mainly on objective measurements that will be able to provide empirical results which will be weighted quantitively between different built cells. Individual testing of the optical assemblies will be able to provide some static attributes that can be linked with the changes made to the optical cells and to further testing results. Additional in-circuit testing will also be carried out by using sine-bursts to help identify the differences created by the modified parameters. Depending on the magnitude of any identified differences, it could be possible to state what types of cells could be used for different audio sources in order to give a specific attack/release characteristic, THD characteristic or possible timbral changes. The timbre refers to the psychoacoustical perceived tone colour or quality of a musical note/piece of music. It is important to mention that even though the testing methodology carried out for all variations of cells will be identical, the results will not necessarily be used to compare cells one against the other, but will be used to point out what effect each modified parameter had on the audio stimuli.

## 4.1 Objective Testing

It is important to first test each cell individually, outside the full compressor circuit in which are placed. When tested in isolation, the cells can be characterised based solely on the modified parameters and static attributes like the resistance curves against input signal level can be plotted. Those curves can therefore be used to predict the behaviour of the cells when audio stimuli would be used and could also be used as a reference for any testing done on the whole compressor. Therefore, it is proposed that two different approaches are undertaken. The first approach is the individual testing of the cells which tests the behaviour of the LDR's resistance versus a known amount of audio stimuli input level. The second approach is to test the different cells in a complete compressor circuit.

### 4.1.1    Testing Optical Cells in Isolation

As mentioned in the previous chapter, the response characteristic of the LDR, which is responsible for the gain reduction non-linearity will be tested under different light sources. The individual testing of the optical cells is done under controlled light output. The attributes tested here are the variation of the output resistance at different illumination levels (represented by the different driving levels from an input signal) with different EL panel colours. To test these attributes according to the different identified parameters, two variations of an optical cell were built, each with a different modified parameter (either the LDR or the colour of the EL panel).

1. A CdS LDR with a changeable green/red/old EL panel + masking tape for exposure area reduction
2. A CdSe LDR with green/red/old EL panel + masking tape for exposure area reduction

The old EL panel reference from Figure 4.1 refers to the panel currently manufactured as a direct replacement for the one used in the old LA-2A compressor, which is manufactured solely in America.

These variations of photocells can be seen in Figure 4.1. To make testing easier with so many changing parameters, the two types of LDR were soldered to a PCB and a separate connection was provided for each of the panels for an easier change. The choice of building just two PCBs and have each LDR soldered to them was made to minimise any tolerance differences in LDRs if more than one from each type would have been used. This way, the findings are consistent throughout testing. Both PCBs were placed in a matt black-painted relay housing which served as a light-tight environment (much like a T4B cell).
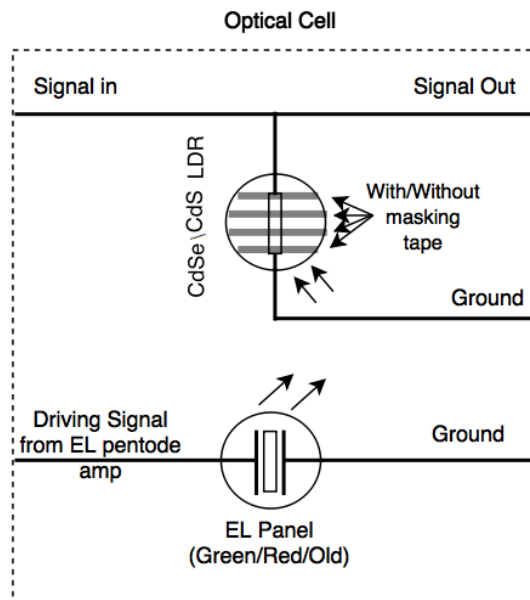


**Figure 4.1: Different optical cell's parameters**

To be able to test the cells with an EL panel (a high impedance device) a high voltage signal is required, obtainable only with a valve amplifier. Such a driving circuit for the EL panel is described in the next chapter.

Individual testing investigates the difference in resistance curves of the two LDRs when different light sources are used and is also looking into the reported colour shift and frequency dependent brightness of the EL Panel. The idea is to control the voltage and frequency that goes to the EL Panel's driver amp and ultimately to the panel itself and correlate them with the results. Therefore, any resulting difference in LDR's resistance at same driving level, but with varying frequency, would prove either the colour shift or the frequency dependent brightness. Testing involves using two different driving signals: sinewaves with different frequencies and also broadband and band-limited pink noise. Pink noise is used as it represents the closest emulation of a musical signal and also relates to the way humans hear by having equal energy per octave. (Foley, 2014).

For the fixed frequency stimuli, a high-performance signal generator is used in order to have complete control over the frequency and signal level. The generator connects to the EL driver amplifier and the output of the amplifier will pass through a DC blocking capacitor connected at the input of the optical cell. To compensate for any deficiencies in the EL driver amplifier, an oscilloscope monitors the amplified voltage on the EL panel and if there are any level changes due to any loading effects, the input is increased to compensate for the level loss. Therefore, what is tested here is the LDR's resistance at a particular frequency with the same voltage on the EL panel. This way, if any change in resistance values are identified, it is due to the frequency dependent brightness of the panel and a resistance curve for that particular LDR with that particular EL panel

colour can be plotted. Unfortunately, this test won't be able to tell if the difference is also attributed to the possible colour shift. Figure 4.2 shows the setup for this test.
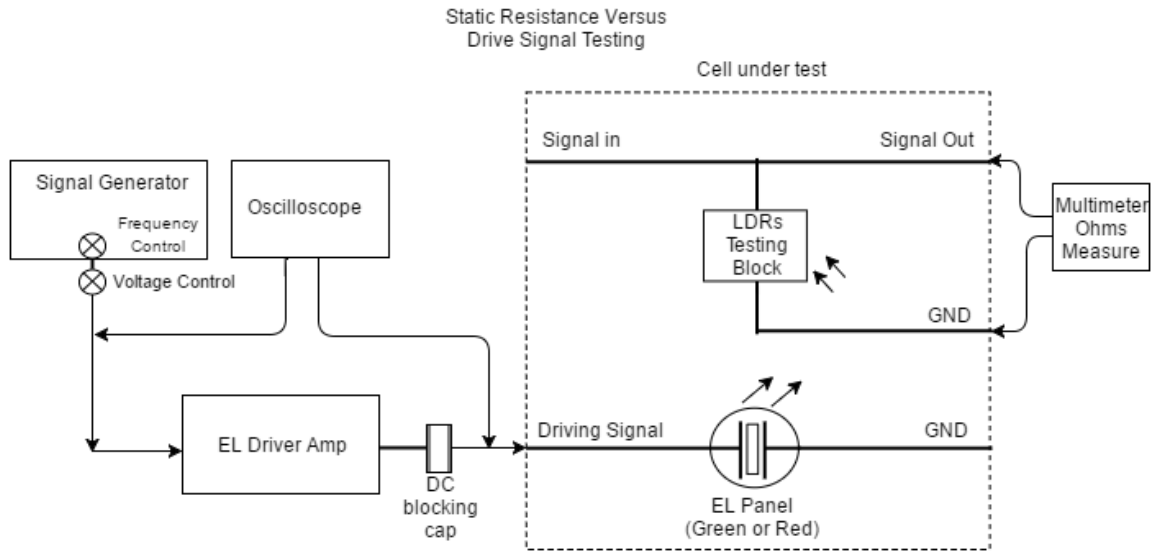


**Figure 4.2: Measurement setup for output resistance with sinewave input**

For pink noise testing, three different pink noise stimuli are pre-rendered in MatLab: Broadband/63 Hz Band/1 kHz Band, each of them with multiple output levels (+4 dBu, +2 dBu, 0 dBu, -3 dBu, -5 dBu, -7 dBu, -9 dBu, -11 dBu, -13 dBu). The processed files are saved as .wav files to be played-back from the laptop through a high-performance digital to analogue converter. The gain of the converter is set to a maximum value so that its output is exactly at the same level of the processed files. The test setup can be seen in Figure 4.3.
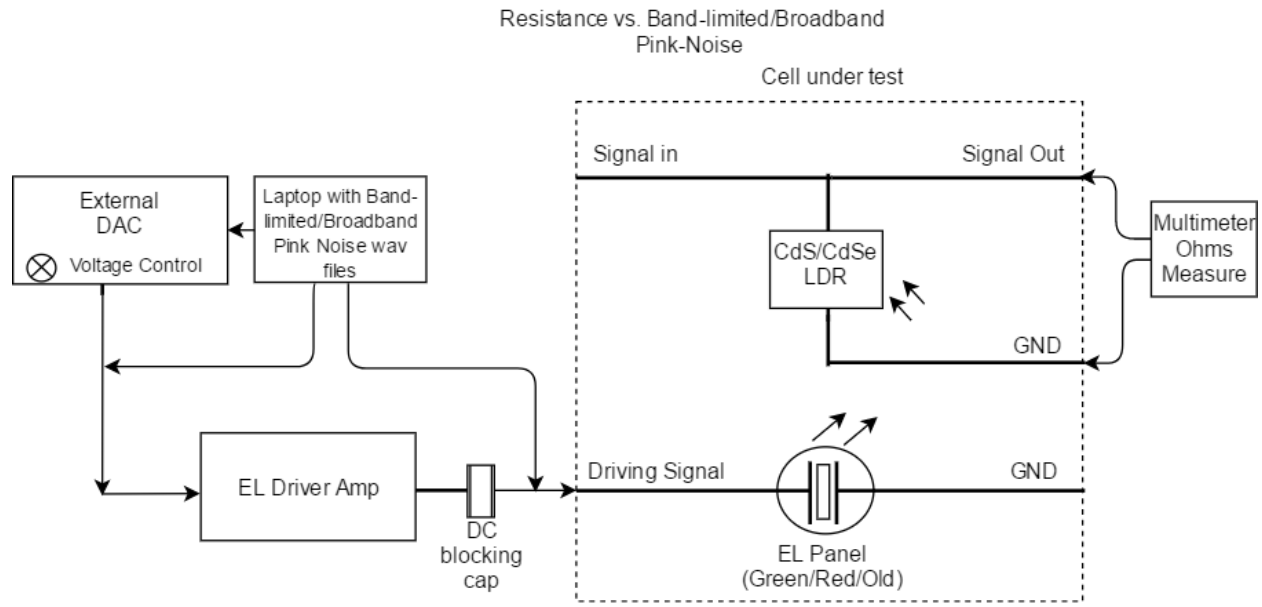
**Figure 4.3: Measurement setup of resistance output with pink noise stimuli**

By using broadband pink noise, a musical signal can be emulated, thus a resistance curve of the LDR can be plotted which can be closely matched to how the optical cell would react to a musical signal. Also, by using different input signal levels, a resistance versus input level curve can be plotted.

The masking tape described in Figure 4.1 will be used to reduce the LDR's exposure area and some of the mentioned tests will be run again. What will be investigated with the reduced exposure area is the resistance curve, to assess whether the slope of the curve changed or remained constant (it is expected to see elevated resistance values due to the lower exposed area, but the resistance slope should in theory be the same). Moreover, attack and release characteristics will be measured, as a change in resistance curve could produce a change in attack and release times.

4.1.2    Testing Optical Cells in the Compression Circuit

Testing the optical cells alone can help determine the static characteristics for that particular configuration and how it reacts to certain stimuli in terms of the resistance drop, but it is not actually helping to determine how a stimuli waveform could be influenced in terms of the attack/release envelope, frequency spectrum and THD. To fully characterise each type of optical cell along with its modified parameters it is necessary to have a fully working compressor circuit in which the cell can be placed. This way, tone bursts can be used and the output of the compressor recorded as audio files to be post-processed and analysed using tools such as the MIRToolbox (Lartillot, 2014). The tone burst is a fast change in an audio waveform, from a very low amplitude level to a high amplitude level. A tone burst can be compared to a transient signal and can be used to emulate a transient signal, but with a slightly longer duration and a known frequency.

Attack and release times can be measured for different tone bursts (different mark-space ratio) to evaluate differences between cells and to assess whether there is any memory effect or not. To do this kind of measurements precisely, the compressed output waveform has to be recorded on the oscilloscope, and by using time division cursors, the attack and release can be measured. If there is any memory effect, after a long compression time the release should be slower. Similar, depending on the mark time, the attack can be faster or slower (depending if the compressor was allowed to fully recover). These measurements can also give an indication of a two-staged attack.

THD during compression and release is another good indication of difference between cells. The problem is that equipment can't measure THD only during a specific time frame, so the output waveform has to be recorded on the computer and then the data has to be post-processed. Tone bursts will be used again, and to properly assess the THD, it is important to have multiple

tone bursts with different mark-space ratios. The space times chosen are 1, 2, 3 and 4 seconds, while the mark times are 250, 500, 750 and 1000ms. Tone bursts will have a combination of each space and mark. The envelope of the recorded outputs can also be used to assess memory effect. Using the MIRToolbox, information such as frequency content can be plotted during the compression and release time-frames in order to evaluate whether there are any spectral differences, and if there are, at what frequencies. Centroid measurements could also be taken to determine if there are any differences in the frequency registers between different audio stimuli, as it is a direct measurement of concentration of energies at particular frequencies, as noted by Lartillot (2017).

THD can also be measured at the compressor's output, while it is compressing at a certain amount of gain reduction. This measurement is relevant, as the compressor spends most of its time compressing, and effectively most of the THD will result from there, as opposed to the THD during attack which is supposed to be greater, but it is for a much shorter period of time. This THD measurement will be done using a +4 dBu signal and a dScope Audio Analyser.

Figure 4.4 describes the test setup for these measurements.
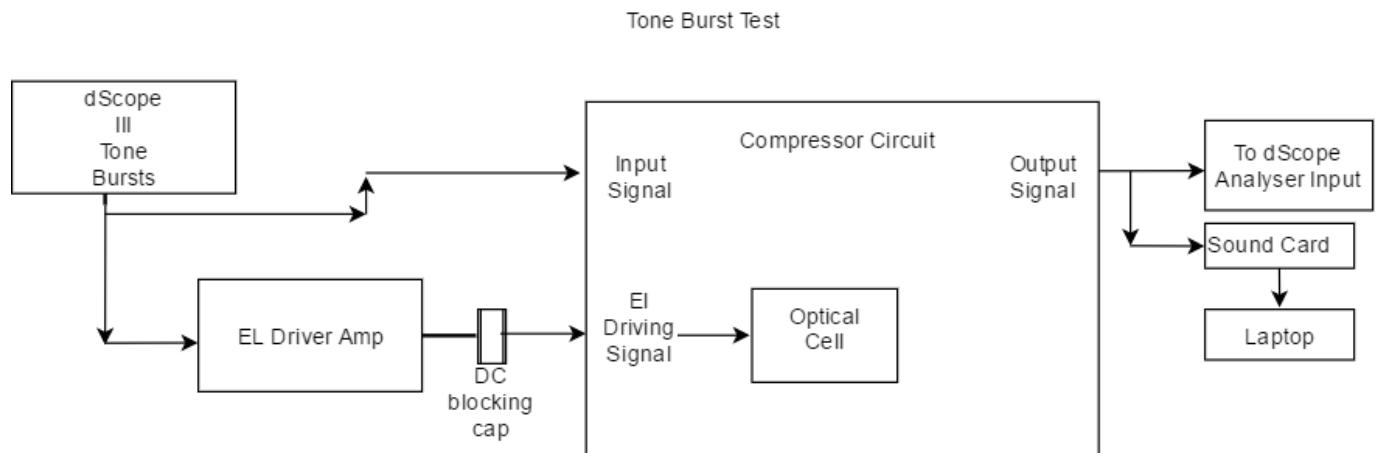


**Figure 4.4: Setup for recording the tone bursts**

# 5 Testing Circuits

## 5.1 EL Driver Amplifier

The EL panel is a high voltage low impedance device that requires around 60V RMS to operate efficiently. To get that amount of voltage amplification of the input signal, two methods were identified, but only one offered the best performance possible. The first method would employ the use of 2 series connected audio transformers on 1:10 ratio that would step-up the voltage by a factor of 100. The main disadvantage of using such a technique is the high voltage which may saturate the transformers and the difficulty of impedance matching between the two which may alter the frequency response. In order to avoid introducing components that may affect the input signal fidelity, a valve-based design was decided upon. To simplify the design and ensure no performance issues for the EL panel driver, its circuit was taken from the LA-2A compressor and replicated with slight tweaks. For purposes of safety, the power supply driving the valves and the amplifier circuit have been designed on separate boards and housed in the same enclosure.

### 5.1.1  Driving Circuit Stage

The driving circuit works by taking an input on the grid of one of the triodes (half of the 12AX7) which is adjustable with a potentiometer. The triode is a diode with 3 electrodes (the diode just has 2) with the extra electrode being called the "the grid" and was developed to be used as an amplification device (Lesurf, n/a).

 The signal input is used to control the amount of signal that goes to the amplification stage, thus the potentiometer (R5) acts as the compressor's threshold. The two triodes' grids are connected together through a 1 kΩ (R10) resistor. Both triodes work under the same quiescent conditions as both cathodes (V2 Pin 3 and 8) and anodes (V2 Pin 6 and 1) are tied together. The 12AX7 valve

acts as a voltage preamplifier for the driver pentode (V1). The gain of the first stage is set by the resistor on the cathode (R7). In order to provide more gain at audio frequencies the resistor is bypassed by using the two capacitors C5 and C6 in parallel. The amplified voltage is further taken to the driving pentode through capacitor C4 thus AC coupling the two stages. R9 is used to tweak the amount of voltage that goes to the grid of the pentode (V1). Just like with the previous stage the gain is set by the cathode resistor R4 bypassed by capacitor C3. Moreover, the pentode provides the necessary current (though small) to drive the El panel. The circuit is taken from the Tektronix LA-2A compressor.
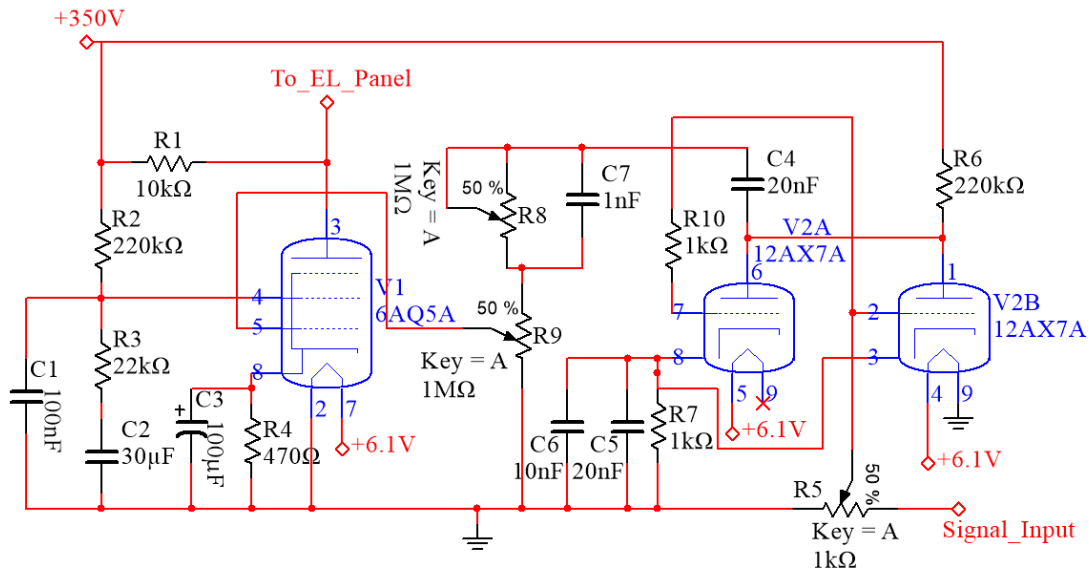


**Figure 5.1: EL Panel driver amplifier**

## 5.1.2    Power Supply

The power supply uses a 100 VA transformer with a 250 V output and 2 x 6.3 V outputs. The fuse on the secondary is rated at 0.1 A fast blow to protect the circuits from any shorts. The main AC voltage is rectified through the full bridge rectifier (D1) which creates a DC voltage with ripple

which is smoothed by filtering capacitors (C2 and C10). The 4.7 kΩ (R6) resistor has a dual function: together with the 3 parallel capacitors (C11-C13) it creates a low pass filter for ripple attenuation and provides the necessary voltage drop, at a certain current, to lower the output voltage to get roughly the same voltages used in the original LA-2A driving circuit. The resistor was selected after the current pulled by the circuit was measured. Resistor R1 is used to discharge the filtering capacitors after the power supply is turned off.

The secondary windings providing a dual 6.3 V output are put in series and the output is rectified by the full bridge rectifier (D2) and then smoothed out by capacitor C14. The resistor (R7) in this part of the circuit also provides the same two functions: It creates a low-pass filter just before the regulator (U2) and also provides a voltage drop to lower the power dissipation on the regulator. The regulator provides a constant 6.1 V output, free of ripple, which is used to drive the heaters of the two valves ( V2 - Pins 5 and 4; V1 – Pin 7).
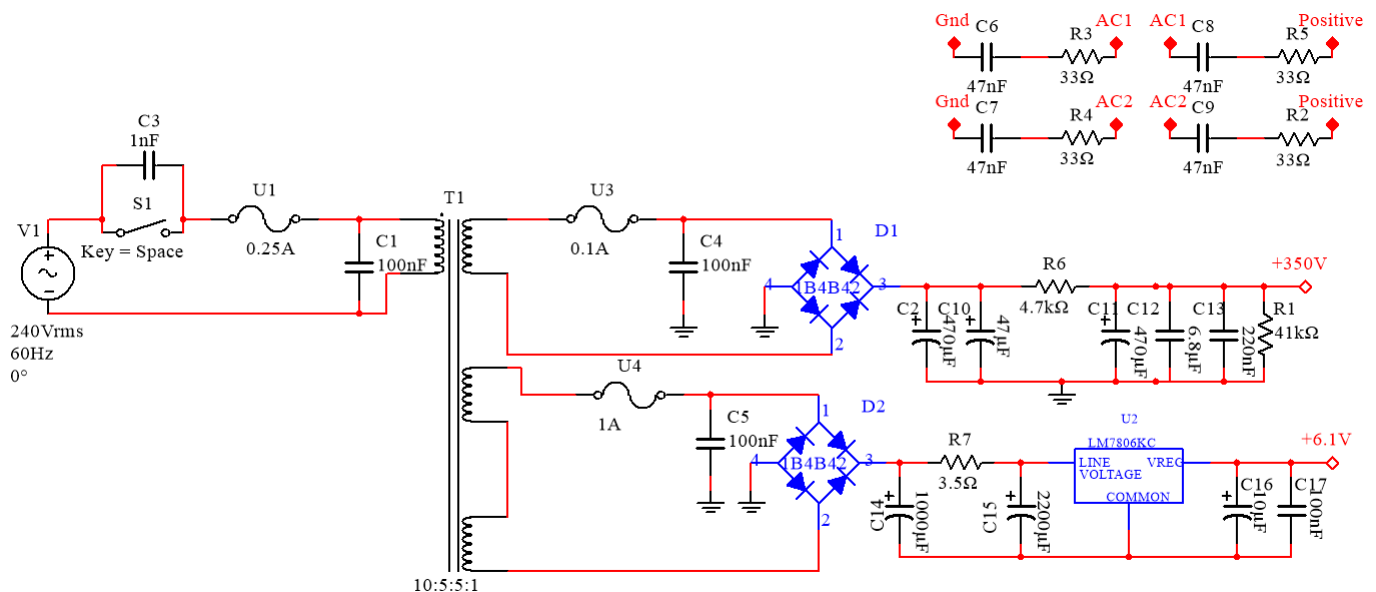


**Figure 5.2: Power supply for EL driver amplifier**

## 5.2 Full Compressor Circuit

The compressor circuit in Figure 5.3 was designed in order to be able to record the gain reduction characteristics of the optical cell and it is a modified version of the UREI LA4 compressor. It basically serves as an impedance buffer before and after the optical cell. The input stage (U1A) was designed to accept a balanced input with 20 kΩ differential input impedance (R1, R3, R4, R5). The balanced input is converted to single ended. The unbalanced signal is taken from the output of the U1A to the input of the EL driver amplifier. The optical cell was placed between U1A and U1B (NE5532 operational amplifiers). Depending on the strength of the signal and the threshold control (located on the EL driver amplifier) the EL will output more or less light, thus changing the resistance of the cell. Lower resistance results in more of the signal getting shunted to ground through the cell's internal LDR. The compressed/reduced signal is then sent through a unity gain buffer (U1B) and its output is further taken to the gain recovery stage (U2A). The gain recovery section comprises of an inverting operational amplifier with a potentiometer (Gain_Recovery) on the feedback path which can be adjusted to provide gain or unity amplification. The output of this stage is sent to the non-inverting input of U3A and the inverting input of U3B which will output two 180 degrees out of phase signals thus converting into a balanced output.
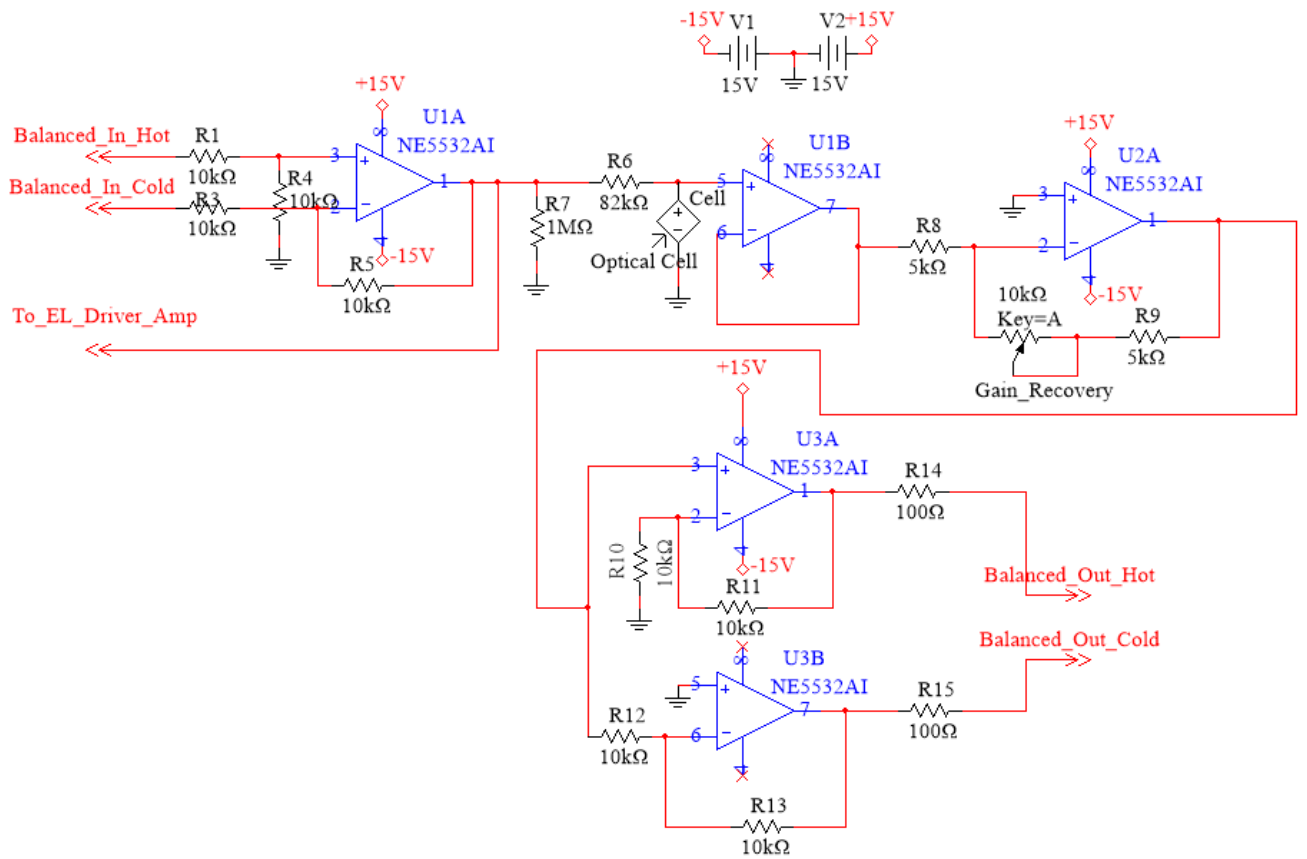
**Figure 5.3: Compressor circuit**

The designed circuits, though not complex, provide the necessary fundamental building blocks for a working optical compressor. Given the fact that the research is looking into identifying parameters of the optical cell that can be changed to provide a certain effect, any differences in the output of the audio waveform will be as a direct result of the modified cell and not of the compressor circuit. Therefore, it is not of interest the amount of noise or distortion the compressor circuit introduces and it is important to only achieve the gain reduction and have a mean of controlling this gain reduction.

# 6  Discussion of Results

## 6.1 Resistance curve versus input stimuli

It was suggested in the research chapter that the two different LDRs will have slightly different responses due to the nature of the material used as a conductor (CdS/CdSe), so the different EL panel colours should create a dissimilar resistance slope. Also, it was suggested that the panel's brightness will be dependent on the frequency applied and that there may also be a frequency dependent colour shift. These parameters have all been identified and confirmed by using the test setup from Figure 4.2 and Figure 4.3.

The first stimulus used was pink noise (broadband, 63 Hz band and 1 kHz band) at different input levels (-13 dBu, -11 dBu, -9 dBu, -7 dBu, -5 dBu, -3 dBu, 0 dBu, +2 dBu and +4 dBu) and the cell's resistance was measured with a digital multimeter, which recorded the data as CSV to be further processed and analysed in Excel.

### 6.1.1    BroadBand Pink Noise

Figure 6.1 and Figure 6.2 show the resistance values measured for different input levels. The optical assembly analysed had a CdSe LDR with three different light sources. Due to the poor resolution of the bottom curve with input levels from -7 dBu to 4 dBu the plot had to be split in two. Same input levels with all three panels means that the amplified voltage of the EL driver was the same across all panels. Even though in reality a sound engineer would adjust the input/threshold level for a certain gain reduction value, the result is meaningful because the resistance drop curve will stay the same. This means that even though he or she may reduce/increase the input level to get a certain amount of gain reduction, that input value will still be on the same resistance curve for that particular LDR + EL panel type combination. As a consequence, the gain reduction will

follow the resistance slope of a particular LDR and EL panel as it can be seen from the figures below. It can also be noted the low resistance value of the LDR when driven by the old modelled panel, which means that this panel is more efficient than the new ones and it does not require to be driven that hard by the amplifier to reach high gain reduction values. Moreover, what is more important is that at a low input level (-13 dBu) the CdSe has a lower resistance value when driven by the green panel and as the input level is increased its sensitivity increases in favour for the red panel. The CdSe used has its peak spectral response in the 690nm region, which is the wavelength of the red colour. It is therefore interesting to note that at a low input level, when the panel's brightness is very low, the CdSe LDR's sensitivity does not necessarily respond better to the red light. But as soon as the light level increases due to an increase in input, the resistance is lower in the presence of red light. Moreover, it could be argued that because the same LDR is used, then its attack time should be the same, but by looking at the graph there's a big difference in resistance between the CdSe Green and CdSe Red curves at -13 dBu. Therefore, if the input signal level would be -11 dBu, it would reach the respective resistance in different amounts of time.
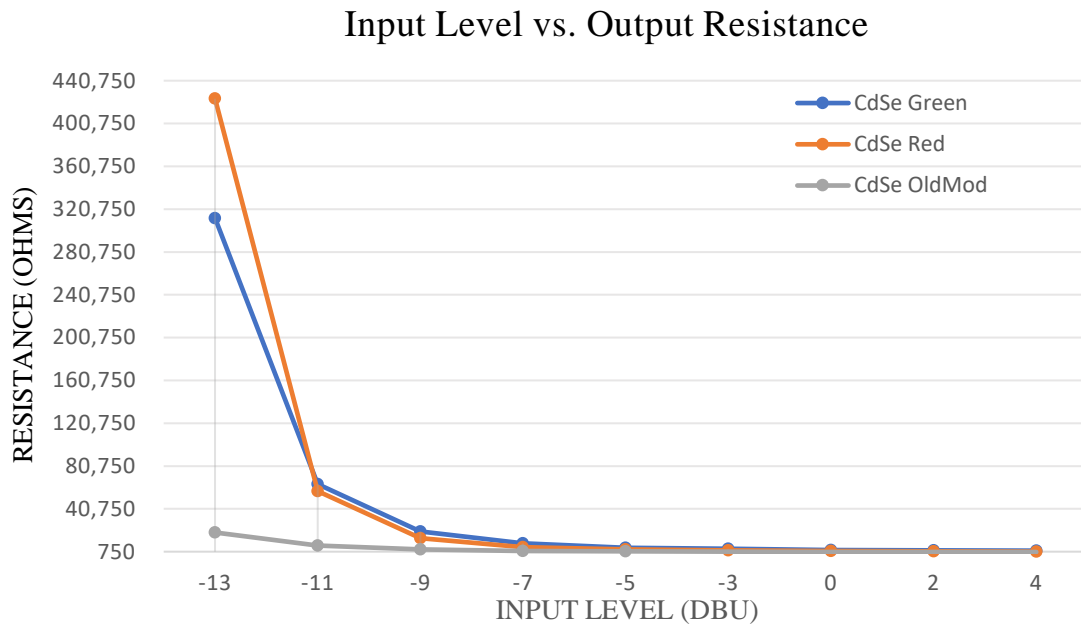
**Figure 6.1: Input Level versus Output Resistance for CdSe**
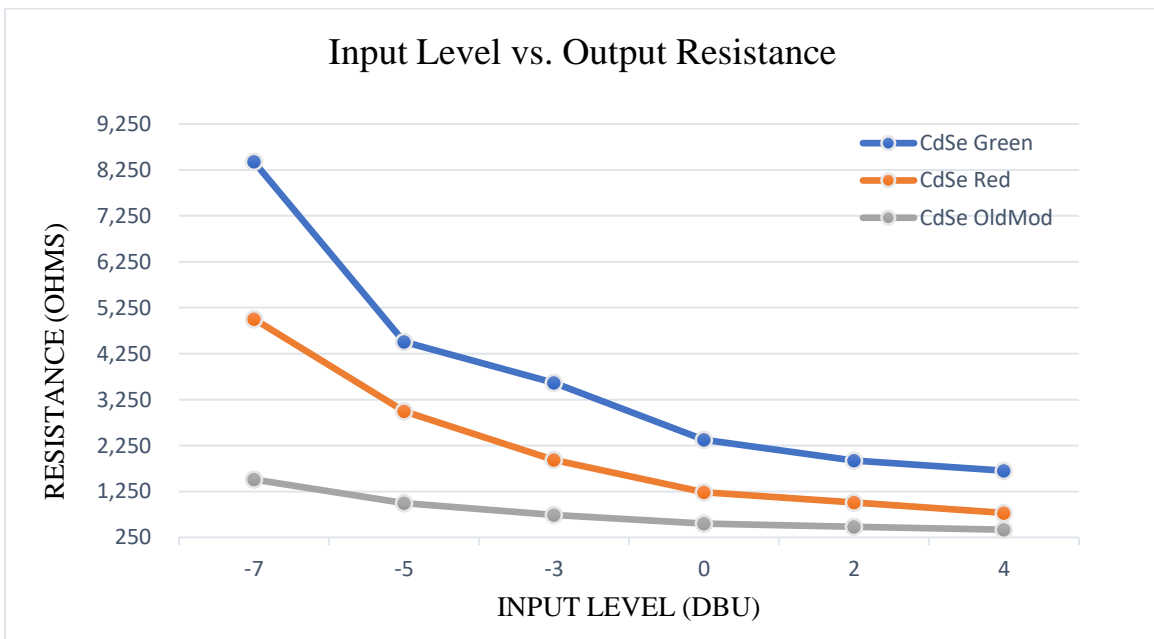


**Figure 6.2: Input Level and Output Resistance for CdSe (zoomed version)**

Figure 6.3 and Figure 6.4 represent the resistance curves at the same input levels for the optical cell containing a CdS LDR. Compared to the curves seen previously, it can be noted the fact that across all input levels the CdS LDR has a lower resistance when driven by the green panel. On the other hand, the figures show that for all input levels above -9 dBu, the CdS Red and CdS Green curves are much closer in resistance compared to the same two curves in the CdSe case (Figure 6.2). This means that with an increase in driving level (increase in brightness in El panel) the CdS LDR's spectral sensitivity decreases. To further show this difference, Table 6.1 contains the differences in resistance between the two curves (Green and Red) for each LDR type at each input level. Also, generally, the resistance values are lower for the CdS LDR with red and green panels at all driving levels compared to CdSe LDR. This could be due to the higher dark resistance of the CdSe.

Another interesting finding, according to the values processed in the table below, is the big difference with the CdS and CdSe between -11 dBu and -9 dBu. At -9 dBu the resultant difference between the two curves yields a resistance value of 1703 Ω for CdS and 6315 Ω for CdSe. Comparing these numbers to the values at the previous input level (-11 dBu) means that the slopes tend to get closer with increasing input levels, but in the case of the CdS there is a very abrupt drop in resultant resistance between -11 and -9 dBu. It has been discussed in Chapter 4 about the possibility to combine different LDRs and light sources to obtain new resistance curves. By taking into consideration the sudden drop in resultant resistance between the afore mentioned levels, which can lead to increase in THD and harsh sounding gain reduction, an optical cell with a combination of CdS LDR and both red and green EL panels would not be recommended.

By looking at the resistance curve with the old modelled EL panel it can be seen that it follows the same trend as the previous LDR, with much lower resistance values, due to its increased efficiency.

Also, as described in the methodology, a test with reduced LDR exposure area was carried out to determine the effects it may have on the resistance curve. It was found that, as expected, the resistance values across all input levels are more elevated (Figure 6.3 and Figure 6.4, yellow line), but as the input level is increased, the difference with the other curves starts decreasing. By analysing the resistance values for the -13 dBu and -11 dBu inputs, it can be noted a very abrupt decrease between these two input levels when compared to the same resistance values of the other curves. This suggests a different attack characteristic.

All the results discussed until now have been obtained by using broadband pink noise, therefore, there was no possible colour shift or increase in brightness as the pink noise contains all frequencies.

| Input Levels (dBu) | -13 | -11 | -9 | -7 | -5 | -3 | 0 | 2 | 4 |
|---|---|---|---|---|---|---|---|---|---|
| CdS(Red-Green) (ohms) | 17179 | 5630.5 | 1702 | 760.1 | 353.1 | 215.1 | 140.7 | 162 | 131 |
| CdSe(Red-Green) (ohms) | 111608 | 6774.5 | 6315 | 3421.2 | 1512.5 | 1675.7 | 1148 | 911 | 918 |
| Total Difference | 94429.1 | 1144.1 | 4612 | 2661.1 | 1159.4 | 1460.6 | 1007 | 749 | 787 |

**Table 6.1: Resistance difference between cells at different input levels**
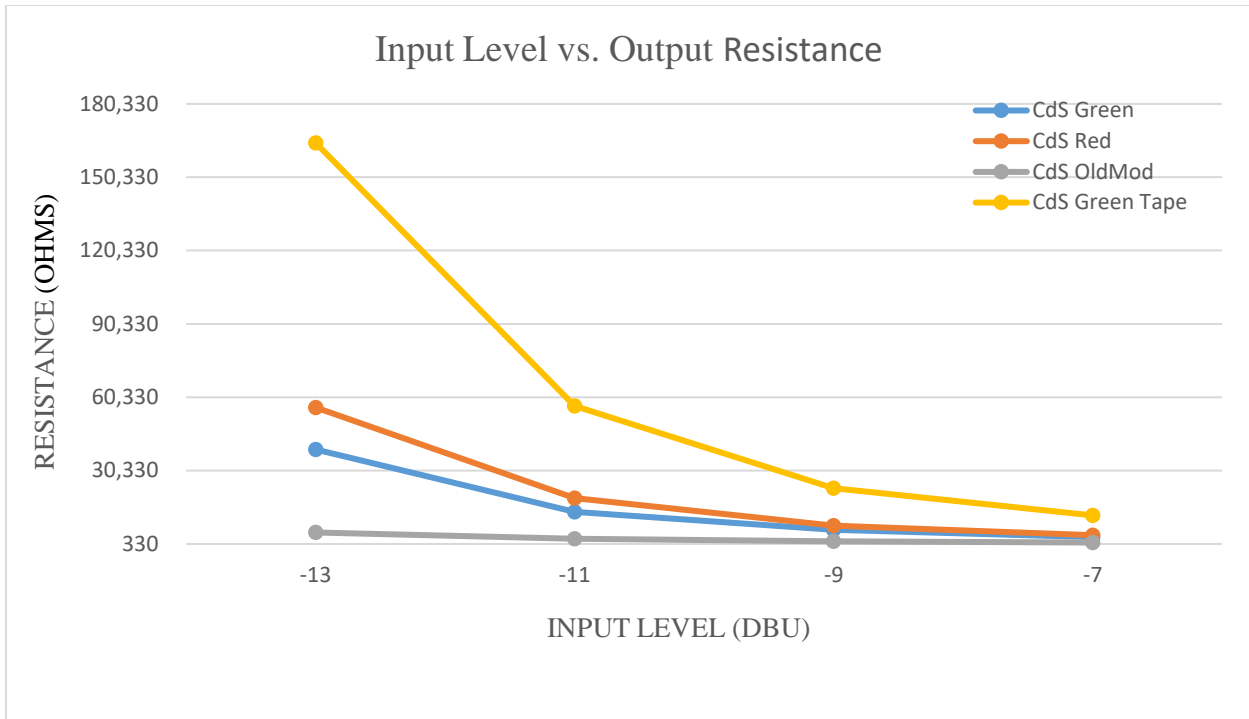
**Figure 6.3: Input Level and Output Resistance for CdS (-13 dBu to -7 dBu)**
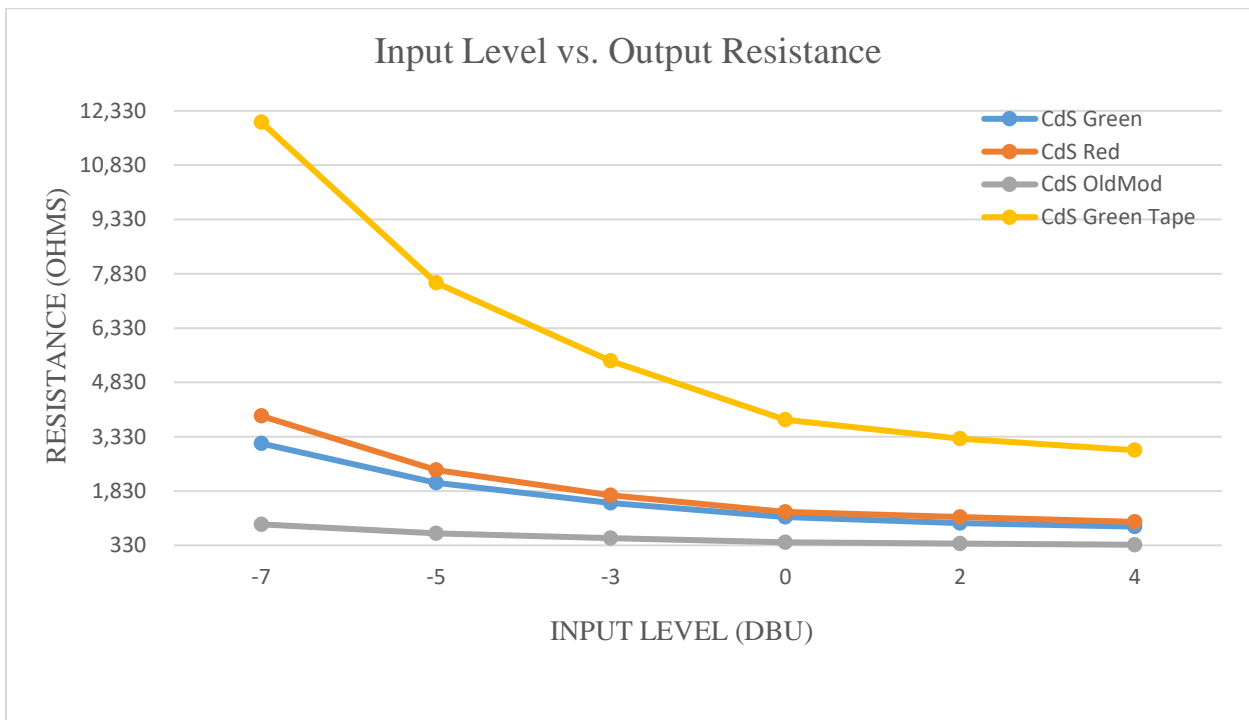


**Figure 6.4: Input Level and Output Resistance for CdS (-7 dBu to 4 dBu)**

72

The following results were obtained throughout the same testing procedure as above, but band limited pink noise was used to test for any colour shift or frequency dependent brightness. Two bands were used in this test: 1 kHz and 63 Hz.

6.1.2   1 kHz Band Pink Noise

Figure 6.5 shows the resistance curves for the different input levels of the 1 kHz band-limited pink noise. Compared to Figure 6.3 it can be noted the lower resistance values for CdS Red and CdS Green. Further processing of the data (Table 6.2) showed that the two curves are almost superimposed starting with -9 dBu input level. This indicates that there is indeed a frequency dependent brightness element for the EL panel.

| Input Level (dBu) | -13 | -11 | -9 | -7 | -5 | -3 | 0 | 2 | 4 |
|---|---|---|---|---|---|---|---|---|---|
| CdS (Red-Green) (ohms) | 11378 | 1556 | 301 | 111 | 59 | 66 | 57 | 60 | 50 |

**Table 6.2: Input Level versus Ouput Resistance difference (CdS Red – CdS Green)**

Like in the previous measurements, biggest difference between the two curves is at -13 dBu.
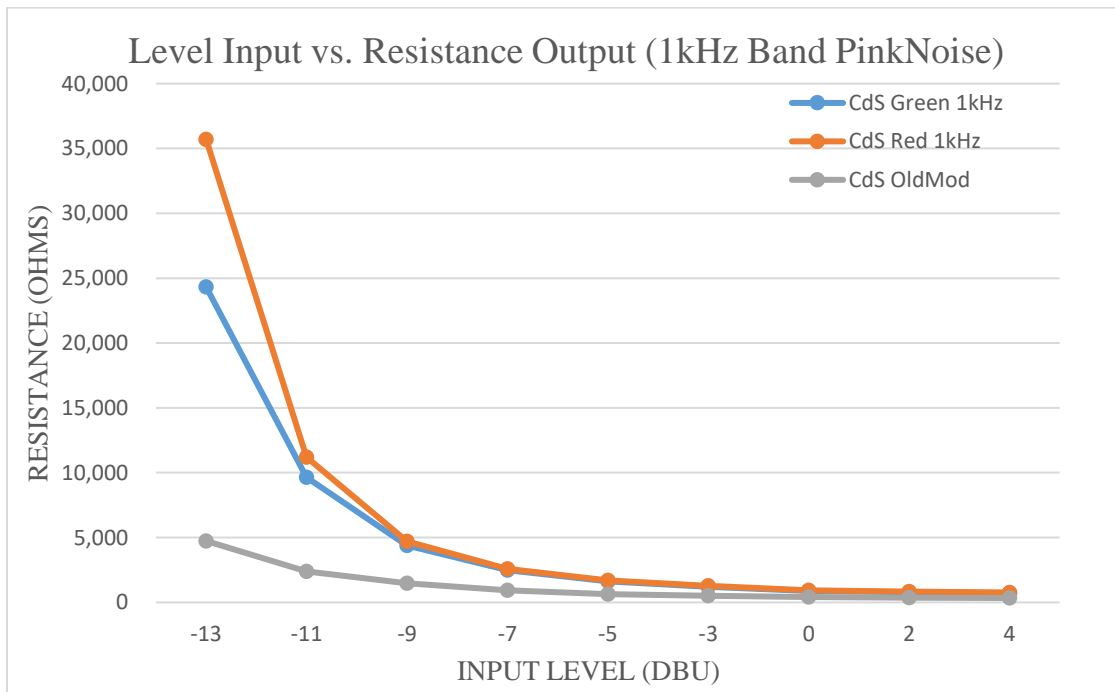


**Figure 6.5: Input Level and Output Resistance for CdS with 1 kHz Band PinkNoise**

### 6.1.3    63 Hz Band Pink Noise

An interesting result was obtained when 63 Hz bandlimited pink noise was used (Figure 6.6). The presence of the frequency dependent brightness is obvious by comparing the resistance values obtained with the old modelled panel with the ones obtained in Figure 6.5, but it did not explain at first why there was such a big resistance difference. Further testing, conducted in a dark room, revealed that the old modelled EL panel, apart from the frequency dependent brightness, also had a colour shift. Further experiments showed that below 100 Hz, the panel's colour was light green and with increasing frequency it changed to violet up to almost blue (around 2 kHz). It seems that the change in manufacturing process between the two panels (old and modern) fixed this occurrence. Compressors such as the LA-2A that use this kind of old panel in the optical cell are therefore "affected" by this colour shift.

Table 6.3 shows that with low frequencies (the 63 Hz band pink noise) there is an increase in difference between resistance curve values at -13 dBu. An explanation would be that at low input levels, with low frequencies, where brightness is low, the colour dominates the response of the LDR. Also, according to the graph in Figure 6.6, there is a small decrease in resistance from -13 dBu to -11 dBu for the CdS Green curve, while then the resistance drops more abruptly at -9 dBu. At the rest of the input levels there is a constant exponential decrease. The sudden decrease between -11 and -9 dBu could be caused by the increase in brightness, which starts dominating the LDR's response above a certain value. On the other hand, below that certain value, the spectral response could be more sensitive to the light's colour.

| Input Level (dBu) | -13 | -11 | -9 | -7 | -5 | -3 | 0 | 2 | 4 |
|---|---|---|---|---|---|---|---|---|---|
| CdS(Red-Green) (ohms) | 94110 | 14945 | 724 | 863 | 747 | 534 | 512 | 569 | 732 |

**Table 6.3: Input Level versus Ouput Resistance difference (CdS Red – CdS Green) at 63 Hz**
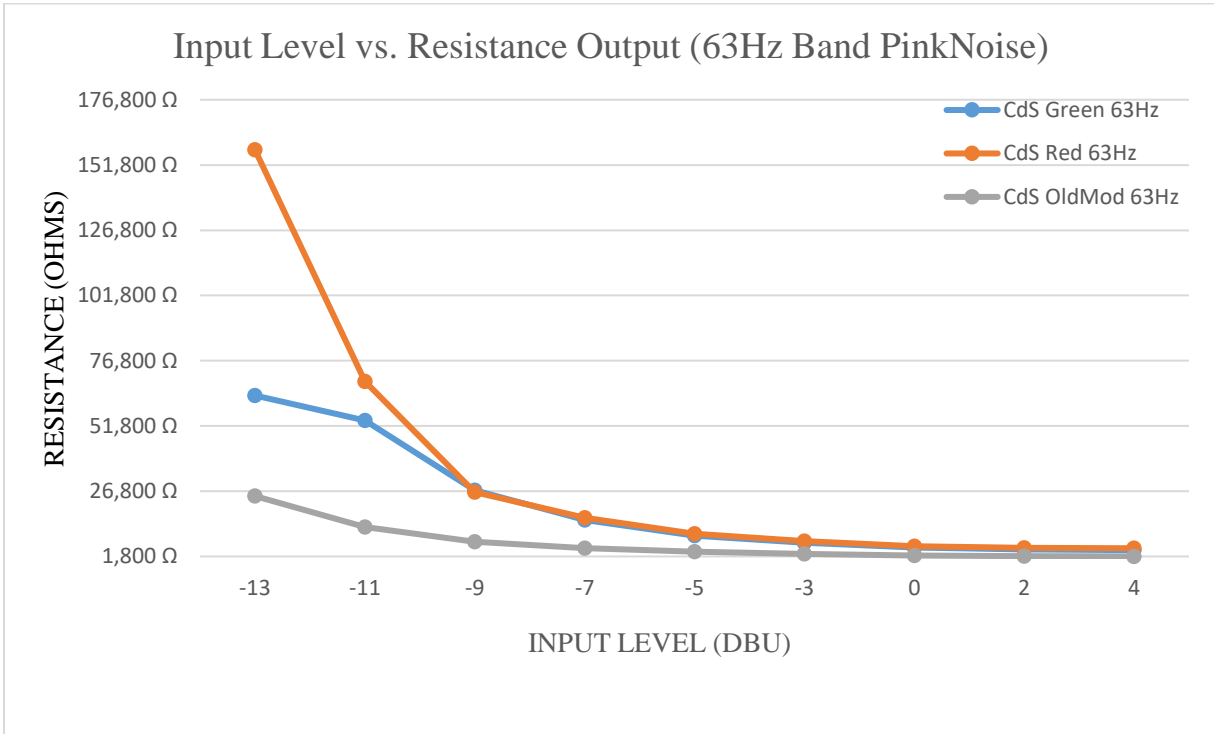


**Figure 6.6: Input Level versus Output Resistance for CdS with 63 Hz Band PinkNoise**

6.1.4    Resistance Output Histogram

An interesting behaviour that was observed during testing with pink noise was that the resistance measured was not constant and was oscillating. Therefore, all the calculated values in the figures above represent the average measured resistance. When plotted as a histogram (Figure 6.7), the measurements show a minimum and maximum deviation of +/- 1.5 kΩ, which in the context of high resistance values (low input levels) won't be able to cause any gain reduction errors.
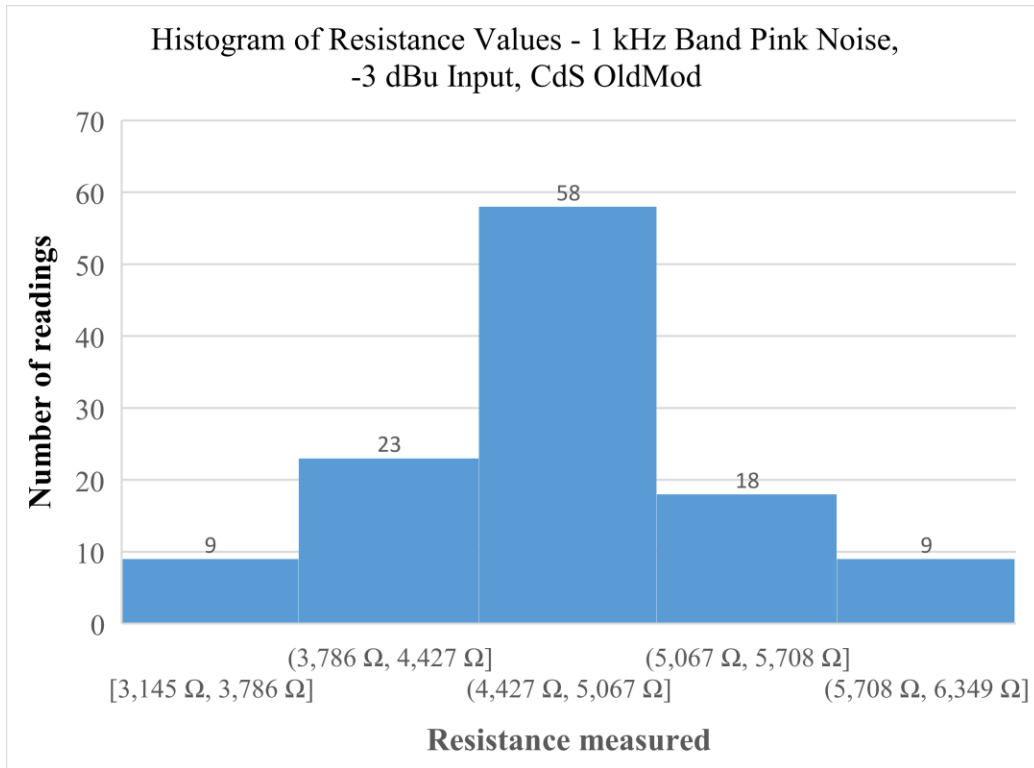
**Figure 6.7: Histogram of Resistance Values**

The problem is that when the input levels are high and the output resistance is low, any kind of deviation in the 1 kΩ range could cause noticeable oscillations of the gain reduction. The problem faced here is that most audio compressors have either analogue VU meters or LED based meters with RMS indication, therefore such oscillations will be averaged with the gain reduction level and can't be spotted. Further testing with the oscilloscope revealed these oscillations. Moreover, they were also present on the recorded audio waveform. Further frequency domain analysis also revealed elevated high-frequency content which may have been caused by these oscillations.

6.1.5    Testing with Sinewaves (40 Hz – 20 kHz)

The next test procedure is almost similar with the one above, but instead of pink noise, sinewaves were used. This test was mainly carried out to show the effect of EL panel frequency dependent brightness on the output resistance. It can also can be used to create resistance curves

for the different combined parameters (EL panel and LDR). Testing used the same set-up as for the pink noise tests, but the input was slightly adjusted for each frequency to compensate for the loading effects of the panel. The purpose of adjusting the input level was to keep the amplified voltage on the EL panel constant (50 V RMS). Moreover, each measurement was repeated twice to make sure the values measured are consistent.

Figure 6.8 shows the resulting curves. This test procedure clearly shows the increase in brightness with increasing frequency, hence the decrease in output resistance. The curves for the CdSe Red and Green seem to be consistent in terms of the relation of one against the other with the curves in Figure 6.1 and Figure 6.2. The resistance values of the CdSe driven by a red panel are higher than the resistance values of the same LDR driven by a green panel for frequencies up to 200 Hz. Above this frequency, the resistance drops more when the LDR is driven by the red panel. Both panels output the same amount of light level (verified with a LUX meter), both are driven by the same voltage, but it seems that with increasing brightness (due to frequency increase) the CdSe achieves lower resistance levels when driven by the red panel, which can only mean that its spectral sensitivity started to have a more noticeable effect. This is not the case for the CdS LDR, which when driven by the green panel has a lower overall resistance, meaning that its green sensitivity has an effect from the beginning. What can be observed thought, with the CdS LDR, is that above 2 kHz the two curves are almost overlaid (with green and red EL panel). Figure 6.9 shows a zoomed version of Figure 6.8 above 1 kHz. In the case of the CdSe, there is a difference between the two curves across all frequencies, but tends to decrease above 10 kHz.

The increased efficiency of the old modelled EL panel can also be seen Figure 6.8. The resistance of the CdSe at 40 Hz when driven by this type of panel is almost ten times lower than when driven by the other two panels, therefore a direct comparison cannot be established. On the

77

other hand, when comparing the two curves for the CdS and CdSe (both driven by the old modelled panel), a difference in resistance can be noticed from 40 Hz up to 1 kHz. Above 2 kHz, the two resistance curves are completely overlaid. The most noticeable differences between them are at 40 and 60 Hz. As mentioned earlier, the old modelled panel emits a light green colour below 100 Hz and above this frequency the colour shifts towards a violet/blue colour. As a result, the differences between the two LDRs at 40 and 60 Hz could be due to the green colour emitted by the panel (affecting the CdS more). Also, at these low frequencies, where light levels are lower (no brightness increase factor), the difference in resistance could also be explained by the increased dark resistance of CdSe cell. This can result in a general elevated resistance curve after initial exposure to light compared to the CdS (something like the values described in Figure 3.6).

Just like with the previous measurements, a CdS with reduce exposure area was used for testing (Cds_Green_Tape). As expected, the resistance curve has higher values compared to the uncovered CdS LDR (driven by red or green panels), but lower than the two CdSe curves. This result can prove useful as:

1. The elevated resistance values could allow for more dynamic range to be used with the threshold control (less sensitive), thus allowing for finer adjustments of gain reduction.

2. The curve has a smooth exponential decrease in resistance, with no abrupt changes in values, which may give a more natural sounding tone during gain reduction.
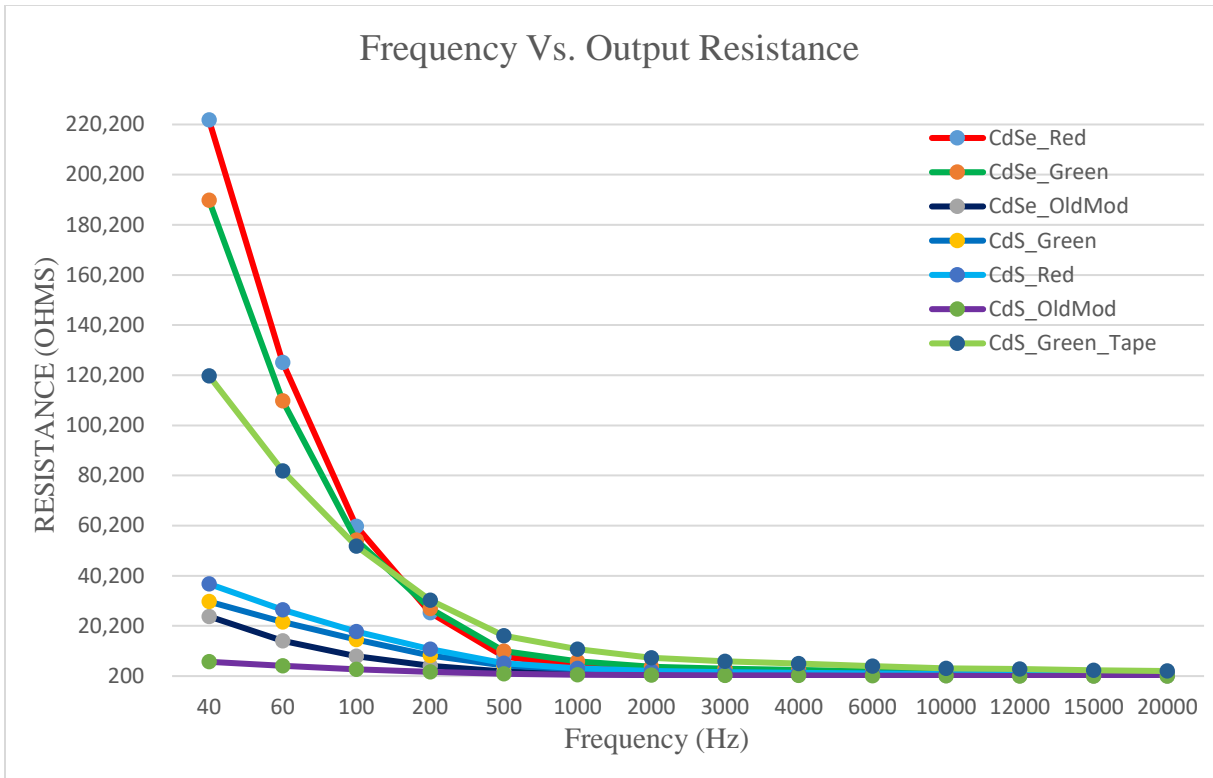
**Figure 6.8: Overall Frequency versus Resistance curves for CdS and CdSe (40 Hz – 20 kHz)**
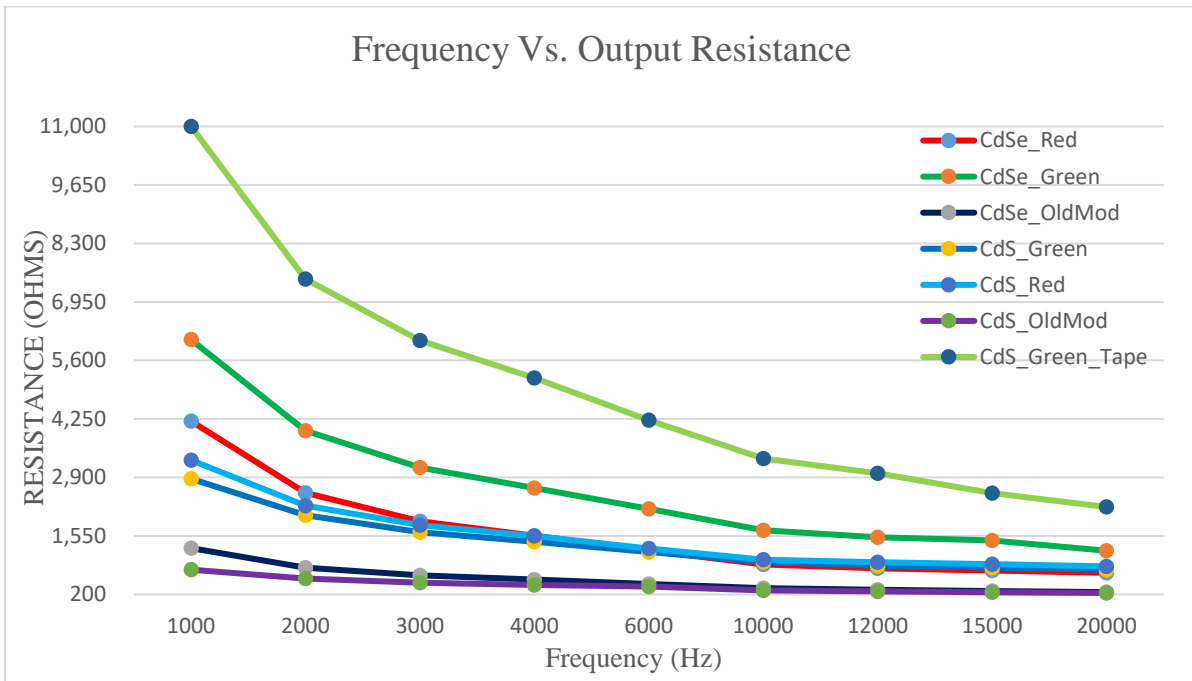


**Figure 6.9: Overall Frequency versus Resistance curves for CdS and CdSe (1 kHz – 20 kHz)**

Table 6.4 shows the difference, as a dB ratio, between the resistance values of each curve at 100 Hz and 1 kHz compared to the values of the CdS LDR driven by green panel (used as the reference value in the dB conversion).

| dB Ratio (@ 1 kHz) compared to CdS_Green | | | | | | |
|---|---|---|---|---|---|---|
| CdS_G | CdS_R | CdS_GTape | CdS_OM | CdSe_G | CdSe_R | CdSe_OM |
| 0 dB | 1.21 dB | 11.67 dB | -11.41 dB | 6.52 dB | 3.31 dB | -7.08 dB |

| dB Ratio (@ 100 Hz) compared to CdS_Green | | | | | | |
|---|---|---|---|---|---|---|
| CdS_G | CdS_R | CdS_GTape | CdS_OM | CdSe_G | CdSe_R | CdSe_OM |
| 0 dB | 1.68 dB | 10.94 dB | -14.04 dB | 11.35 dB | 12.19 dB | -5.23 dB |

**Table 6.4: Resistance difference as dB Ratios at 1 kHz and 100 Hz**

It was proposed in Chapter 3 that it is possible to obtain different resistance curves when pairing a CdS with a CdSe in either series or parallel combinations. As values were measured individually for each LDR with all three EL panels, Excel was used to mathematically post-process these values and obtain the equivalent curves for any parallel or series combination. Figure 6.10 and Figure 6.11 show the results obtained. Figure 6.12 presents all the previously measured curves for an overall comparison.
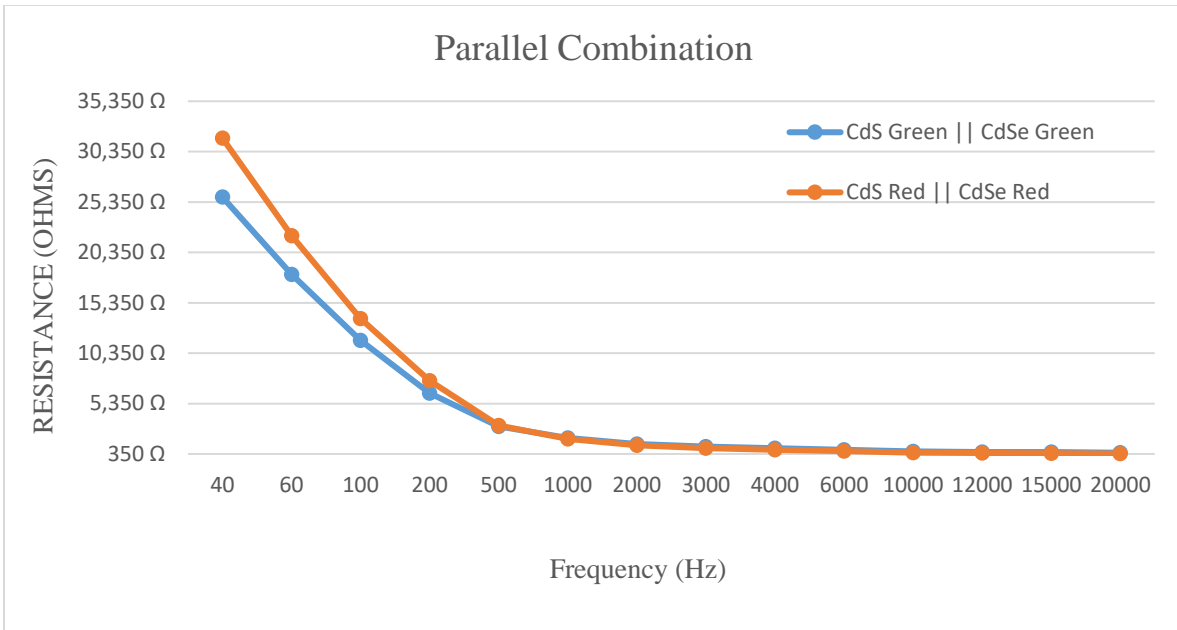
**Figure 6.10: CdS Parallel Combination**
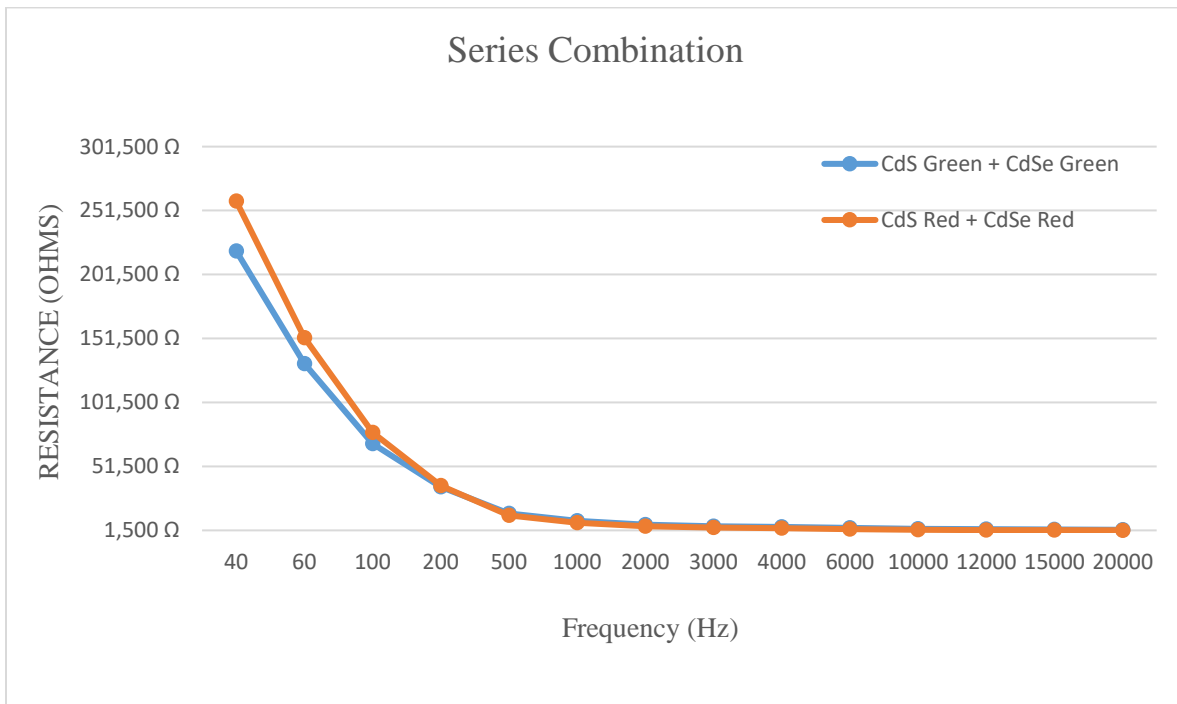


**Figure 6.11: CdS Series Combination**
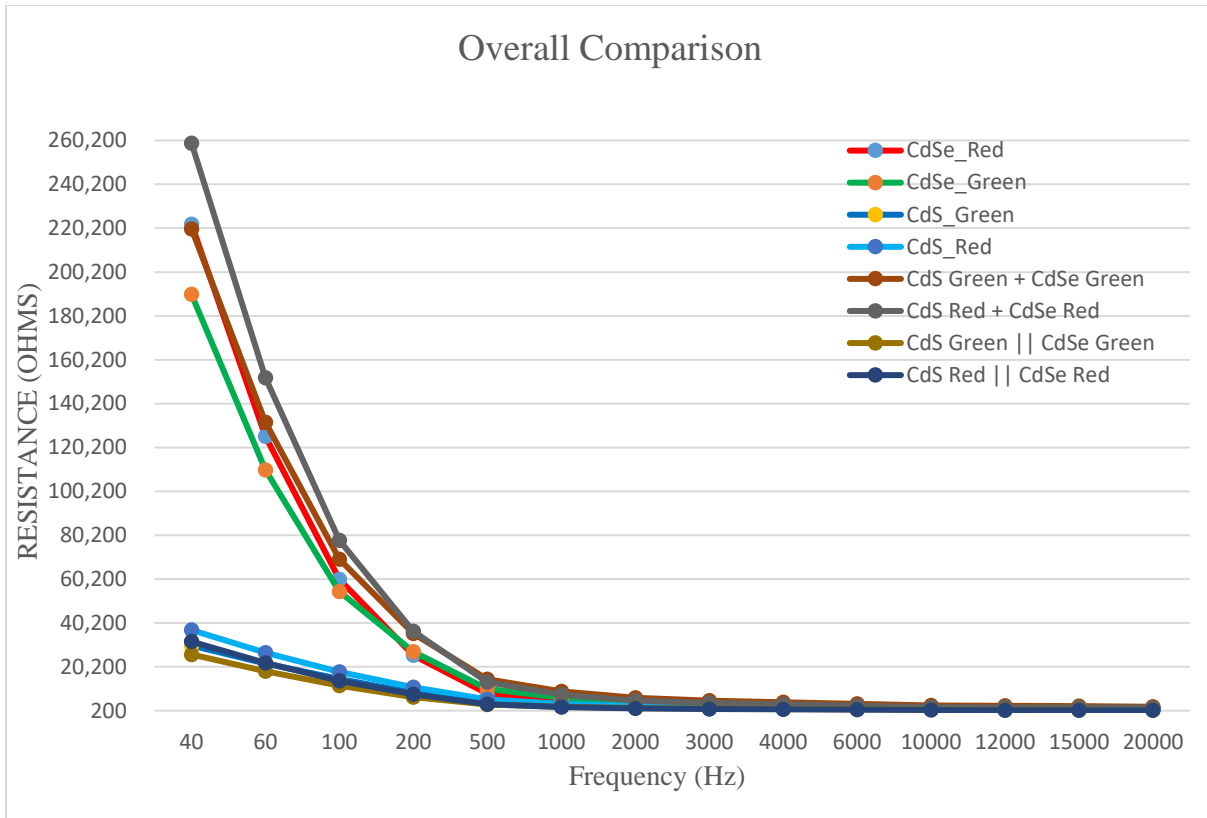
**Figure 6.12: Resistance Curves - Overall Comparison**

The difference between series/parallel combination of the LDRs coupled with different light sources is theoretically not enough to create any perceived difference in compression, but some curves tend to have a smoother exponential decay. Tests could be further undertaken to verify if they do have any musical effect during gain reduction, but these tests are outside the scope of this research.

## 6.2 LDR Resistance Oscillations

The oscillations in resistance were observed when using both pink noise and sinewaves stimuli. As mentioned earlier, further tests were undertaken to identify whether these oscillations in resistance could have any effect over the used stimuli. Figure 6.13 and Figure 6.14 show a sinewave under constant compression. The threshold of the compressor was adjusted to give 10 dB of gain reduction and the reduced amplitude of the sinewave was measured on an oscilloscope. To be able to record any possible oscillations, the persistence mode was turned on. Figure 6.13 represents the CdS LDR driven by a green panel. The orange waveform is the sinewave and the other trace underneath represents the persistence. As it can be seen, the peaks are not constant over time and there are also some noise spikes, possibly due to the resistance variation or internal LDR imperfections.
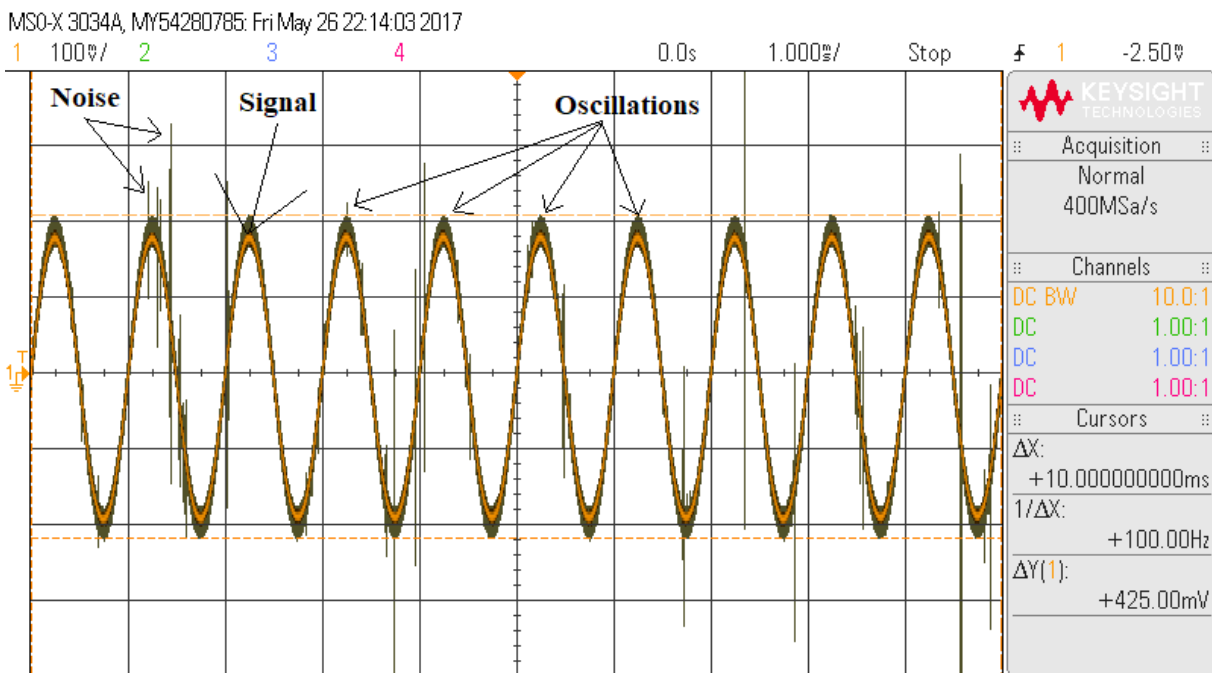


Orange Waveform - Measured Signal
Green Waveform - Oscillations of the signal observed in Persistance Mode.

**Figure 6.13: Oscillations of the CdS LDR + Green El Panel**

Figure 6.14 represents the CdSe LDR driven by a green EL panel. In this situation, the oscillations are worse than previously measured with the CdS. The same noise spikes are also present. Again, the orange waveform represents the measured signal and the other waveforms represent the oscillations which can only be caught in persistence mode, but because they appear and disappear very fast, it should not have any noticeable impact on a musical signal. Although, with age, the LDR may degrade further and these oscillations could be responsible for the ripple modulation (present for example in the LA-2A) mentioned by Moore, Till and Wakefield (2016)

While measuring the Total Harmonic Distortion and Noise (THD+N) of the compression circuit under different gain reduction values, an increase in upper harmonics was identified, which could be due to these noise spikes. The next chapter discusses the results from FFT measurements for the optical cells under different gain reduction values.



**Figure 6.14: Oscillations of the CdSe LDR + Green El Panel**

## 6.3 FFT Analysis

To further investigate the oscillations and noise spikes identified on the time domain measurement, an FFT analysis was used (4096 points, Prism maximum dynamic range window). In order to capture the effects compression has on the signal, FFT was also used to measure the output spectrum of the compressor without any gain reduction applied, with and without an optical cell connected. In theory, the optical cell is just a variable resistor to ground, therefore the difference should be small to none in terms of FFT analysis when it is not connected. Through the use of FFT, the THD+N of the output signal can be measured and any differences, if any, between the optical cells can be further identified. Figure 6.15 shows the output spectrum of the compressor without any optical cell connected. No relevant problems can be identified in the FFT, so the compressor circuit itself it's not introducing any unwanted artefacts. Therefore, any differences that will show up in testing will be mainly due to any of the optical cells used.
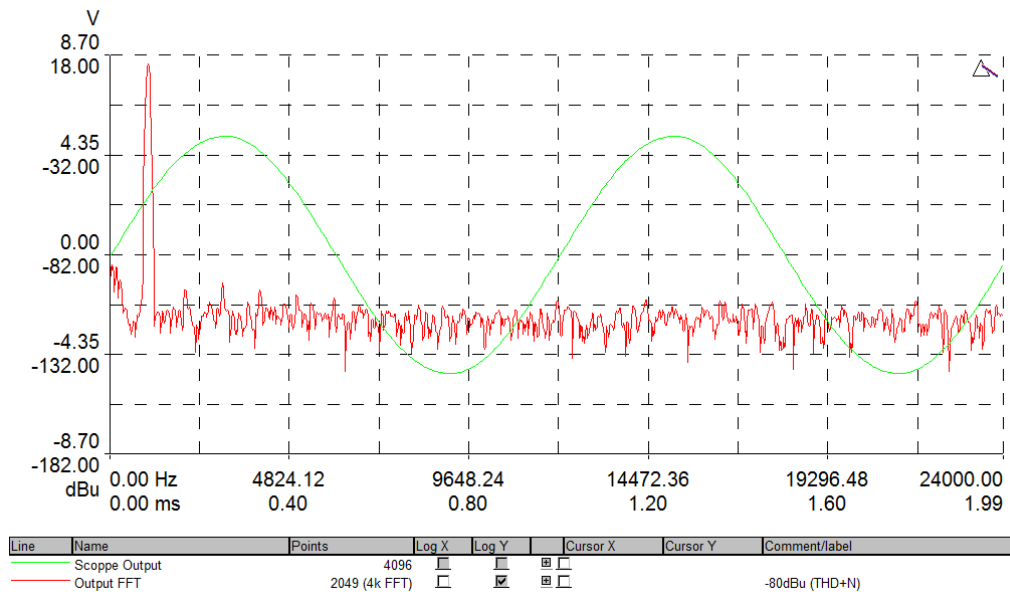


**Figure 6.15: FFT output of the compressor without an optical cell connected**

In order to compare the optical cells at different amounts of gain reduction, it is necessary to record the output spectrum of the compressor with the two optical cells connected at no gain reduction. Figure 6.16 shows the output of the compressor circuit with the CdS optical cell connected and Figure 6.17 shows the same output but with the CdSe cell. While no gain reduction was applied while taking those measurements, both FFTs show an increase in the overall spectrum. Figure 6.16 which represents the CdS cell shows a pronounced increase in the third harmonic (-57 dBu). There is also an increase in the ninth and tenth harmonic. Throughout further investigations, it was discovered that after around 10 seconds, the third harmonic decreased in level, but was still elevated compared to the value in Figure 6.15. On the other hand, the other two harmonics ($9^{th}$ and $10^{th}$) were still present regardless of how much time passed since the cell was connected in the compressor.
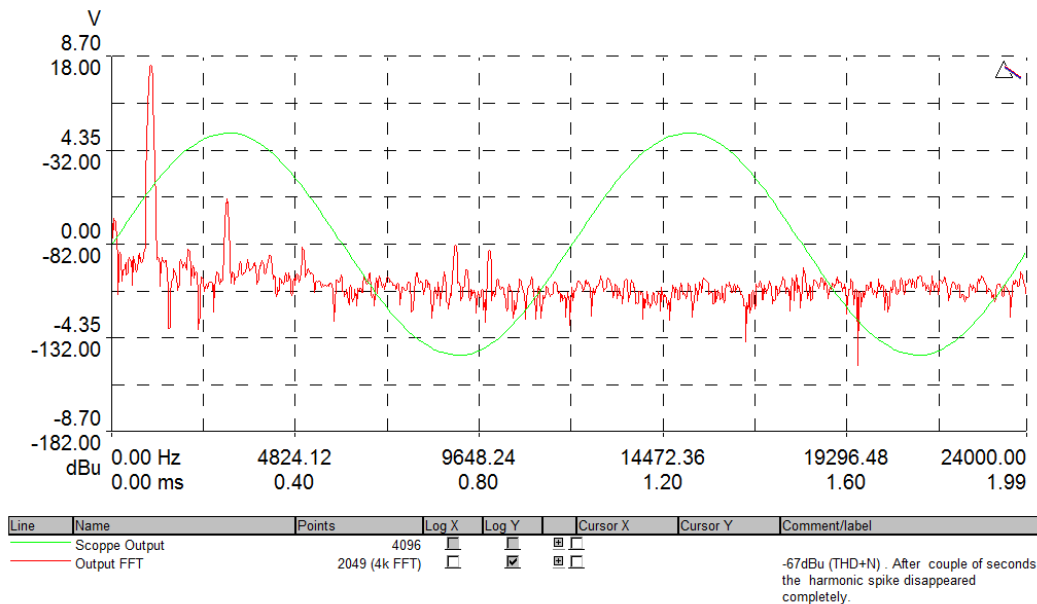


**Figure 6.16: Compressor FFT output with a CdS cell connected**

Furthermore, looking at the output FFT with the CdSe cell (Figure 6.17), the third harmonic is not present, but an overall increase in THD+N is observed between 2.4-4.8 kHz. The 9th and 10th harmonics are present in this output as well, but at a lower level. Comparing both these two measurements to Figure 6.15 it can definitely be concluded that those distortions are a function of the LDR itself, more likely the chemical interactions at a molecular level which cannot be controlled and which may also produce the oscillations seen before.
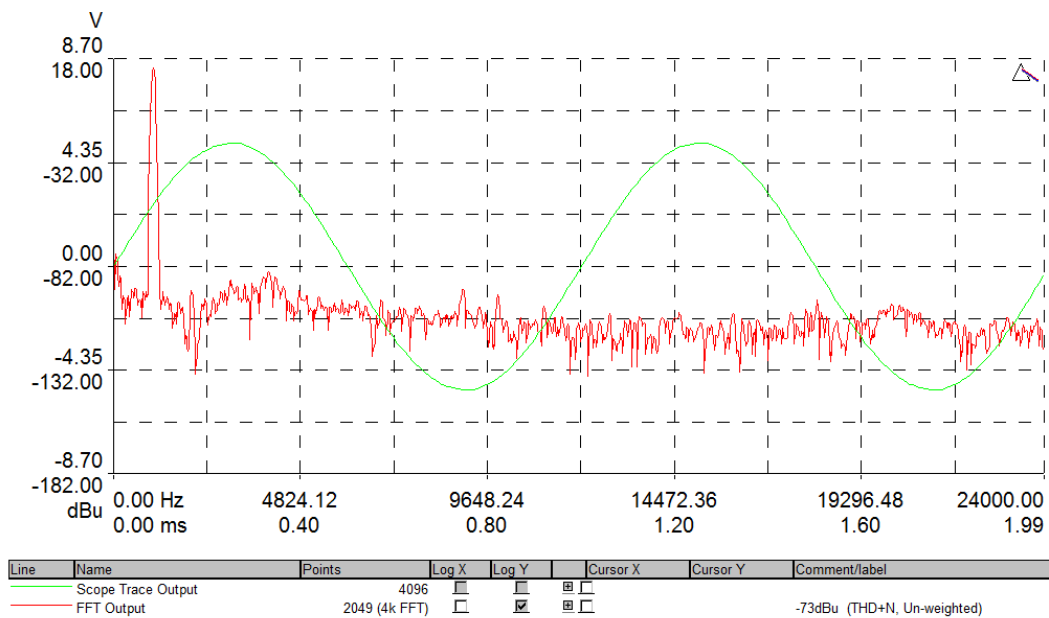


**Figure 6.17: Compressor FFT output with a CdSe cell connected**

As previously mentioned, these measurements were also taken during constant compression. Three gain reduction values were used to measure the THD+N and compare the output spectrum between cells. These values are 6 dB, 12 dB and 20 dB. The FFT measurement in all figures were taken only after the cell has fully reached the mentioned gain reduction value, not during the attack stage. Following subchapters present the obtained result for each gain reduction amount.

### 6.3.1    FFT at 6 dB Gain Reduction

For a more detailed look at the FFT output at 6 dB gain reduction please see Section A: FFT at 6 dB Gain Reduction in the Appendix.

The FFT output with a CdS + Green Panel showed that the $2^{nd}$ and $3^{rd}$ harmonics are almost equal in level and so is the case for any other harmonic pair ($6^{th}$ and $7^{th}$, $8^{th}$ and $9^{th}$.). On the other hand, with the spectrum output when a CdSe LDR is used, the odd harmonics have an increased level compared to the even ones. Also, there is an increased harmonic content in the upper frequency range when using a CdSe LDR. Overall, the difference in total THD+N between outputs is around 4 dB (-41.1 dBu when using a CdS LDR and -37.1 dBu when suing a CdSe LDR). Solely by analysing this data, the CdS based cell would be much more fitted for use within a compressor, not only because the overall level of THD is lower, but also because of the increased even harmonics.

Same FFT measurement was carried out on a CdS + Red panel cell and a CdSe + Red panel cell, the only difference to the above measurement was the use of a red panel to drive the two LDRs. The difference in total THD+N in this instance is around 0.7 dBu, which is much lower than the previous result due to the decrease in distortion levels with the CdSe + Red panel cell. Multiple readings were taken to ensure the distortion values are not oscillating or changing in time. The FFT of the CdS + Red panel cell showed there aren't any noticeable changes in the amplitude of the harmonics below 18 kHz (compared to CdS + Green panel), but there is a small increase above that frequency (which in reality it would never affect a musical signal).

Overall, with 6 dB of gain reduction, there are differences in spectrum between the CdS and the CdSe cells. The most important change is the increased level difference between odd and

even harmonics for the CdSe cell. The increase in spectrum content in the upper frequencies is a direct result of the oscillations and noise spikes that were described above. This claim is further reinforced by the fact that the CdSe LDR, as discussed above, has worse oscillations compared to the CdS, which spectrally results in higher THD in the upper frequency range. This was also identified on the FFT measurements. In terms of distortions, to reduce the THD level, using a red panel to drive the CdSe cell seems a better approach than using a green panel. This may be a direct result of the fact that CdSe is much more sensitive to the red-light spectrum.

Once all LDRs were tested with the modern EL panels, it was decided to pair a CdSe with the old modelled panel. It was discovered during testing that with this light source the THD + N was even lower than the one recorded with same LDR and a green EL panel (-36.4 dBu compared to -37.1 dBu). The difference of 0.7 dBs is not really making much difference, but what is interesting is the fact that the amplitude of the $2^{nd}$ harmonic was found to be bigger than the $3^{rd}$ harmonic. The test was carried out multiple times in order to be able to say for certain that it was not a measurement issue. While the CdSe + old modelled panel cell was tested at other GR values (3 dB, 12 dB, 20 dB), the same behaviour was identified with regards to the relationship between $2^{nd}$ and $3^{rd}$ harmonic. In terms of THD+N levels, the combination of CdSe and old modelled panel gave the same low overall distortion values as the combination of CdSe and green panel.

### 6.3.2    FFT at 12 dB Gain Reduction

For a more detailed look at the FFT output at 6 dB gain reduction please see Section B: FFT at 12 dB Gain Reductionin the Appendix.

CdS and CdSe LDRs were paired again with a green panel and another FFT measurement was taken at 12 dB of constant GR. The overall THD+N at the output of the compressor when using a CdS cell decreased by 6 dB, linearly with the output level which also decreased by 6 dB compared to the previous measurements. The relation between odd and even harmonics for this cell is the same, while harmonics above 14 kHz increase in amplitude, probably due to elevated oscillations caused by an increase in gain reduction, thus a decrease in resistance which could make the LDR a bit more unstable. When the CdS LDR is driven by the red panel, the output spectrum looked exactly the same, but with a small decrease in THD+N of about 0.1 dB which can be neglected as it won't have much of an impact on musical material. Same small amount of decrease in THD+N was noted between CdS + green panel and CdS + red panel at 6 dB gain reduction.

On the other hand, CdSe + green panel cell's total THD+N only decreased by 1.5 dBu and just like in the previous measurement (at 6 dB GR), the level of the odd harmonics is higher compared to the even ones. Also, an increased distortion is present in the upper frequency region compared to the same measurement done at 6 dB gain reduction. Overall, it seems that both outputs exhibit lower distortion figures with increasing gain reduction, but the CdS seems to achieve a better THD performance.

An important difference was discovered when measuring the THD+N of the compressor when using a CdSe + green panel cell with the THD+N when using the same LDR but with a red

panel. When driven by the red panel, the distortions decreased by 6.2 dBu (thus halving). It has to be stated again that both the LDR and the audio stimuli were the same, the only different element being the red panel. What was noted when analysing the two FFTs is that the 2nd harmonic decreased more than the 3rd. Another notable decrease in level was that of the 5th harmonic. The high frequency distortion is still present. Again, it looks like when the CdSe is driven by a red panel, the THD level decreases, as it was seen in the figures above at 6 dB gain reduction.

### 6.3.3    FFT at 20 dB Gain Reduction

For a more detailed look at the FFT output at 6 dB gain reduction please see Section C: FFT at 20 dB Gain Reductionin the Appendix.

With increasing amount of gain reduction, the THD+N drops even more. The distortion figures for CdS + green panel, just like in the previous measurements are a lot lower than the ones for CdSe + green panel. They both drop in level with increasing gain reduction values, but the combination of CdS and green panel achieves better overall THD values and decreases in this measurement at a faster rate compared to CdS + red panel. The improvement in THD+N value is about 5.6 dB at 20 dB gain reduction when using CdS + green panel and around 3.2 dB when using CdSe + green panel. (These results are reported against the values measured at 12 dB gain reduction.)

Same as in the previous measurements, CdS/CdSe + Red panel cells present better THD+N levels than CdSe + Green panel, but with 20 dB of GR, the CdS + Red panel cell exhibits for the first time a slightly better value than CdS + Green (-54.1 dBu compared to -52.5 dBu).

So far, it seems that with increasing GR values the THD+N levels drop. The difference between certain LDRs and light sources seems to follow the same trend with increasing GR, the

only noted difference being at 20 dB GR when the CdS + red panel cell exhibited the lowest

THD+N. Moreover, it seems that the CdSe + green panel exhibits the biggest difference between

the 2nd and the 3rd harmonic, while with increasing amounts of GR, the level difference between

the two harmonics increases for the CdS + red panel cell.  Another interesting fact is that, overall,

the THD+N values of the CdS cells under different GR values are better than the values obtained

with a CdSe cell, even though, with no GR, the system's THD+N value was better when a CdSe

cell was used (Figure 6.16 and Figure 6.17).

Table 6.5 summarises the measurements above and represents a shortened version of all FFT

measurements in the Appendix.

| Cell | THD+N with no GR (EL panel not important) | THD+N at 6 dB GR | THD+N at 12 dB GR | THD+N at 20 dB GR | Comments |
|---|---|---|---|---|---|
| CdS + Green EL | -67 dBu | -41.1 dBu | -47.1 dBu | -52.5 dBu | 2nd and 3rd harmonics almost equal in level |
| CdSe + Green EL | -73 dBu | -37.1 dBu | -38.6 dBu | -41.8 dBu | Odd harmonics higher than even harmonics. Higher spectrum content in the upper frequencies.<br><br>Highest difference between 2nd and 3rd harmonics at 12 dB GR. |
| CdS + Red EL | | -40.3 dBu | -44.8 dBu | -57.1 dBu | Lowest THD+N at 20 dB GR |
| CdSe + Red EL | | -41 dBu | | | Higher spectrum content in the upper frequencies. |
| CdSe + OldMod EL | | -36.4 dBu | | | Higher 2nd harmonic |

**Table 6.5: Parameters overview at different compression levels**

## 6.4 Attack and Release Characteristics

This sub-chapter discusses the attack and release characteristics of the two LDR types when combined with different light sources. This measurement was done to assess if there are any differences between the cells and whether any possible conclusion could be drawn that could indicate that one cell type might be better suited for certain audio material than others. In order to test the dynamic behaviour of the optical cells, a sinewave burst test signal was used, as described by Metzler (2005). The tone consisted of three portions: a low-level portion with a signal below the threshold, a high-level portion with signal going above the threshold for a certain amount of time and then another low-level portion with below-threshold signal to allow the compressor to recover. To be able to assess and further prove any memory-effects, three different burst test tones were used, having either 5 seconds, 1 second or 300 ms of above-threshold burst length.

All test results containing attack and release values are compiled in Table 6.6. Values for the three parameters have been extracted using oscilloscope measurements on the recorded compressed waveforms. An example of a recorded tone burst under compression can be seen in Figure 6.18. The figure clearly shows the difference in release between CdS and CdSe with the same panel.
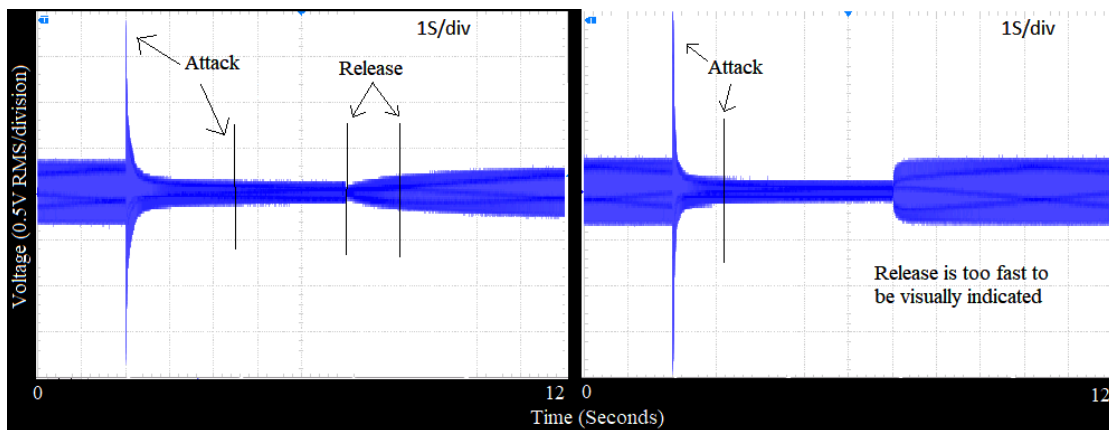


**Figure 6.18: Tone burst compression (CdS + Green left and CdSe + Green right)**

| Optical Cell/ Tone burst | 1st Attack (ms) (63% of GR) | 2nd Attack (ms) (63% to full GR) | Release (ms) (63% to full level) |
|---|---|---|---|
| | | | |
| CdSe + Green EL | | | |
| 5 Sec. Burst | 65 | 1000 | 60 |
| 1 Sec. Burst | | | 30 |
| 300 ms Burst | | | 18 |
| | | | |
| CdSe + Red EL | | | |
| 5 Sec. Burst | 500 | 1700 | 260 |
| 1 Sec. Burst | | | 30 |
| 300 ms Burst | | | Unmeasurable |
| | | | |
| CdSe + Old Modelled | | | |
| 5 Sec. Burst | 96 | 1360 | 130 |
| 1 Sec. Burst | | | 32 |
| 300 ms Burst | | | 16 |
| | | | |
| CdS + Green EL | | | |
| 5 Sec. Burst | 90 | 1500 | 1600 |
| 1 Sec. Burst | | | 1200 |
| 300 ms Burst | | | 150 |
| | | | |
| CdS + Tape + Green EL | | | |
| 5 Sec. Burst | 106 | 1000 | 1350 |
| 1 Sec. Burst | | | 320 |
| 300 ms Burst | | | 150 |
| | | | |
| CdS + Red | | | |
| 5 Sec. Burst | 280 | 2350 | 2200 |
| 1 Sec. Burst | | | 1600 |
| 300 ms Burst | | | 606 |
| | | | |
| CdS + Old Modelled | | | |
| 5 Sec. Burst | 128 | 1000 | 1560 |
| 1 Sec. Burst | | | 580 |
| 300 ms Burst | | | 90 |

**Table 6.6: Attack and Release values**

As it can be seen from the table, all LDRs exhibit different attack and release times when paired with different light sources. All cells have pretty fast attack values apart from the CdSe + Red panel and CdS + Red panel, which are a bit slower, with the former being the slowest of all. Looking at the resistance curves from Figure 6.1 and Figure 6.2 it can be seen that the CdSe has a higher resistance value across multiple measurements than all other LDRs when driven with a red panel, which could explain the slow behaviour, but does not explain entirely the big difference between when it's driven by a red panel and when it's driven by a green one. Also, the slower attack for the CdSe + Red panel could be a cause for obtaining better THD+N performance than with a green panel.

Looking at the attack times of the CdS based cells, it can be seen that the fastest attack is obtained when driven by a green panel due to the peak spectral response of that type of LDR. Also, by controlling the exposure area of the LDR, the attack time can be changed, and in this case, it increased from 90 ms to 106 ms. The difference should not make any difference on an audio source, but by further decreasing the exposure area this time can be increased even more. The practicality in such a compressor is that, given the fact of how it works, there is no real time-constant control, but by using this kind of approach, a crude attack control could be implemented. With the case of using an old modelled panel as a light source it seems that the attack values are in between the ones obtained with CdSe + Red and CdSe + Green panel. With the CdSe based cells, the attack times are not as expected. Considering the peak spectral response of the CdSe LDR it was anticipated that the attack time would be much faster when using a red panel, whereas the results are exactly opposite. Same test was repeated with replacing the LDR, but the results were pretty much the same. As in the previous case, when pairing a CdS LDR with an old modelled panel, the attack values sit in between CdS + Red and CdS + Green panel.

The table also contains a column for the second attack, which was necessary to be added due to the fact that in order to get to full GR value the compressor will spend a lot of time compressing the last 37% of the remaining amplitude. Figures used above, when presenting the resistance curves expressed in ohms against input level can't tell precisely what happens at low resistance values and how do the curves differ between different cells. By using the values of the $2^{nd}$ part of the attack, a better understanding of the differences between cells at high gain reduction values can be made. Also, due to the fact that all cells were set to achieve the same amount of GR means that all results are comparable.

Three of the cells seem to need the same amount of time to get to full GR, even though the $1^{st}$ part of the attack time is different. Therefore, between CdSe + Green, CdS + Tape + Green and CdS + Old Modelled cells is no difference in attack /resistance curve once it reached 63% of GR, therefore they are only comparable during the $1^{st}$ part of the attack.

The long $1^{st}$ attack time of the CdSe + Red panel also translates through to the $2^{nd}$ attack time, which is 700 ms slower compared to the 1000 ms of the CdSe + green panel cell. Again, this is an interesting finding, as the CdSe has the peak spectral response in the red-light region, therefore should be more sensitive and have a faster attack curve when driven by the red panel.

The slowest $2^{nd}$ attack time was obtained with the CdS + red panel cell, which was expected to happen due to the different peak spectral response of the LDR.

Even though CdSe + red and CdS + green panel cells have very different $1^{st}$ attack times, the second part of the attack is pretty similar, with only 200 ms of difference, which means both resistance curves at high GR are almost the same.

Interestingly, when the exposure area of the CdS LDR was reduced, the 1$^{st}$ attack time increased (by 16 ms), but the second attack time decreased way more (by 500 ms), even though the same LDR and panel were used and the same GR was set. This results in the fact that, modifying exposure area affects the LDR's resistance drop rate more at the low resistance values (high GR).

Regarding the release times there are two important findings to note:

- The CdSe is a lot faster during release, compared to the CdS, with differences of up to 2000 ms between the two.

- Depending on the time length of the above-threshold burst, different release times could be noted. This is due to the memory effect, showing that the less amount of time the panel illuminates the LDR the faster the release is (More light means the resistance drops more, more time the light falls on the LDR means more electron-hole pairs are formed, thus the longer the recombination process will take, hence the different release times.).

## 6.5 Frequency response of optical cells

As mentioned previously, the EL panel has a frequency dependent brightness which was demonstrated through individual frequency testing. Figure 6.19 and Figure 6.20 show the output of the compressor with two different optical cells, measured across the audio spectrum. Both cells used a green EL panel and the same driving signal was used in both instances (a frequency sweep). There are two main things resulting from the two plots. First of all, they further prove the frequency-dependent brightness of the EL panel, which can be seen as the increase in gain reduction with increasing frequency. It is furthermore demonstrated the drop in EL panel's efficiency above 5 kHz, which is a direct result from a combination of two different elements: The

actual physical and chemical construction of the EL panel and the response of the EL driver amplifier, which gets loaded as the EL panel's impedance drops with increasing frequency.
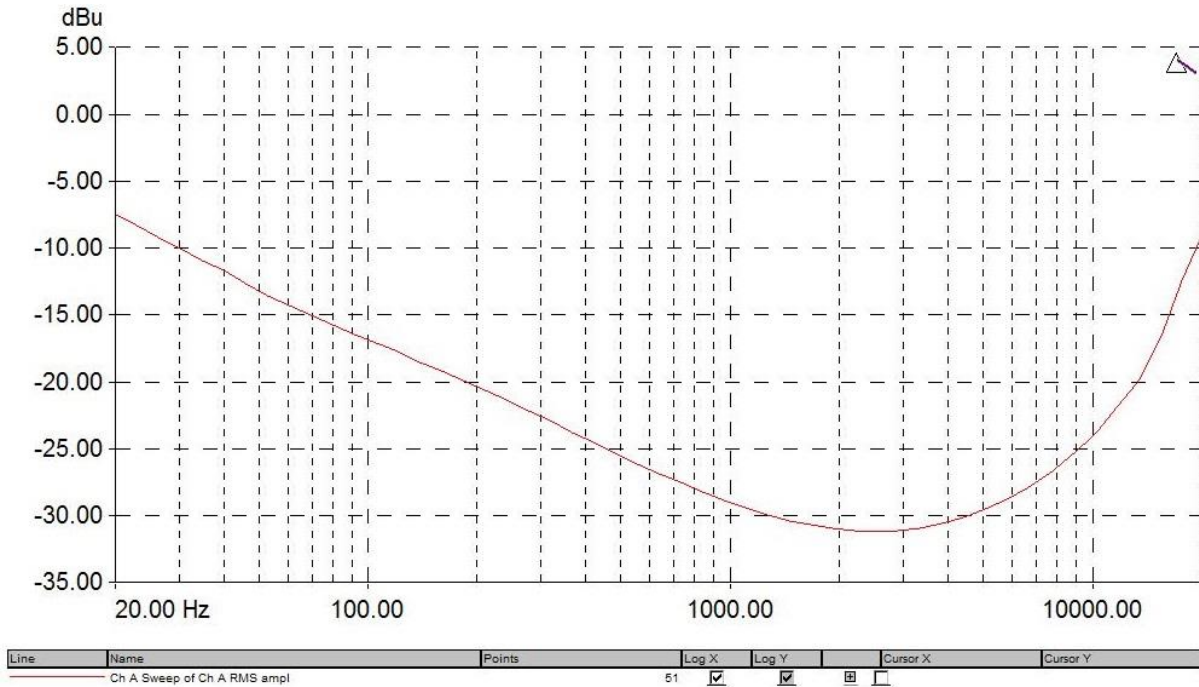


**Figure 6.19: Frequency response with CdS + Green at max threshold**
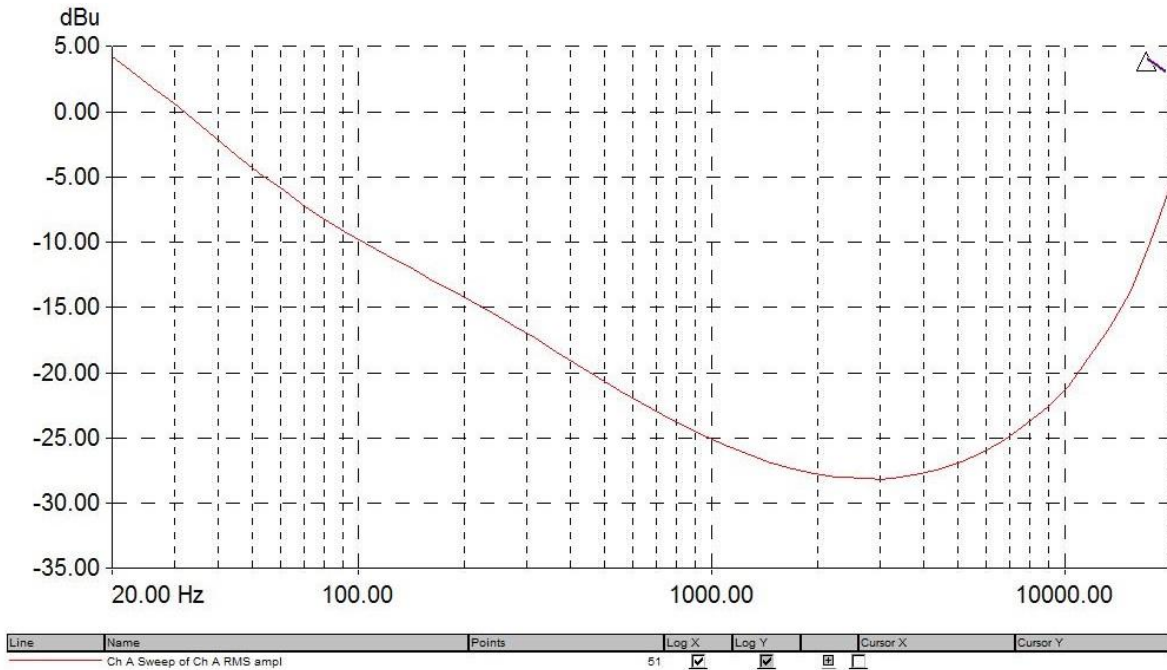


**Figure 6.20: Frequency response with CdSe + Green at max threshold**

This impedance drop was further measured and the results are showed in  EL Panel Impedance and Capacitance.

Analysing the frequency range between 20 Hz and 200 Hz in the two frequency response figures below, there is an approximate 12 dB of gain reduction difference at 20 Hz and 5 dB at 150 Hz. It is worth mentioning that the compressor was at maximum threshold level and the same input signal level was used, therefore the difference between the two output curves could only come from the LDR's output resistance. One reason could be the difference between CdS and CdSe, in resistance after dark adaption, with the latter having a higher value and also the difference in peak spectral response which would make the CdS based cell more sensitive (as the test was carried out with a green panel). As a result, by having a CdSe based optical cell, the compressor would require a higher threshold level to achieve the same amount of gain reduction at low frequencies compared to a CdS based cell.  On the other hand, as the frequency increases, the amount of gain reduction difference between the two cells decreases, with a maximum difference of 3 dB at 1 kHz, which proves once more that brightness dominates the LDR's resistance curve more than light colour does. The only place light colour seems to make a difference is at low frequencies due to lower light levels. Therefore, it is safe to state that at low light levels, the spectrum sensitivity curve of the LDR dominates its resistance response curve. On the other hand, at high levels of light, the LDRs have almost identical resistance curves. The increased light levels do not necessarily have to be achieved by an increase in driving level, but it is enough to have higher frequencies present in the signal.

## 6.6 EL Panel Impedance and Capacitance

With regards to Figure 6.21 and Figure 6.22 that show the impedance and capacitance values of the three El panels, an important result can be extracted by analysing them. First of all, it is interesting to find that the two modern panels have different impedance values when compared at the same frequencies. Secondly, starting with 2 kHz and above, there is a very small difference between the red modern panel and the old modelled one. In terms of capacitance, there are pretty similar values between the green and the old modelled panel, while the red panel measures higher values. Considering the fact that the panels are driven (in this case) by a pentode amplifier and that with increasing frequency the impedance drops, there will be a point above which the panel will start having a loading effect on the pentode. Considering the impedance values that the panels seem to drop to, it is explainable why above a certain frequency the light level begins to fall, as the pentode can no longer output the same driving voltage. Moreover, the capacitance values of all panels, especially red panel's ones, are pretty elevated for such a high impedance driving circuit and could therefore affect the frequency response of the driver amplifier, affecting the EL panel further. This results in a non-uniform gain reduction across the audio frequency spectrum.

As a result, it seems that in such an optical cell it is not only down to the LDR element to control the attack/release characteristic and the amount of gain reduction. It is a combined effect of itself, the light element with its output colour, brightness level and the driving amplifier.
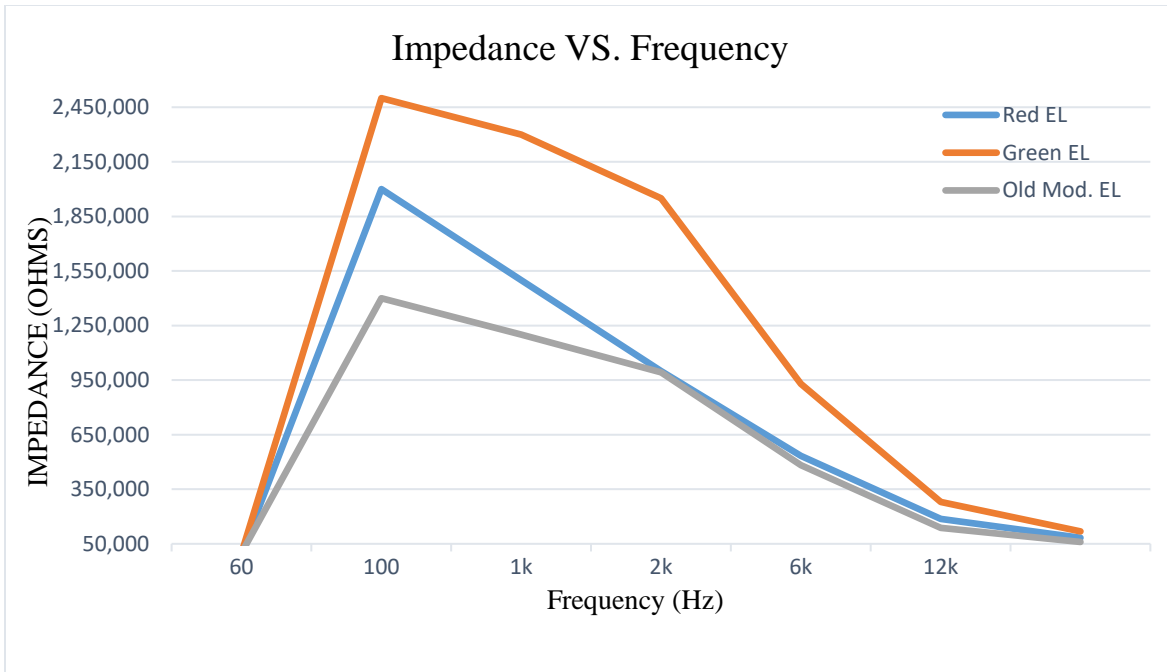
**Figure 6.21: EL Panel's Impedance vs Frequency**
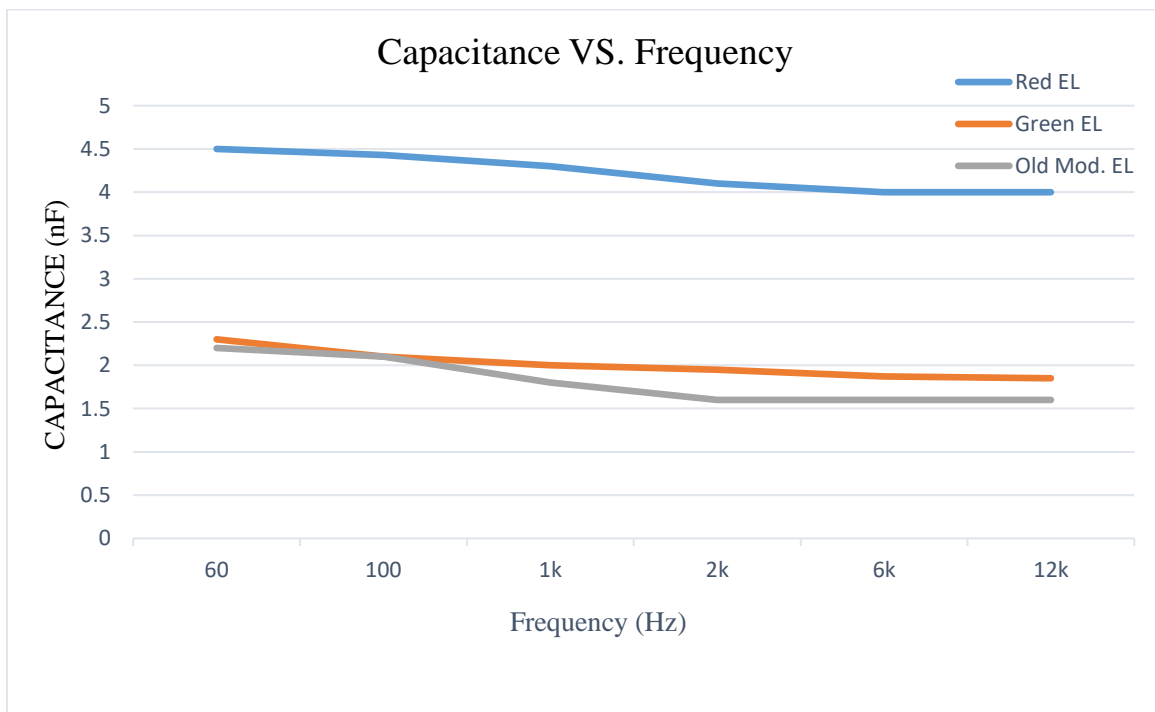


**Figure 6.22: EL Panel's Capacitance vs. Frequency**

## 6.7 Matlab analysis of recorded data

### 6.7.1    Spectrogram and Centroid Measures during constant compression

While the results described above give a good indication of the LDR-light source relationship and the effect the modified parameters have on the stimuli, it is also important to investigate what happens with the audio waveform (spectrally) during the 1$^{st}$ attack period and release. It would be interesting to find out what is the THD difference between a fast attack/release and a slow attack/release and to try and identify whether there is any difference imposed by the panel's colour.  To allow this, in-depth spectral analysis was carried out on the recorded output of the compressor without any cell connected, with a cell connected and no gain reduction applied and with a cell connected with gain reduction.

Figure 6.23 shows the spectral output of the compressor without any optical cell connected in the system. A simple 1 kHz signal was passed through and the spectrum of the output was generated in Matlab. It is kind of a THD analysis, but instead of showing the harmonic frequencies and amplitudes, the spectrogram computes the energy levels of different frequencies and how they are spread. A cold colour indicates less energy in that particular area, while a warm colour indicates the opposite. Therefore, the 1 kHz signal energy can be seen in red because it has the highest amplitude, thus the highest energy. It can be noted that most of the harmonic content lays in between 1 kHz and 3 kHz. Low spectral energies appear to be concentrated from around 6 kHz to 20 kHz between 0.5 S and 3 S timeframe. A good question would be why is this low spectral energy present between this timeframe as the driving signal was a continuous 1 kHz tone. Figure 6.24 and Figure 6.25 present the same spectral measurement carried out on the recorded output of

the compressor with two different cells connected (no gain reduction applied). The main identified differences are:

- For the CdSe cell, the low spectral energy area shifted towards right, between the 1.5 S and 3.5 S timeframe. It also shows a slight increase in energy levels between 0 S and 1 S timeframe compared to the spectrum that has no cell connected.

- For the CdS cell, the low spectral energy area shifted toward left, vanishing almost completely. Also, by comparing the spectrum output of this cell to the other two, it can be clearly noted a more elevated energy content across the entire frequency spectrum.
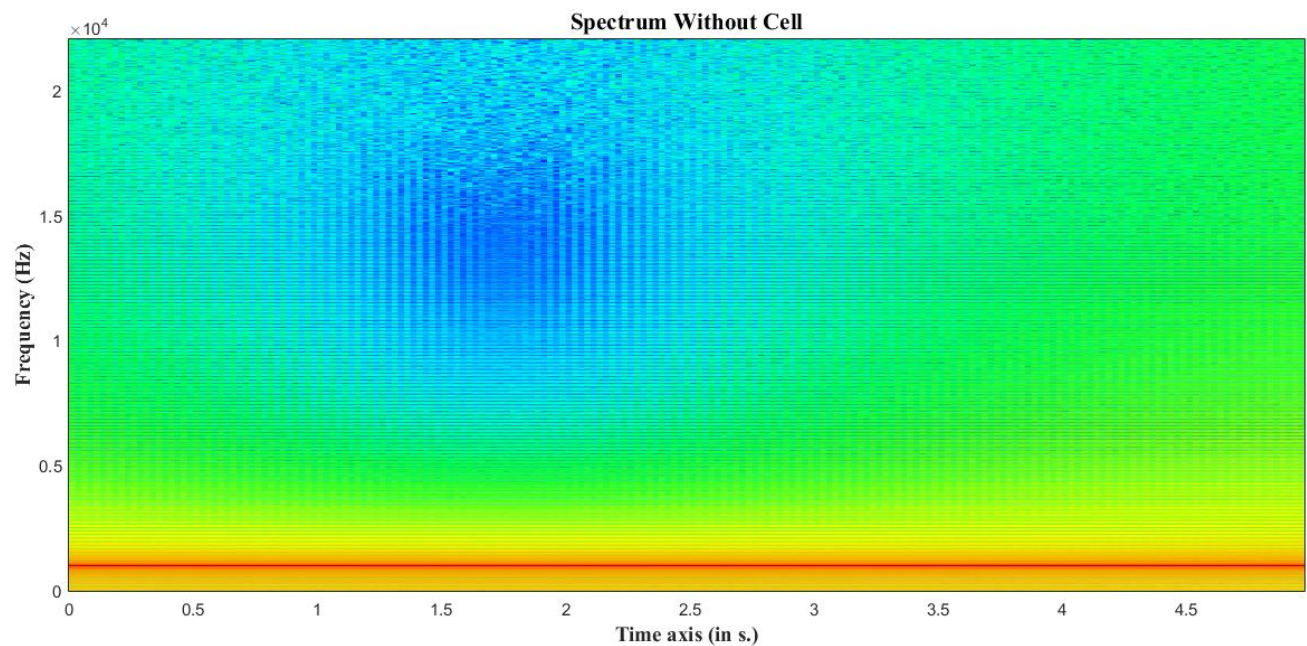


**Figure 6.23: Compressor's output spectrum without cell connected**
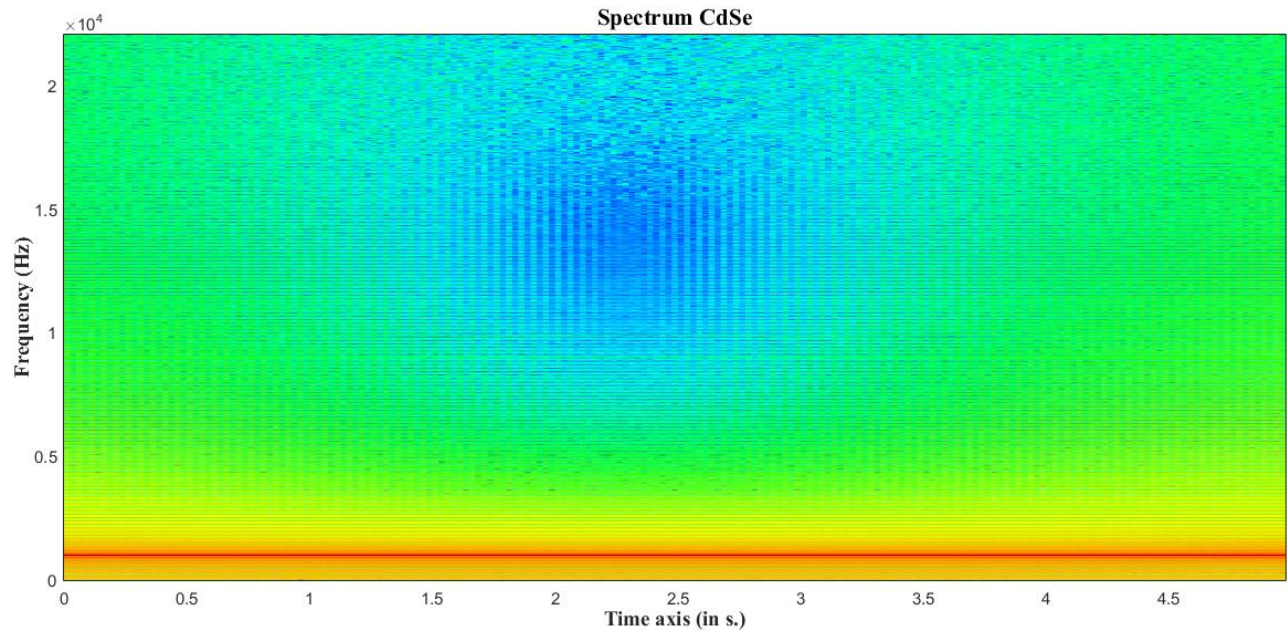
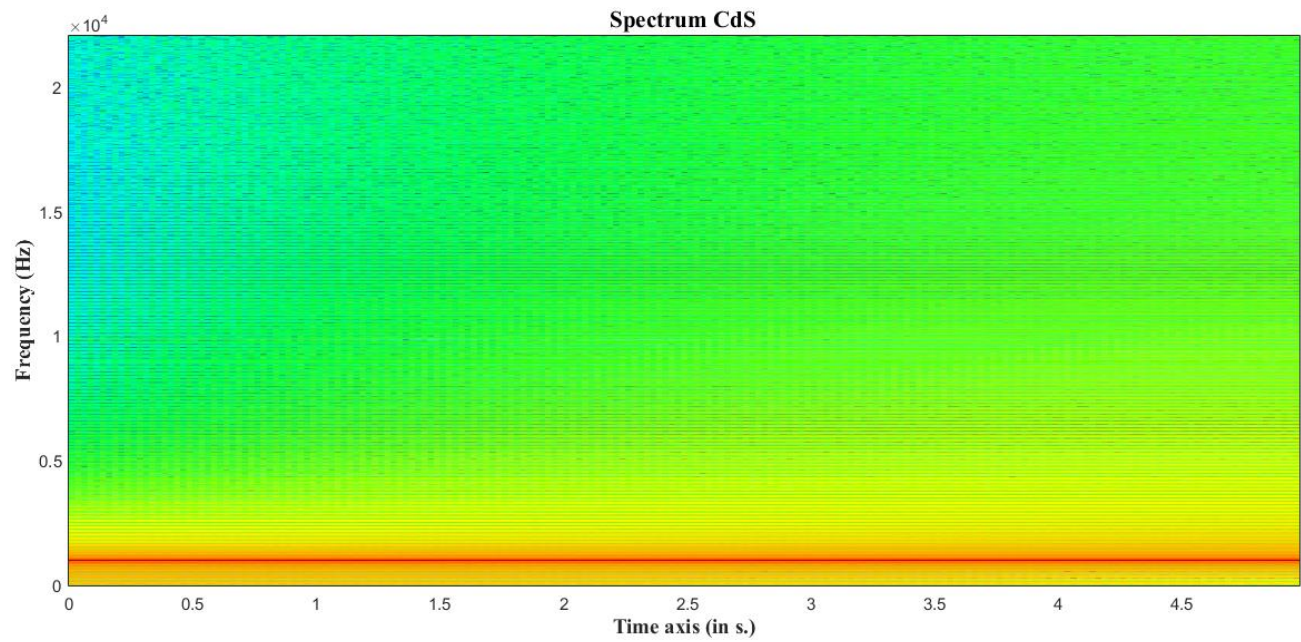**Figure 6.24: Output spectrum with CdSe Cell**



**Figure 6.25: Output spectrum with CdS Cell**

While differences appear in the spectrum by just connecting an optical cell, a further step was taken and a signal was applied through the compressor and a set amount of 10 dB GR was applied. While it was constantly compressing the 1 kHz signal, the output was recorded and a spectral analysis was carried out. The two figures below represent the spectrum with the different cells (CdS + Green, CdSe + Green). Figure 6.26 and Figure 6.27 show the differences between CdS + Green and CdSe + Green cells. As it can be seen, the output of the compressor with the CdSe + Green cell has a higher amount of energies in the odd and even harmonics, which are spread across the entire audio spectrum. These harmonics are represented as the yellow/orange strips. For the compressor output with the CdS + Green cell it can be noted that just the first three harmonics ($2^{nd}$, $3^{rd}$ and $4^{th}$) are visible with such high energy levels (the yellow bands).

The same results were obtained for the compressor output when connecting a CdS + Red and a CdSe + Red cell. There are increased energy levels in the odd and even harmonics spread across the entire audio spectrum for the output with the CdSe + Red cell, while the output with the CdS + Red cell only shows high energy levels for the first three harmonics. Moreover, the output with the CdS + Red cell seems to have a slightly elevated overall energy level across the entire spectrum, result that is also confirmed by the FFT measurement.
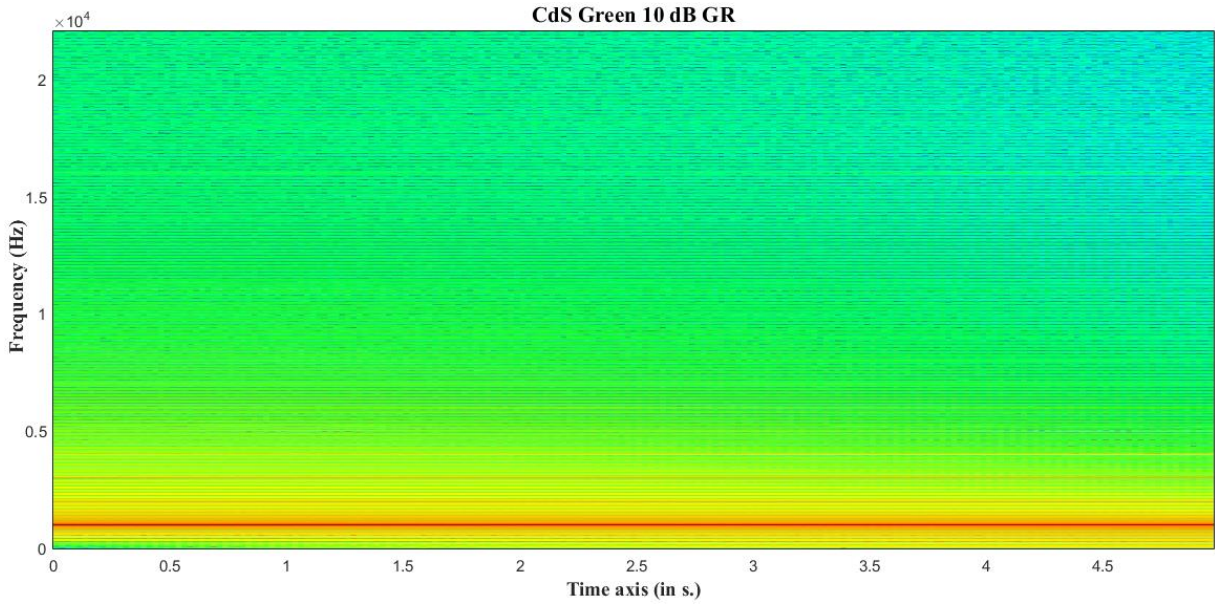
**Figure 6.26: CdS output spectrum at constant gain reduction**
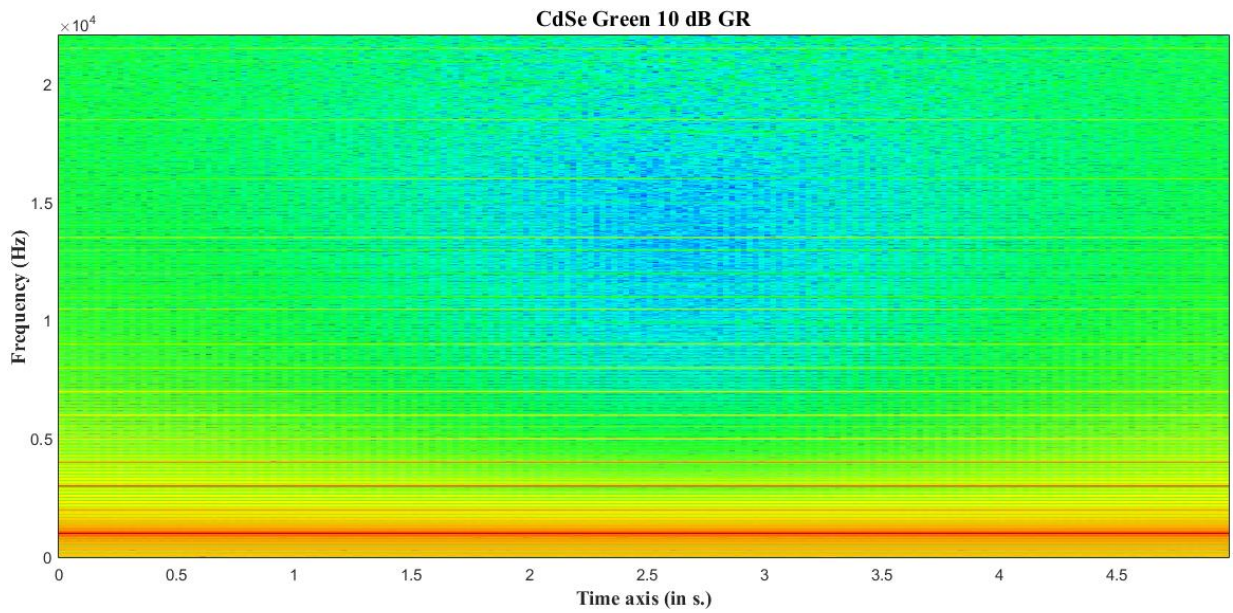


**Figure 6.27: CdSe output spectrum at constant gain reduction**

Further investigation in Matlab of the output of the compressor with a CdS + Green and CdS + Red cell has been carried out by analysing the centroid values using the MIRToolbox. The purspose was to see if there are any low-level differences in centroid values that might suggest a certain impact on the musical signal. According to Nam (2001) the cetroid represents the measure that relates to the perceived brightness of a sound measured using the frquency and magnitude information of fourier transform. Tests have indicated an almost perfectly equal centroid curve for both of the recorded outputs, which means that by using a musical signal there would be no notable difference in brightness during compression. This conclusion was somewhat valid just by looking at the difference in FFT during compression when using these two different cells. On the other hand, what was noted is that the centroid values are not uniform under the entire compression time-frame. As it can be seen in Figure 6.28, there is a linear rise of the centroid with time, which indicates that even though there are no essential differences between the two cells, there is an increased brightness element the more the cell is kept under compression.
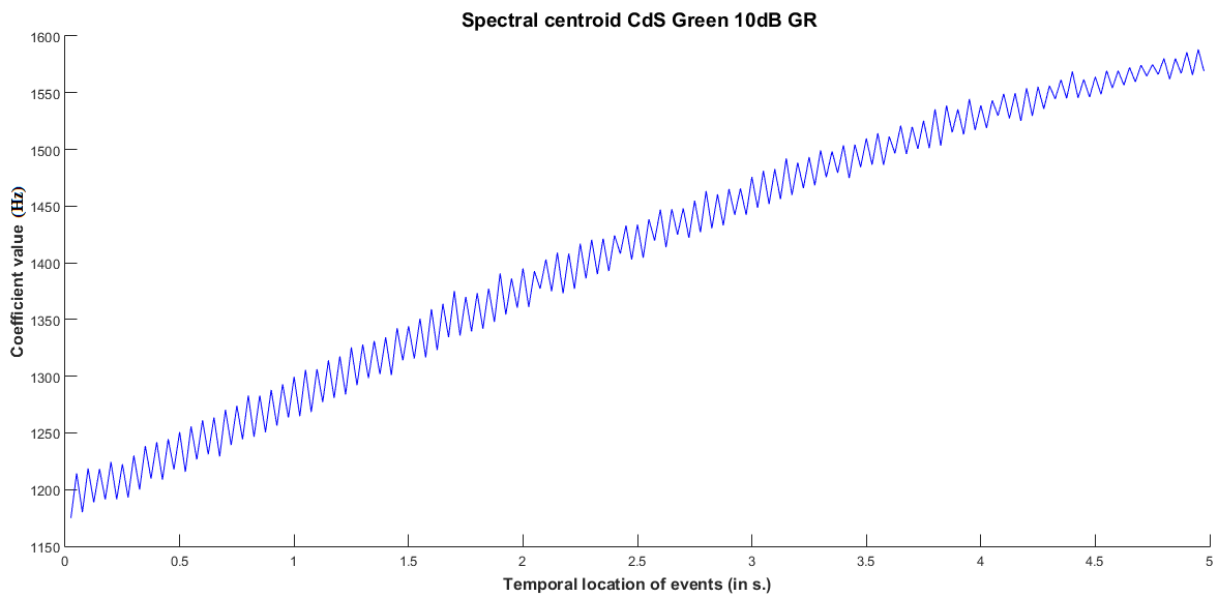


**Figure 6.28: Spectral Centroid with CdS + Green panel at constant gain reduction**

Same results were obtained by comparing the output of the compressor when using the CdSe + Green and CdSe + Red cell.

## 6.7.2    Spectrogram and Spectral Centroid during Attack Timeframe

Further investigations have been carried out during the attack timeframe to determine whether there are any differences in spectrogram during this moment, when the signal suddenly drops in level. The measurements were done by feeding a high-level signal through the compressor, of a certain length, and then followed by a very low-level signal of a certain length. This On-Off burst was repeated a couple of times in order to investigate if the attack characteristic changes during more compression cycles.

Analysis of the recorded waveforms showed that attack values are very close to the ones measured on the oscilloscope, but are only valid for the first attack of the first tone burst. All recorded compressor outputs with any of the cells showed that after compression of the first tone burst, the attack characteristic of the cell changes by reacting faster to the following tone bursts. A possible explanation for this phenomenon is that after the compression of the first burst, the cell's resistance is low and it takes some time to recover (release characteristic), depending on the 'under threshold' value. Therefore, depending on this time, the cell's resistance value could be higher or lower. Now, depending on where on its resistance curve this resistance value is, the faster or the slower the attack time will be. Therefore, due to the slow reacting nature of the cell, if it is not allowed to fully recover its resistance value until the next compression, the attack time will inevitably vary. Figure 6.29 and Figure 6.30 show the same waveform, but with a different 'under threshold' time (1 second and 250 ms) and it can be noted that there is no important difference in attack slope between the two. The only difference is the initial amplitude of the second tone burst due to the longer 'under threshold' time between the two bursts.
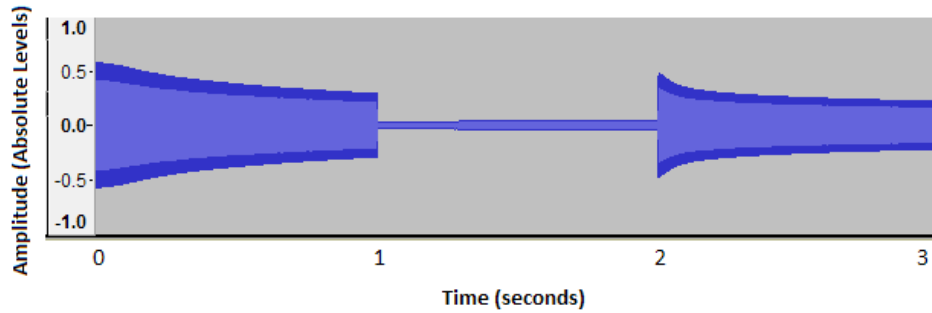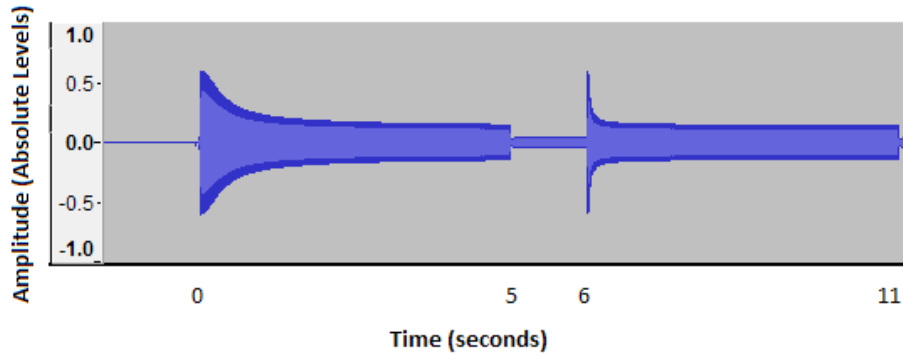
**Figure 6.29: Compressed waveform - CdS based cell – 1 S under threshold**
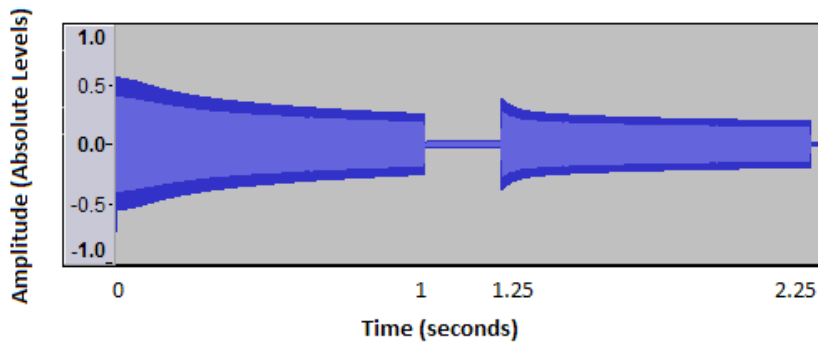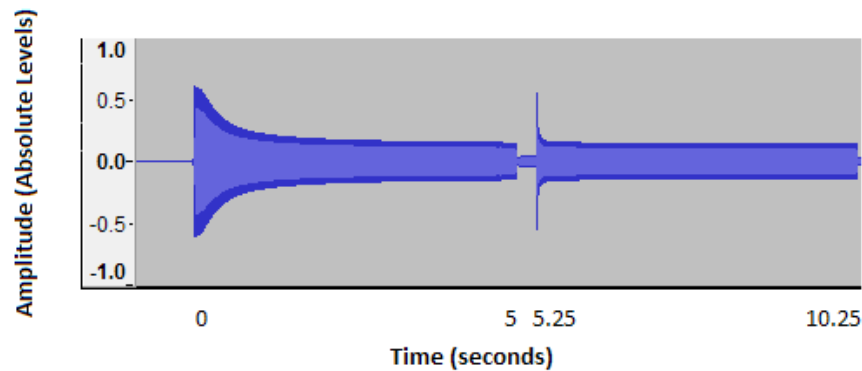


**Figure 6.30: Compressed waveform - CdS based cell – 250 ms under threshold**

Even though this is valid for all cells, the CdSe based ones have a much faster attack on the second tone burst than the CdS based ones. What is interesting is the fact that the CdSe LDR, as shown earlier, has a much faster release characteristic compared to the CdS LDR. It would therefore be expected that its resistance increases back up to a higher value, in the same amount of time, compared to the other LDR, therefore the attack time on the second tone burst would be pretty much equal to the first attack. Figure 6.31 and Figure 6.32 show the compressor output with two different 'under threshold' times, just like the two previous figures. As it can be noted, the attack on the second burst is much faster compared to the one on the first burst, even though the cell's resistance was almost fully recovered (the initial amplitude of the second tone burst is almost equal to the one in the first burst). The difference in the attack characteristic on the second tone burst between the two figures is that in Figure 6.32 is clearly faster due to the shorter 'under

threshold' time (250 ms compared to the 1s), which resulted in a lower resistance value at the time of compression onset.
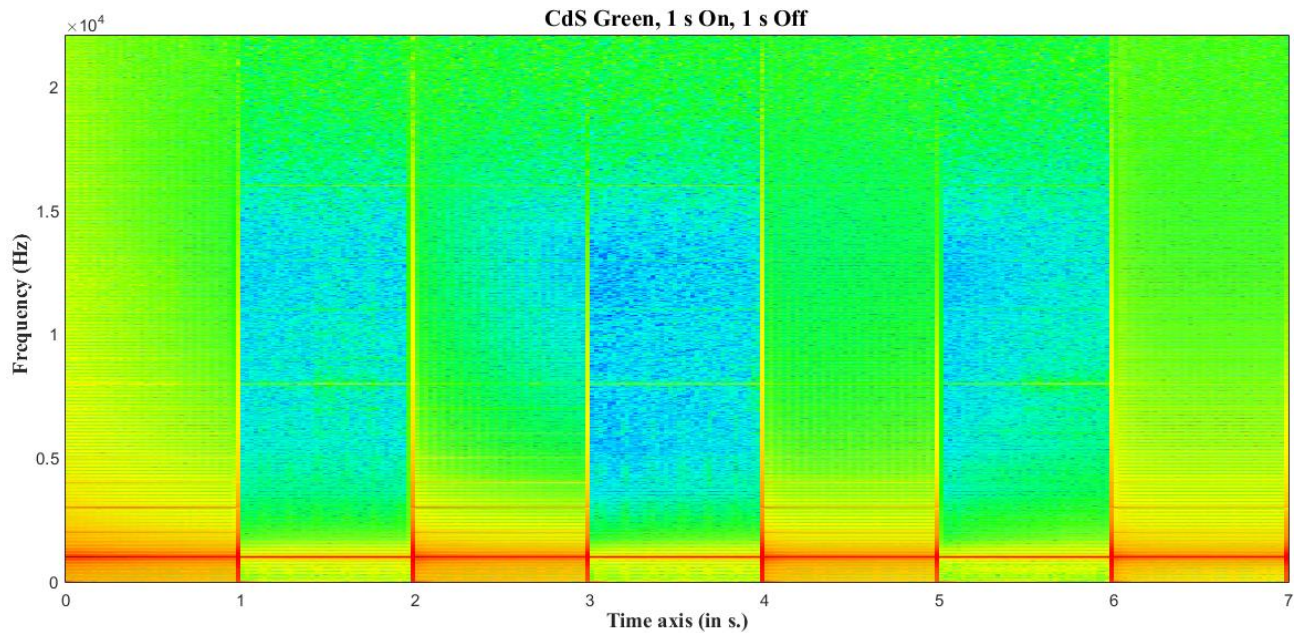


**Figure 6.31: Compressed waveform - CdSe based cell – 1 S under threshold**



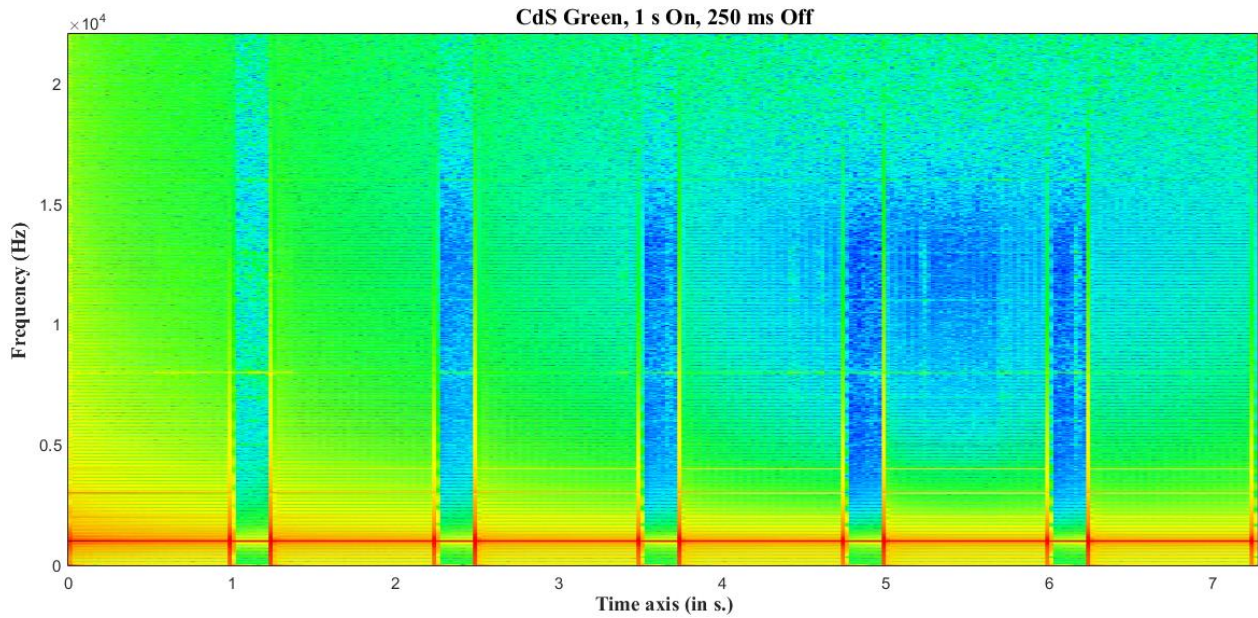**Figure 6.32: Compressed waveform - CdS based cell – 250 ms under threshold**

Matlab analysis of the same compressor output (with CdS + Green cell) at different burst times shows a different spectral content during the 'below threshold' timeframe. With a 1 second of 'below threshold' the spectrum is pretty much repetitive and shows almost constant harmonic content, whereas with a 250 ms of 'below threshold' things differ a lot with each successive tone burst applied, showing a diminished harmonic content (Figure 6.33 and Figure 6.34). Furthermore, there is also a different spectral content during the attack period between the two which may be as a direct result of the 'under threshold' time. It can be noted that, when the compressor has more time to recover (Figure 6.33), the harmonic content is almost the same across each successive tone

burst compared to the decreasing harmonic content from Figure 6.34, where the compressor is not allowed to recover much. By not allowing it to recover as much it means that there is less compression to apply in the same 1 second time frame, therefore less distortion. As seen in the FFT analysis carried out during constant compression, there is also an increased upper harmonic content (above 15 kHz) in each of the two figures below, which may be a direct result of the oscillations described above.
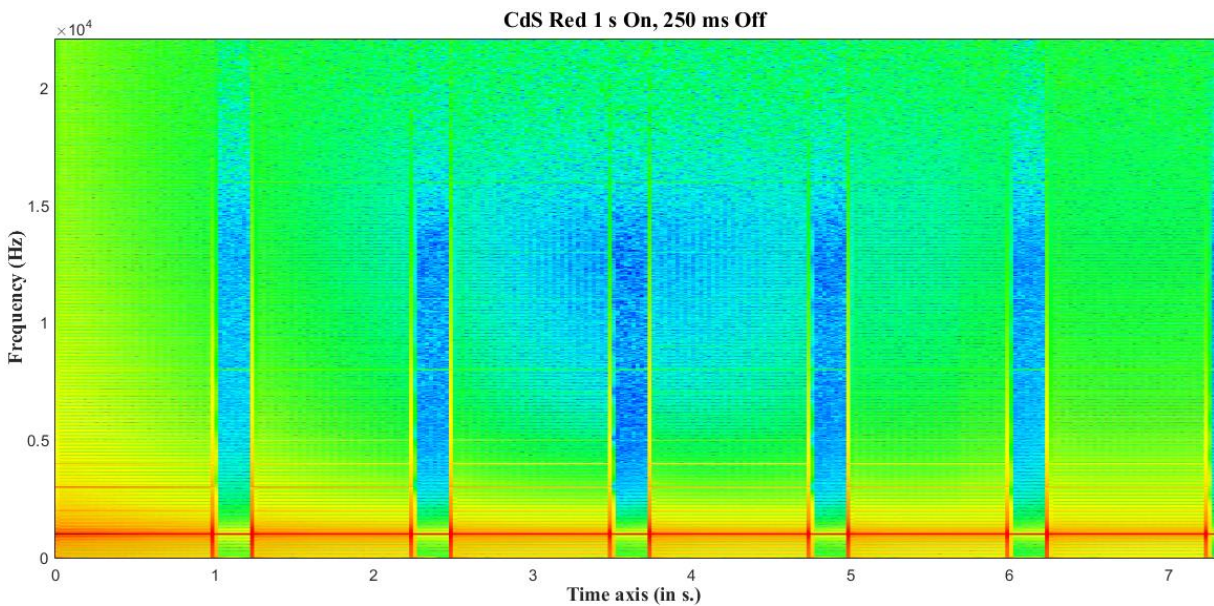


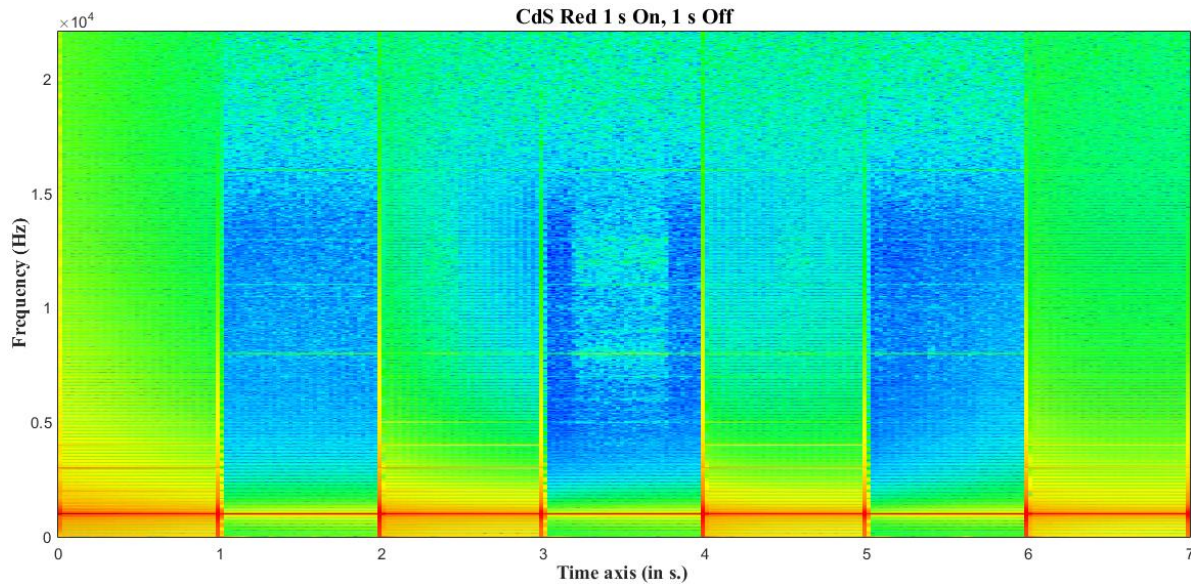**Figure 6.33: Compressed waveform spectrogram - CdS + Green – 1 S On, 1 S Off**

**Figure 6.34: Compressed waveform spectrogram - CdS + Green – 1 S On, 250 ms Off**

When using a CdS + Red cell it seems that there is a decreased spectral content during 'below threshold' timeframes as seen in Figure 6.35 and Figure 6.36. There is also an artefact present during one of these timeframes in Figure 6.36, which again may be due to some oscillations (which may cause an increased harmonic content).
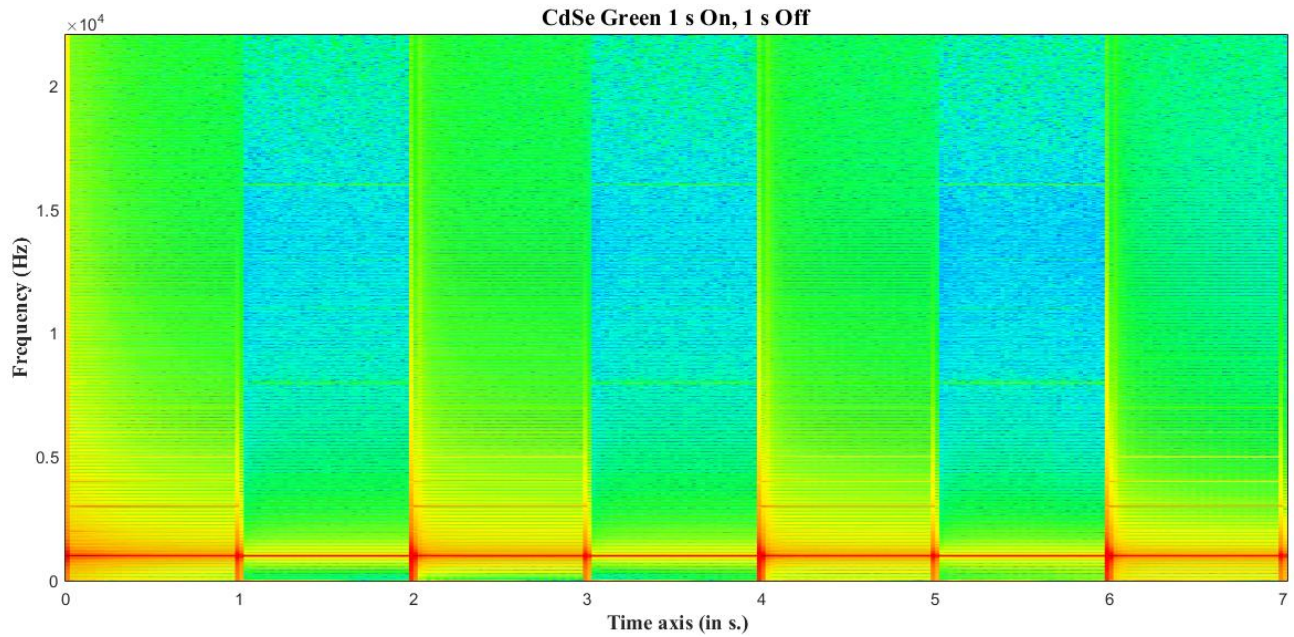


**Figure 6.35: Compressed waveform spectrogram - CdS + Red – 1 S On, 250 ms Off**
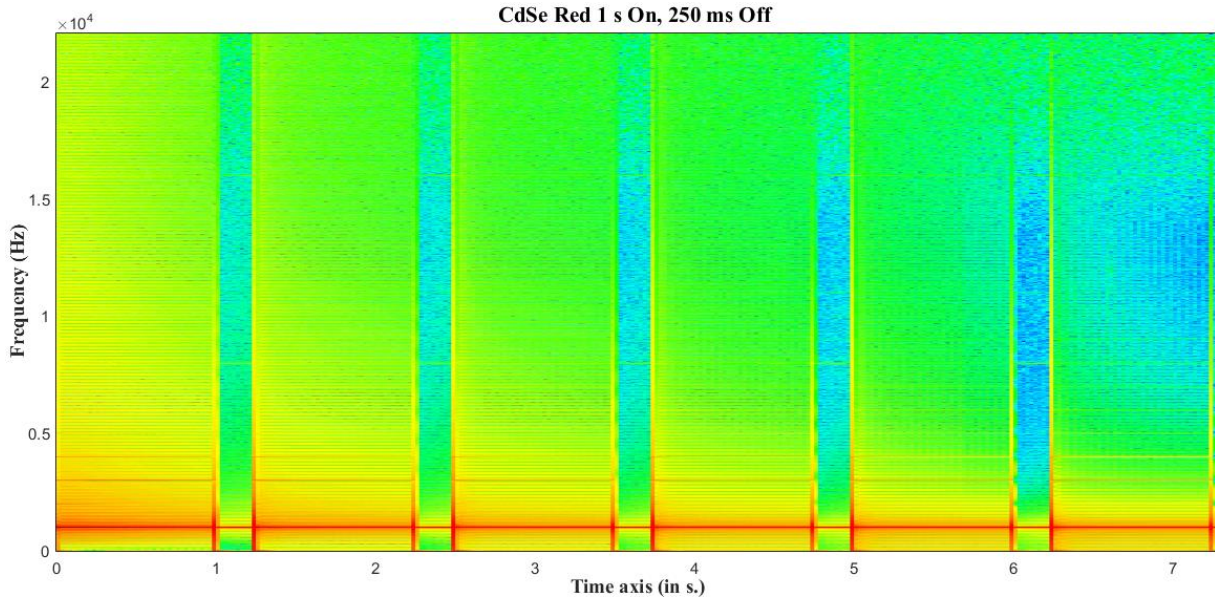
**Figure 6.36: Compressed waveform spectrogram - CdS + Red – 1 S On, 1 S Off**

The spectrum output of the compressor with a CdSe + Green cell shows almost the same harmonic distribution across frequencies compared to the spectrum of the CdS + Green cell, the only difference being in the upper frequencies. The colour map shows a decreased level of the upper harmonics above 15 kHz. On the other hand, what is more relevant is that the output spectrum of the CdS + Green cell has more harmonic content around the fundamental frequency compared to the output of the CdSe + Green cell, which may have a more noticeable effect on a musical signal. It is therefore interesting to see that during the attack period, the output of the compressor with a CdS + Green cell shows increased harmonic content, whereas measuring the harmonic distortions during constant compression, the output with CdSe + Green cell shows an increased value. Other differences are small and therefore should not have increased influence over a musical signal.

**Figure 6.37: Compressed waveform spectrogram - CdSe + Green – 1 S On, 1 S Off**

Comparing the spectral colour map of the compressor output with CdSe + Red cell against the output with a CdS + Red cell, at the two different burst times, shows a small increase in spectral content during attack for the CdSe + Red output, as it can be seen in Figure 6.38. This difference is especially visible when comparing against each successive tone burst. Just like before, they seem to show different behaviour during the attack than during constant compression (when the CdSe + Red has a lower THD level).
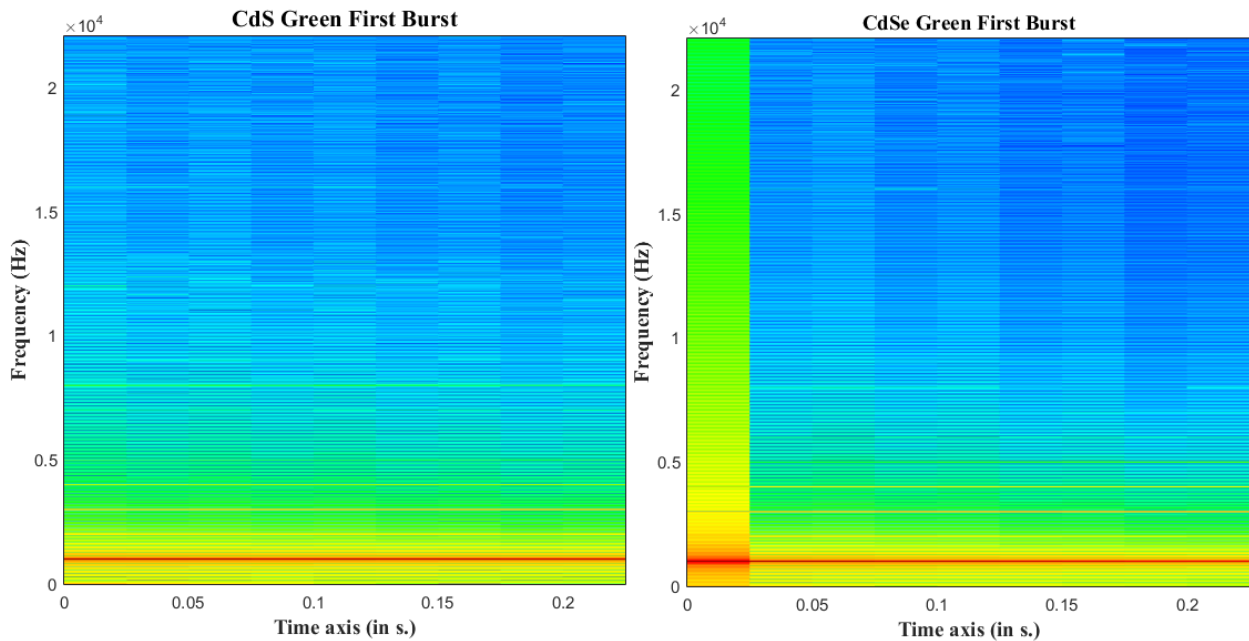
**Figure 6.38: Compressed waveform spectrogram - CdSe + Red – 1 S On, 250 ms Off**

Figures above show the spectral colour map of a single burst repeated a couple of times in order to identify and compare the evolution the spectrum with different optical cells. It is important to also analyse the spectrum output during attack timeframe to get a better understanding of what is actually happening in terms of harmonic content. Therefore, figures below show the first 250 ms of the attack timeframe for the first and second burst only. They do not provide any information whatsoever about the harmonic content during release, as the interest is mostly in how the cell is able to deal with an impulse signal that goes above its threshold. Moreover, the time difference between the first and second burst is 1 second (the 'below threshold' value).

Figure 6.39 and Figure 6.40 show the spectrum output of the compressor with two different optical cells. It can be noted an important difference between the two (Figure 6.39), in the first 25 ms, with an increased harmonic content across the entire audio spectrum for the output with the CdSe + Green cell. Apart from the first 25 ms there are no relevant differences in spectrum between the two. The audio recording was further analysed for any possible defects in the waveform or for

115

the presence of oscillations or modulations, but nothing was found. It can be noted in Figure 6.40, the same increased harmonic content in the first 25 ms, but in this case, it is present in both outputs. A difference between the first 25 ms in the two spectrograms in Figure 6.40 and the spectrogram of the CdSe + Green (Figure 6.39) is that the latter shows a more emphasized harmonic content around the fundamental frequency (red bands). Comparing the two spectrograms of the compressor output, with a CdS + Green and a CdS + red cell, it can be noted an overall difference in harmonic content across the entire 250 ms of attack, with the CdS + Red cell having a richer harmonic spectrum. The same is also valid when comparing the output with a CdSe + Green and CdSe + Red cell, with a richer harmonic content for the latter. Even though it is not entirely visible in Figure 6.39, the output spectrogram with the CdSe + Red cell shows a slightly more elevated harmonic content compared to the output with a CdS + Red cell.
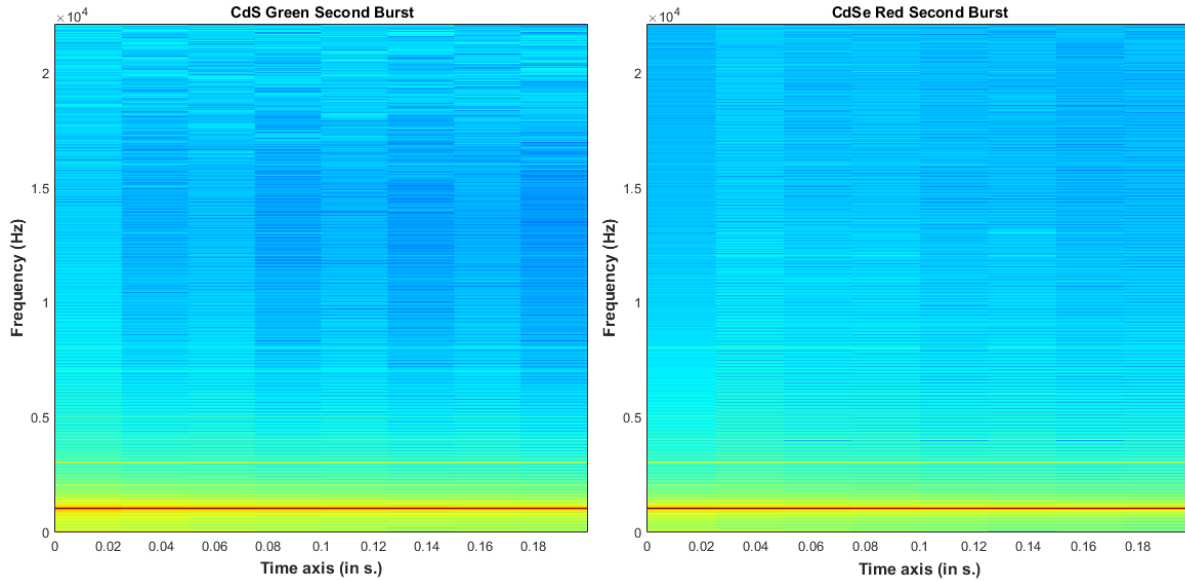


**Figure 6.39: Compressed waveform spectrogram - CdS/CdSe + Green – First 250 ms**
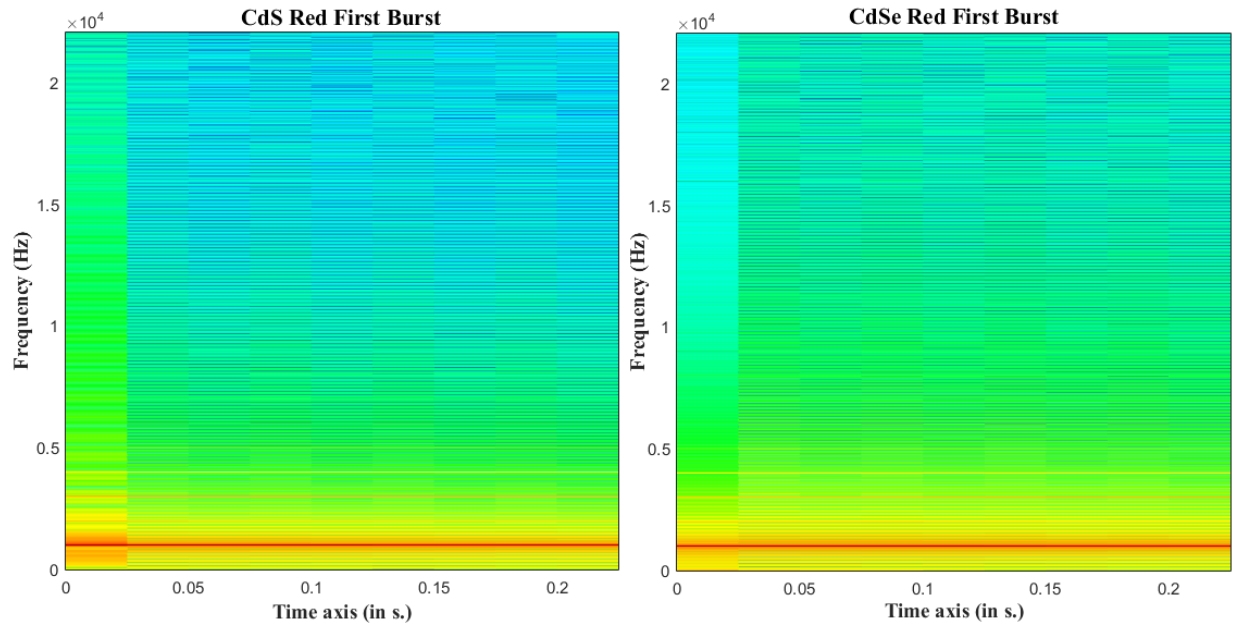
**Figure 6.40: Compressed waveform spectrogram - CdS/CdSe + Red – First 250 ms**

While analysing the attack of the second tone burst, the only identified difference was between the output spectrum with the CdS + Green and CdSe + Red cell (Figure 6.41). They both had almost identical distribution of the harmonic content around the fundamental frequency. The output with the other two cells (CdS + Red, CdSe + Green) presented increased harmonic content compared to the other two in the first 25 ms of the attack, but less around the fundamental frequency. Above 500 Hz, the spectral output with any optical cell is almost identical, but yet different compared to the spectrum of the first burst. This could be explained by the fact that during the second burst, the optical cell's resistance is already low (more or less across each cell) and the amount of gain reduction applied is not as much as with the first burst. Further tests showed that if the cell is allowed to recover more, then the spectral output of the attack during the second burst looks closer to the spectrum of the attack during the first burst.

**Figure 6.41: Compressed waveform spectrogram - Second Burst - First 200 ms**

Another interesting finding arising from the spectrum analysis in the figures above is the repetitively changing harmonic content at each 25 ms. This is displayed as a rectangular block. Previously, these blocks represented the level changes in the audio waveform, such as transitions from the 'below threshold' to the 'above threshold' values and their width was equal to the timeframe. This time, Figure 6.39, Figure 6.40 and Figure 6.41 are the spectral outputs of the waveform during attack time. There is indeed a level decrease, but it should not be displayed like a constant changing block every 25 ms. Further analysis of the waveforms revealed a small ripple modulation effect present, which could be the cause of these repetitive blocks. It is to be noted that even though the rectangular blocks are repetitive, the harmonic content across the audio spectrum is not always the same in each block. All this could be a combination of the ripple modulation and oscillations.

Figure 6.42 shows the measured centroid values for the output of the compressor with each of the four cells. This measurement was carried out as an extension to the previous spectrum measurements in order to be able to see the harmonic content distribution with numerical values. This measurement relates directly to the perceived brightness (due to increase in harmonic content), and therefore, its usefulness comes in when assessing whether these optical cells would have an impact on a musical signal. Even though all four outputs have different centroid values, the difference between them is not large and should therefore not have a very noticeable effect on a musical signal. The repetitive rectangular blocks discussed before can also be seen here as the rising and falling curves every 25 ms. As noted on the spectrogram, the blocks are repetitive, but do not have the same harmonic content distribution, a fact that can be seen in the value of the rising and falling curves.
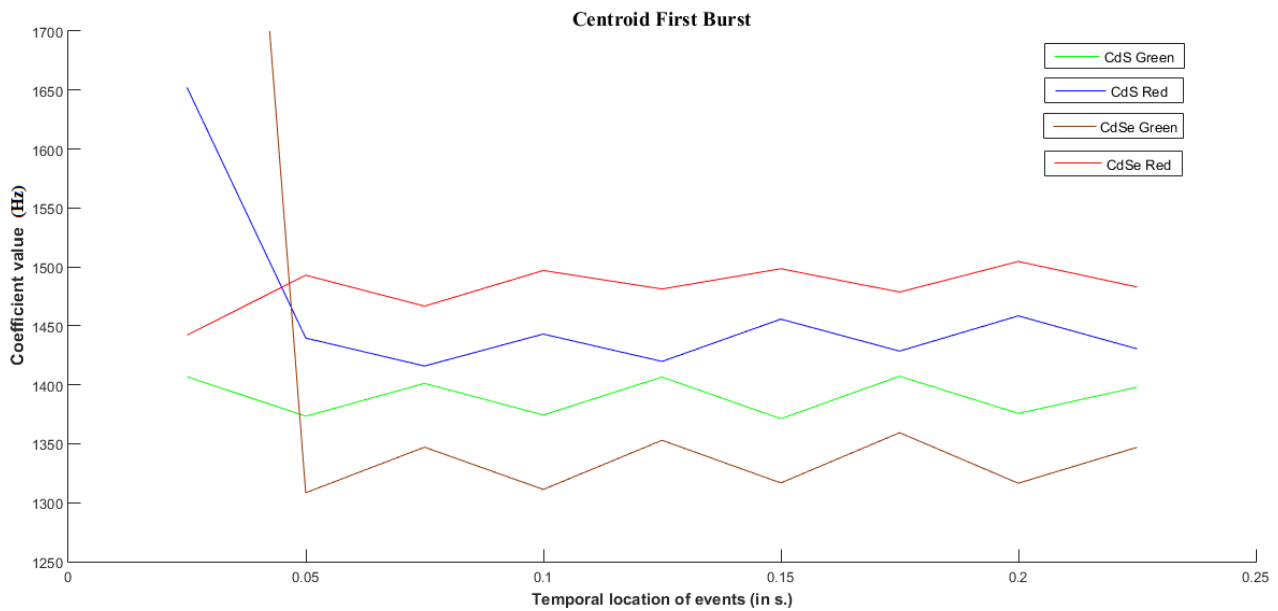


**Figure 6.42: Centroid measurement of the first 250 ms of attack - First Burst**

Figure 6.43 describes the same measurement, but done on the 250 ms attack timeframe of the second burst. As discussed above, there are differences in the attack characteristics between the first compression and the second compression timeframes, which determine a different harmonic behaviour of the compressed waveform. The biggest visible difference is in the output with the CdSe + Green cell, which has an average centroid value of 1325 during the attack of the first burst and an average value of 1550 during the attack of the second burst. This is a better representation of the difference than just by looking at the spectral map and it suggests an increased harmonic content. During the attack on the second burst, the output with the CdS + Green cell shows a lower centroid value, as a result of less compression applied due to a lower amplitude of the second burst (slower recovery rate of the CdS LDR). On the other hand, the centroid of the output using a CdS + Red cell shows an increased value, behaving totally opposite than the CdS + Green cell.
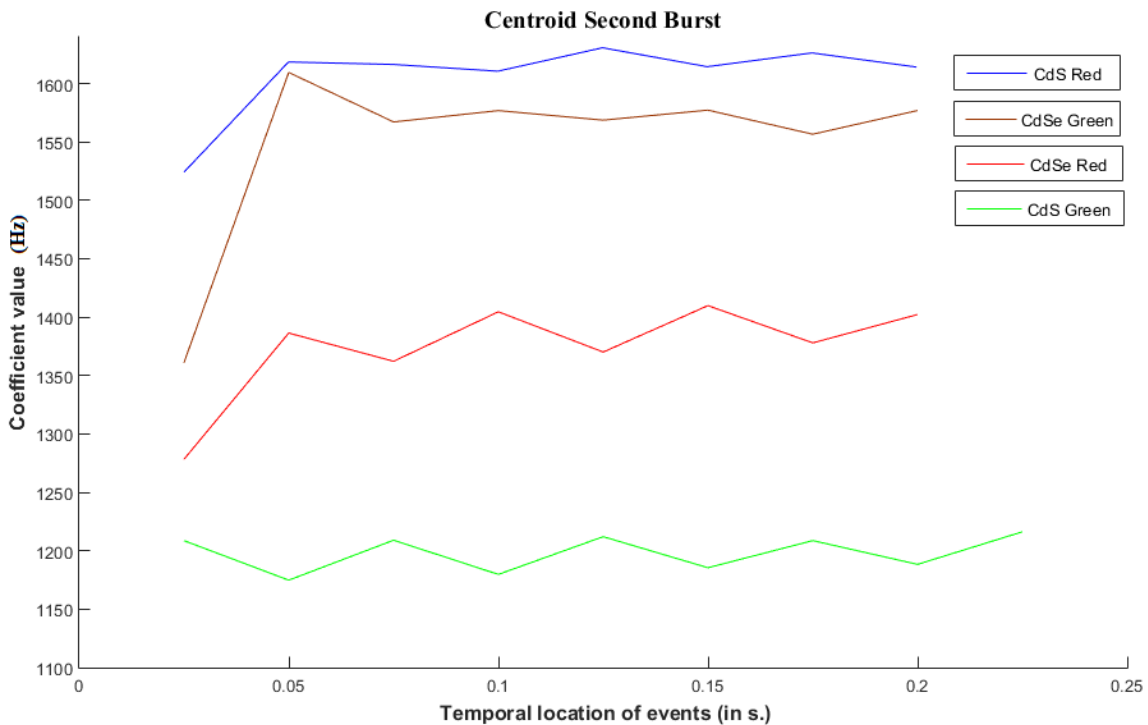


**Figure 6.43: Centroid measurement of the first 200 ms of attack - Second Burst**

Figure 6.44 shows the envelope of the energy in the first 250 ms of the attack on the first burst. It is therefore a measure of the attack slope characteristic with different cells, and as expected, the fastest attack is obtained by using a CdSe + Green cell, while the slowest attack is obtained with the CdSe + Red cell. This data perfectly correlates to the attack values measured on the oscilloscope and presented in Table 6.6.
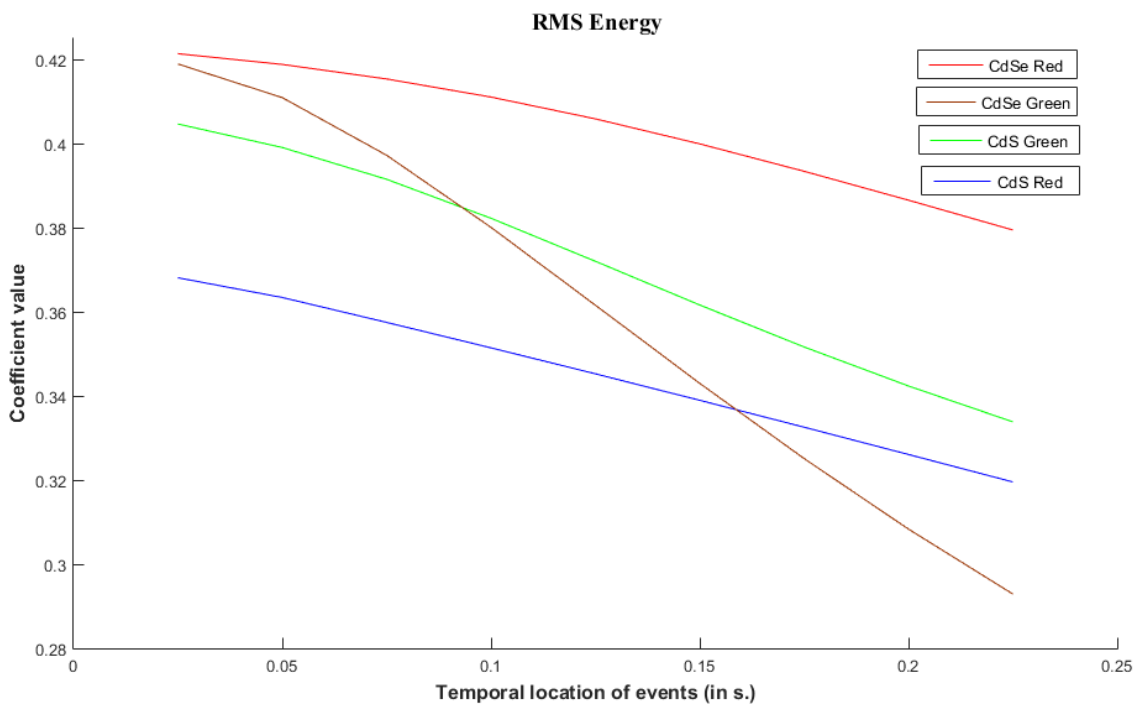


**Figure 6.44: RMS Energy of the first 250 ms of attack - First Burst**

## 6.8 Summary of results and key findings

The key objectives of this study were to review different methods of optical cell implementation with a view to ascertaining the effect of the low-level parameters on the overall sound of the compressor. The research questions were how does the time versus brightness influence the response of the LDR and is there any difference in compression if using a totally different LDR and light source? Also, what parameters would affect the compression characteristics?

| Parameter | Key Findings |
|---|---|
| Modern El Panel (Red, Green) | Presents a frequency dependent brightness. Efficiency drops above 6 kHz due to impedance drop, thus having a loading effect on the El driver amplifier |
| Old Modelled El Panel | Has both frequency dependent brightness and colour shift. Below 100 Hz the panel has a light green colour. With increasing frequency, the colour changes to violet up to almost blue (2 kHz) |
| LDRs (CdS and CdSe) | With constant brightness the resistance of the LDR oscillates. It could be this oscillation in resistance that becomes more unstable with LDR aging and causes the ripple modulation. |
| Reducing LDR exposure area | As expected, the resistance increases, but also the resistance curve of the LDR has a smoother exponential decay. This also affects the attack and release times of the optical cell. |
| Parallel and Series combination of LDRs | Resistance curves have a smoother exponential decay. Series combination leads to an increased total resistance, thus allowing for greater sensitivity and dynamic range. |
| CdS/CdSe LDR + El Panel (Red, Green or Old Modelled) | 1.Resistance curves of the LDRs differ the most in the 40 Hz-1 kHz bandwidth. In this frequency range, the panel's colour seems to dominate the response of both LDR types. As frequency increases, so does the brightness, and with increasing light levels the LDRs' curves begin intersecting. 2. All combinations presented a two-staged attack. 3. Very fast release with CdSe LDRs 4. More compression results in slower release (Memory effect) |
| CdSe + Red El panel | Slowest attack |
| CdSe + Green El panel | Highest THD+N |
| CdSe LDR | Increased odd order harmonics compared to CdS LDR and increased overall harmonic content |

**Table 6.7:Key findings**

# 7 Conclusions

The aim of the research was to do an in-depth investigation into the optical cells and identify key low-level parameters that can be changed in order to modify the behaviour of the optical cell, which would ultimately change the effect it has over a musical signal. Individual testing of the optical cells provided an insight into the LDR's resistance curve change with input levels, frequencies and EL panel colour.

Investigations with different frequencies and pink noise, but with the same voltage output level on the panel showed that:

- Between 40 Hz and 1 kHz the change in brightness had the most impact on the LDR's resistance.

- Panel's efficiency drops above 6 kHz which could be due to the loading effect that it may have on the driver amplifier, as with increasing frequency the panel's impedance drops.

- The obtained resistance curves when pairing different LDRs and EL panel colours seem to be different, especially in the low frequency range (40 Hz to 1 kHz).

- With increasing frequency, the resistance curves start intersecting and achieving pretty much equal resistance values due to an increase in brightness.

- At low frequencies, the brightness element is not taken into consideration allowing the spectral sensitivity of the LDRs to dominate the response.

- With increasing brightness over the LDR, the less the panel's colour matters and light level dictates LDR's resistance curve.

- Oscillations and modulation are present in all LDRs with light colour having no effect over these parameters. It could be these oscillations that cause the "ripple modulation" some people refer to.

- The old modelled EL panel does have a colour shift depending on the driving frequency with an effect on the LDR's output resistance.

- Modern EL panels did not show any colour shift.

- All EL Panels do show a frequency dependent brightness.

The difference between series/parallel combination of the LDRs coupled with different light sources is theoretically not enough to create any perceived difference in compression, but some curves tend to have a smoother exponential decay.

Control over the LDR's exposure area showed that:

- The obtained resistance curve has higher resistance values across the entire frequency spectrum, but with a smoother curve.

- The above stated increased resistance could allow for an improved sensitivity and higher threshold dynamic range.

- Changes are made to the attack/release characteristic of the optical cell which may have a perceptual impact on the audio signal. To fully assess if any difference is made a further subjective testing would be required.

FFT analysis during constant compression showed that:

- All cells exhibit almost the same THD level, apart from the CdSe + Green panel cell that showed increased THD levels during 6 dB and 12 dB GR.

- With increasing GR all cells seem to exhibit lower THD levels.

- CdSe based cells tend to have increased odd order harmonics compared to CdS cells.

- Light colour has a small effect over the distortion levels.

Attack and release values measured for all the cells showed that:

- CdSe + Red panel cell exhibited the slowest attack than any other cell, which was unexpected given the fact that a CdSe LDR is supposed to be very sensitive with red light and have a better response.

- The $2^{nd}$ attack (from 63% to full GR) made the most difference between the cells.

- $1^{st}$ attack values range from 95 ms to 500 ms while $2^{nd}$ attack values range from 1 S all the way to 2.3 S.

- Optical cells do have a two-staged attack characteristic

- As mentioned by many researchers, the optical cells do exhibit a two-staged release that is dependent on the amount of GR achieved previously (the so-called memory-effect).

- Release times show that the CdSe based cells are almost up to 15 times faster than CdS based ones.

Spectral and centroid analysis of the recorded audio during the attack timeframe showed that:

- There are some more harmonic elements present when using CdSe based cells resulting in an extra layer of distortion added to the audio signal and possibly increased brightness.

# 8  Further Work

Further work could be carried out to establish differences between the EL panel based optical cells and the LED ones. Testing could include hand-built optical assemblies using LEDs instead of EL panels and comparing these to the factory-built ones available on the market from Vactrol. It would be interesting to determine the characteristics of an optical cell that uses both an EL panel and an LED, with different LDRs. Further improvements to tests could be made by using real musical signals, which can be analysed with MIRToolbox to determine the real effect of different optical cells. Subjective testing can also be added in addition to the objective measurement to provide a full package of tests that would be able to fully assess the differences and better correlate a certain modified parameter to the resulting perceptual attribute.

# References

-, -. (2002). *What's so good about optical compressors?*. [online] SweetWater.com. Available at: https://www.sweetwater.com/insync/what-so-good-optical-compressors/ [Accessed 26 Aug. 2017].

Abel, J. and Berners, D. (2003). On Peak-Detecting and RMS Feedback and Feedforward Compressors. In: *Audio Engineering Society 115th Convention*. New York: Audio Engineering Society, pp.2-6.

*Analog Optical Isolators VACTROLS®*. Retrieved from http://denethor.wlu.ca/pc300/optoisolators/analogoptoisolatorintroduction.pdf

*Audio level control with resistive optocouplers*. (2010). *Silonex*. Retrieved 14 September 2017, from https://web.archive.org/web/20101117022736/http://www.silonex.com:80/audiohm/pdf/level control.pdf

Ballou, G. (2008). *Figure 14-22 Volume control using a light-dependent resistor*. Retrieved from https://books.google.co.uk/books?id=eh60Ue_K2QkC&pg=PA778&dq=glen+ballou+Volume+control+using+a+light-dependent+resistor&hl=en&sa=X&ved=0ahUKEwio17mZ0qnWAhVIIcAKHTcKCX8Q6AEIKDAA#v=onepage&q=glen%20ballou%20Volume%20control%20using%20a%20light-dependent%20resistor&f=false

Ballou, G. (2008). *Handbook for sound engineers*. 4th ed. Oxford: Focal.

Bani, N., Abdul-Malek, Z., & Ahmad, H. (2015). Charateristic of electroluminescene phenomenon in virgin and thermally aged LDPE. Aberdeen: Robert Gordon University. Retrieved from https://openair.rgu.ac.uk/bitstream/handle/10059/1426/MUHAMMAD-SUKKI%202015%20AIP%20Conference%20Proceedings.pdf?sequence=1&isAllowed=y

Berners, D. (2006). Ask the Doctors: Analysis of Dynamic Range Control (DRC) Devices. [Blog] *Universal Audio WebZine*. Available at: http://www.uaudio.com/webzine/2006/september/text/content2.html [Accessed 26 Aug. 2017].

Berners, D. (2006). *Input signal and compressed outputs*. Retrieved from http://www.uaudio.com/webzine/2006/september/text/content2.html

Bohn, D. (2000). *AUDIO SPECIFICATIONS*. 1st ed. [ebook] Mulkiteo: Rane Corporation, p.7. Available at: http://www.rane.com/pdf/ranenotes/Audio_Specifications.pdf [Accessed 26 Aug. 2017].

Ciletti, E. (1998). *LA-2A Input Circuit*. Retrieved from http://www.tangible-technology.com/dynamics/art_o_dynamics.html

Ciletti, e. (1998). *The Art of Dynamics: The essence of popular compressor/limiters*. [online] Tangible-technology.com. Available at: http://www.tangible-technology.com/dynamics/art_o_dynamics.html [Accessed 26 Aug. 2017].

Ciletti, E. and Hill, D. (1999). *GAIN CONTROL DEVICES, SIDE CHAINS, AUDIO AMPLIFIERS*. [online] Tangible-technology.com. Available at: http://www.tangible-technology.com/dynamics/comp_lim_ec_dh_pw2.html [Accessed 26 Aug. 2017].

Detection and the Dynamics Duo. (2017). 1st ed. [ebook] Sandy: DBX, pp.1-3. Available at: https://www.manualslib.com/manual/561140/Dbx-Detection-And-The-Dynamics-Duo.html#manual [Accessed 26 Aug. 2017].

*Digital oscilloscope persistence modes*. (2018). *Picotech.com*. Retrieved 15 January 2018, from https://www.picotech.com/library/oscilloscopes/digital-persistence-modes

*Direct and Indirect Band Gap Semiconductors*. (2015). *Doitpoms.ac.uk*. Retrieved 14 September 2017, from https://www.doitpoms.ac.uk/tlplib/semiconductors/direct.php

Droney, M. and Massey, H. (2001). *Compression Applications*. 1st ed. [ebook] n/a: T.C. Electronic, pp.8-9. Available at: https://www.tcelectronic.com/media/1018549/droney_massey_2001_compres.pdf [Accessed 26 Aug. 2017].

EL Panel Tape. *EL Panel Layers*. Retrieved from http://elpanelandtape.co.uk/wp-content/uploads/2015/06/layers-of-el-panel-explained-450x800.png

*EL Parallel Panels*. (2017). Sheffield. Retrieved from http://www.surelight.com/images/products/el_panels/el_parallel_panels/downloads/brochure/el_parallel_panel.pdf

Entner, R. *Carrier Generation and Recombination*. *Iue.tuwien.ac.at*. Retrieved 14 September 2017, from http://www.iue.tuwien.ac.at/phd/entner/node11.html

Floru, F. (1998). Attack and Release Time Constants in RMS-Based Feedback Compressors. In: *Audio Engineering Society Convention*. Amsterdam: Audio Engineering Society, p.8.

Foley, D. (2014). *White Noise Definition Vs. Pink Noise – Acoustic Fields*. *Acoustic Fields*.

Retrieved 18 September 2017, from https://www.acousticfields.com/white-noise-definition-vs-pink-noise/

Giannoulis, D., Massberg, M. and Reiss, J. (2012). Digital Dynamic Range Compressor Design - A Tutorial and Analysis. *Audio Engineering Society*, 60(6), pp.399-401.

Goetzberger, A., Knobloch, J., & Voss, B. (1998). *Crystalline silicon solar cells*. Chichester: Wiley.

Gowdham, S. *Absorption coefficient*. Retrieved from http://www.kprblog.in/cse/sem1/absorption-coefficient-determination/

Green, M. (2003). *Third Generation Photovoltaics: Advanced Solar Energy Conversion* (1st ed.). Germany: Springer.

Grovenor, C. (1998). *Microelectronic materials*. London: Taylor and Francis.

Hicks, M. (2017). *Audio Compression Basics | Universal Audio*. [online] Uaudio.com. Available at: http://www.uaudio.com/blog/audio-compression-basics/ [Accessed 26 Aug. 2017].

Honsberg, C., & Bowden, S. *Electroluminescence*. *Pveducation.org*. Retrieved 14 September 2017, from http://www.pveducation.org/pvcdrom/characterisation/electroluminescence

Horowitz, P. and Hill, W. (2016). *The art of electronics*. 3rd ed. Cambridge: Cambridge University Press.

Johnsen, R. (1998). *Detection and the Dynamics Duo* (1st ed.). Sandy: dbx. Retrieved from http://ftp://ftp.dbxpro.com/pub/PDFs/WhitePapers/DetectionandDynamicsDuo.pdf

Joshi, N. (1990). *Figure 7.15: A demonstrative example of sensitivity variation*. Retrieved from https://books.google.co.uk/books?id=lv-Nb5-H3pQC&pg=PA285&dq=Photoconductivity:+Art:+Science+%26+Technology+photoelectric+fatigue&hl=en&sa=X&ved=0ahUKEwi-5K7F2qnWAhXJCcAKHfwDCNYQ6AEIKDAA#v=onepage&q=Photoconductivity%3A%20Art%3A%20Science%20%26%20Technology%20photoelectric%20fatigue&f=false

Joshi, N. (1990). *Photoconductivity*. New York: Marcel Dekker, Inc.

Kadis, J. (2012). *The Science of Sound Recording*. 1st ed. Waltham: Elsevier Inc., pp.108-114.

Khauser. (2012). *Op-Amp Peak Detector*. Retrieved from https://www.circuitlab.com/forums/audio-electronics/topic/s87a7uju/op-amp-peak-detector/

King, C. *Electroluminescent Displays*. Beaverton: Planar Systems. Retrieved from http://ch00ftech.com/wp-content/uploads/2012/05/mrsnf98.pdf

Kleczkowski, P. (2001). The Reduction of Distortion in the dynamic compressor. In: *Audio Engineering Society 111th Convention*. New York: Audio Engineering Sociey, p.2.

Korsunskaya, N., Krolevets, N., Markevich, I., Pekar, G., & Sheinkman, M. (1973). Photoelectric Fatigue. *Fizika I Tekhnika Poluprovodnikov*, *7*(275).

Kraftmakher, Y. (2015). *Experiments and demonstrations in physics* (2nd ed.). Link: World Scientific.

Lartillot, O. (2014). *MIRtoolbox 1.6.1*. [ebook] Aalborg University. Available at: https://www.jyu.fi/hytk/fi/laitokset/mutku/en/research/materials/mirtoolbox/MIRtoolbox1.6.1 guide [Accessed 9 Sep. 2017].

Lartillot, O. (2014). *MIRtoolbox 1.6.1*. Aalborg University. Retrieved from https://www.jyu.fi/hytk/fi/laitokset/mutku/en/research/materials/mirtoolbox/MIRtoolbox1.6.1 guide

Lartillot, O. (2017). *MIRtoolbox*. [ebook] University of Oslo, pp.129-135. Available at: https://www.jyu.fi/hytk/fi/laitokset/mutku/en/research/materials/mirtoolbox/manual1-7.pdf [Accessed 26 Aug. 2017].

Lawrence, JR., J. (1964). An Improved Method of Audio Level Control for Broadcasting and Recording. *Journal of the SMPTE*, 73(n/a).

Lerner, S. *Compression Knee*. Retrieved from http://www.dilettantesdictionary.org/index.php?search=1&searchtxt=soft%20knee%20compression

Lesurf, J. (2018). *Valve Diodes and Triodes*. *St-andrews.ac.uk*. Retrieved 15 January 2018, from https://www.st-andrews.ac.uk/~jcgl/Scots_Guide/audio/part9/page2.html

Lewis, E., & Henry, K. (1988). *Transient responses to tone bursts* (1st ed., pp. 1-3). Elsevier. Retrieved from https://people.eecs.berkeley.edu/~lewis/Ken3.pdf

*Light Dependent Resistors*. (1997). Retrieved from http://www.bilimteknik.tubitak.gov.tr/sites/default/files/gelisim/elektronik/dosyalar/40/LDR_NSL19_M51.pdf

Lisa, F. (2013). *Types of Compressor | Audio Undone*. [online] Audioundone.com. Available at: http://audioundone.com/types-of-compressor [Accessed 26 Aug. 2017].

Marston, R., & van Roon, T. (2010). *Photosensitive Devices*. Retrieved from http://ugweb.cs.ualberta.ca/~c274/resources/hardware/PhotoResistor/MarstonRoonTutorial.pdf

Marston, R., & van Roon, T. (2011). *Cutaway view of a photocell*. Retrieved from http://ugweb.cs.ualberta.ca/~c274/resources/hardware/PhotoResistor/MarstonRoonTutorial.pdf

Mehrotra, S., & Klimeck, G. (2010). *Diffusion of holes and electrons*. *Nanohub.org*. Retrieved 14 September 2017, from http://nanohub.org/resources/8820

Metzler, B. (2005). The Audio Measurement handbook (2nd ed.). Audio Precision, Inc.

Mnats. (2003). *The Weak Joe Optical Compressor*. Retrieved from http://mnats.net/images/weak_joe_schematic.gif

Mohankumar, D. (2012). Electroluminescent display.How Stuff Works. *Electronics hobby*. Retrieved from https://dmohankumar.wordpress.com/2012/12/07/electroluminescent-display-how-stuff-works/

Moore, A., Till, R. and Wakefield, J. (2016). *An Investigation into the Sonic Signature of Three Classic Dynamic Range Compressors - University of Huddersfield Repository*. [online] University of Huddersfield Repository. Available at: http://eprints.hud.ac.uk/28482/ [Accessed 26 Aug. 2017].

Nam, U. (2001). Special Area Exam Part II (1st ed., pp. 1-2). n/a: n/a. Retrieved from https://ccrma.stanford.edu/~unjung/AIR/areaExam.pdf

Nanite. (2013). *Band Structure*. Retrieved from https://en.wikipedia.org/wiki/Valence_and_conduction_bands#/media/File:Band_filling_diagram.svg

Nave, R. (2017). *Band*. *Hyperphysics*. Retrieved 14 September 2017, from http://hyperphysics.phy-astr.gsu.edu/hbase/Solids/band.html

Nave, R. *P- and N- Type Semiconductors*. Retrieved from http://hyperphysics.phy-astr.gsu.edu/hbase/Solids/dope.html

Neamen, D. (2003). *Semiconductor physics and devices* (3rd ed.). Boston: McGraw Hill.

Newt. (2004). *The Visible Spectrum*. Retrieved from http://www.aquaticplantcentral.com/forumapc/lighting/38014-lighting-spectrum-photosythesis.html

PerkinElmer Optoelectronics (n.d.). *Analog Optical Isolators VACTROLS®*. [online] Available at: http://denethor.wlu.ca/pc300/optoisolators/analogoptoisolatorintroduction.pdf [Accessed 26 Aug. 2017].

PerkinElmer. (2001). *Typical Variation of Resistance with Light History*. Retrieved from http://skpang.co.uk/datasheet/BRO_PhotoconductiveCellsAndAnalogOptoiso.pdf

PerkinElmer. *Figure 2: Resistance vs. Time, Figure 5: Hours on Test*. Retrieved from http://denethor.wlu.ca/pc300/optoisolators/analogoptoisolatorintroduction.pdf

Perkowitz, S. *Photoconductivity*. *Encyclopedia Britannica*. Retrieved 14 September 2017, from https://www.britannica.com/science/photoconductivity

Petrosjan, S., Shik, A., Vul', A., & Sheinkman, M. (1977). On the nature of photoelectric fatigue in semiconductors. *Solid State Communications*, *23*(6), 385-387. http://dx.doi.org/10.1016/0038-1098(77)90238-1

*PHOTOCONDUCTIVITY*. (2017). *Physics-assignment.com*. Retrieved 14 September 2017, from http://www.physics-assignment.com/photoconductivity

*Physics of Semiconductors in Nonequilibrium*. Retrieved from http://dunham.ee.washington.edu/ee482/Fall02/Nonequil.pdf

Potter, A., & Schalla, R. (1967). *MECHANISM OF CADMIUM SULFIDE FILM CELL*. Washington: Nasa. Retrieved from https://ntrs.nasa.gov/archive/nasa/casi.ntrs.nasa.gov/19670008178.pdf

*PROPERTIES OF CADMIUM SULFIDE, ZINC SULFIDE AND MERCURIC SULFIDE*. (1961). Arlington. Retrieved from http://www.dtic.mil/dtic/tr/fulltext/u2/256763.pdf

Rainbow Light. (2017). *1931 CIE Chromaticity Diagram*. Retrieved from http://www.rainbow-light.com.tw/en/faq/Whats-CIE1931-chromaticity-Coordinate-x-y-/rainbow-light_faq-01.html

Resistorguide. (2017). *Wavelength dependency Read more http://www.resistorguide.com/photoresistor/*. Retrieved from http://www.resistorguide.com/pictures/wavelength-detectivity.png

Rouse, M. (2005). *What is photoconductivity?*. *WhatIs.com*. Retrieved 14 September 2017, from http://whatis.techtarget.com/definition/photoconductivity

RS (1997). *Light Dependent Resistors*. Corby: RS, pp.1-4.

RS Components. (1997). *Figure 2: Spectral Response, Figure 5: Spectral Response*. Retrieved from http://www.bilimteknik.tubitak.gov.tr/sites/default/files/gelisim/elektronik/dosyalar/40/LDR_NSL19_M51.pdf

Safwan, A. (2012). *Resistance versus Illumination*. Retrieved from http://artic12.blogspot.co.uk/2012/10/a-light-sensor-generates-output-signal.html

Schiavello, M. (1985). *Photoelectrochemistry, photocatalysis and photoreactors*. Dordrecht [u.a.]: Kluwer.

Scott, J. *Model LA-2A Leveling Amplifier*. Santa Cruz: Universal Audio. Retrieved from https://web.archive.org/web/20061113094825/http://www.uaudio.com/_works/pdf/manuals/LA-2A_manual.pdf

*Selecting a Photocell*. (2012). Retrieved from
http://www.ladyada.net/media/sensors/gde_photocellselecting.pdf

Shanks, W. (2003). *UA WebZine "Compression Obsession" July 03 | Long Live the T4 Cell!*.
[online] Uaudio.com. Available at:
https://www.uaudio.com/webzine/2003/july/text/content4.html [Accessed 26 Aug. 2017].

Signality. (2012). *Peak-Detector*. Retrieved from
https://www.circuitlab.com/circuit/75p326/basic-peak-detector-01/

Simmer, U., Schmidt, D. and Bitzer, J. (2006). Parameter Estimation of Dynamic Range
Compressors: Models, procedures and Test Signals. In: *Audio Engineering Society 120th
Convention*. Paris: Audio Engineering Society, pp.3-7.

S-kei. (2006). *Electronic Band Structure*. Retrieved from
https://en.wikipedia.org/wiki/Electron_hole#/media/File:BandDiagram-Semiconductors-
E.PNG

Sobczyk, I. *Optical Cells*. Retrieved from
http://file:///C:/Users/RecordMaster/Downloads/t4bx.pdf

Stark, G. *Light | Physics*. *Encyclopedia Britannica*. Retrieved 14 September 2017, from
https://www.britannica.com/science/light

Strock, L. (2014). *Electroluminescence: Theory and Practice, January 1965 Electronics
World*. *Rfcafe.com*. Retrieved 14 September 2017, from
http://www.rfcafe.com/references/electronics-world/electroluminescence-january-1965-
electronics-world.htm

Strock, L. (2014). *Fig. 2: Brightness versus lamp voltage, Fig. 3: Effect of frequency on
wavelength distribution*. Retrieved from http://www.rfcafe.com/references/electronics-
world/electroluminescence-january-1965-electronics-world.htm

Sun, G. (2010). *Figure 1: Illustration of a photon emission process*. Retrieved from
https://www.intechopen.com/books/advances-in-lasers-and-electro-optics/the-intersubband-
approach-to-si-based-lasers

Surelight. *Figure 1: Brightness versus accumulated lighting time*. Retrieved from
http://www.surelight.com/images/products/el_panels/el_parallel_panels/downloads/brochure/
el_parallel_panel.pdf

*The P-N Junction (The Diode)*. Retrieved from https://ocw.mit.edu/courses/materials-
science-and-engineering/3-024-electronic-optical-and-magnetic-properties-of-materials-
spring-2013/lecture-notes/MIT3_024S13_2012lec18.pdf

The University of Toledo. (2012). *Absorption Coefficient*. Retrieved from http://www.iue.tuwien.ac.at/phd/entner/node11.html

*The Visible Spectrum*. (2004). Retrieved from http://www.aquaticplantcentral.com/forumapc/lighting/38014-lighting-spectrum-photosythesis.html

*Unit Conversions - Halas Research Group*. *Halas.rice.edu*. Retrieved 14 September 2017, from http://halas.rice.edu/conversions

University of Cambridge. (2007). *Direct and Indirect Band Gap Semiconductors*. Retrieved from https://www.doitpoms.ac.uk/tlplib/semiconductors/direct.php

Whelan, M. (2013). *Electroluminescent Lamps - How They Work & History*. *Edisontechcenter.org*. Retrieved 14 September 2017, from http://www.edisontechcenter.org/electroluminescent.html#works

White, P. (2003). *What is Optical compression?*. [online] Focusrite Audio Engineering. Available at: https://support.focusrite.com/hc/en-gb/articles/207548655-What-is-Optical-compression- [Accessed 26 Aug. 2017].

Yano, Y., & Nagano, K. (2003). EL Panel. United States.

Zeghbroeck, B. (1996). *Temperature dependence of the energy bandgap*. *Ecee.colorado.edu*. Retrieved 14 September 2017, from http://ecee.colorado.edu/~bart/book/eband5.htm

Zhao, H. (2007). *Impurity and Back Contact Effects on CdTe/CdS Thin Film Solar Cells*. PhD. University of South Florida.

# Appendix

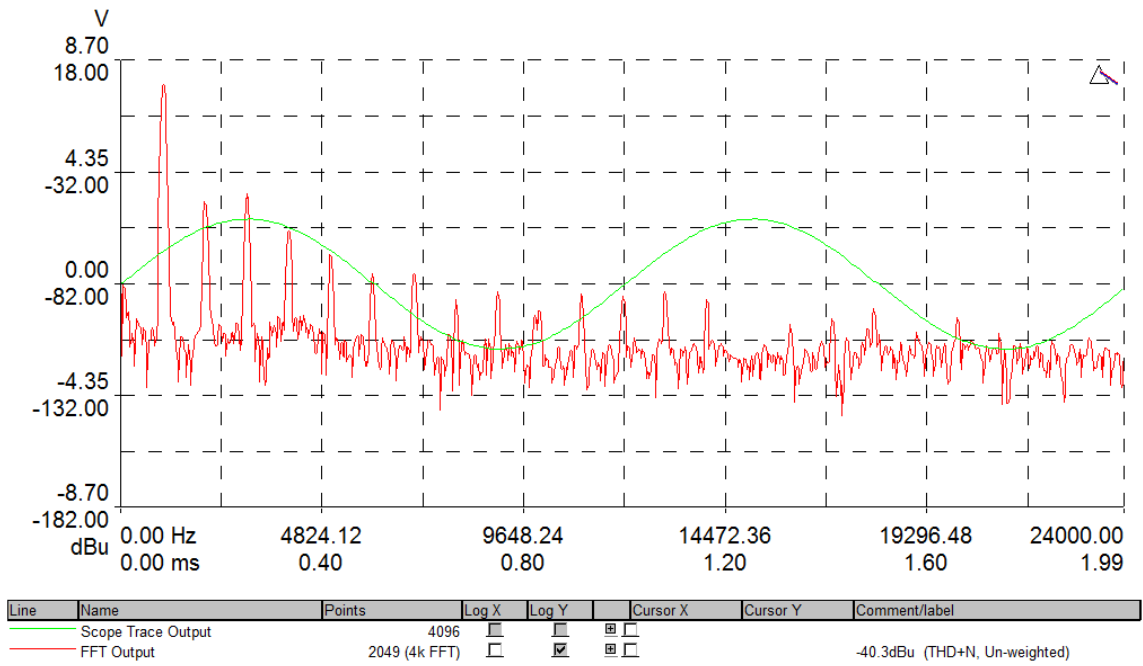## Section A: FFT at 6 dB Gain Reduction
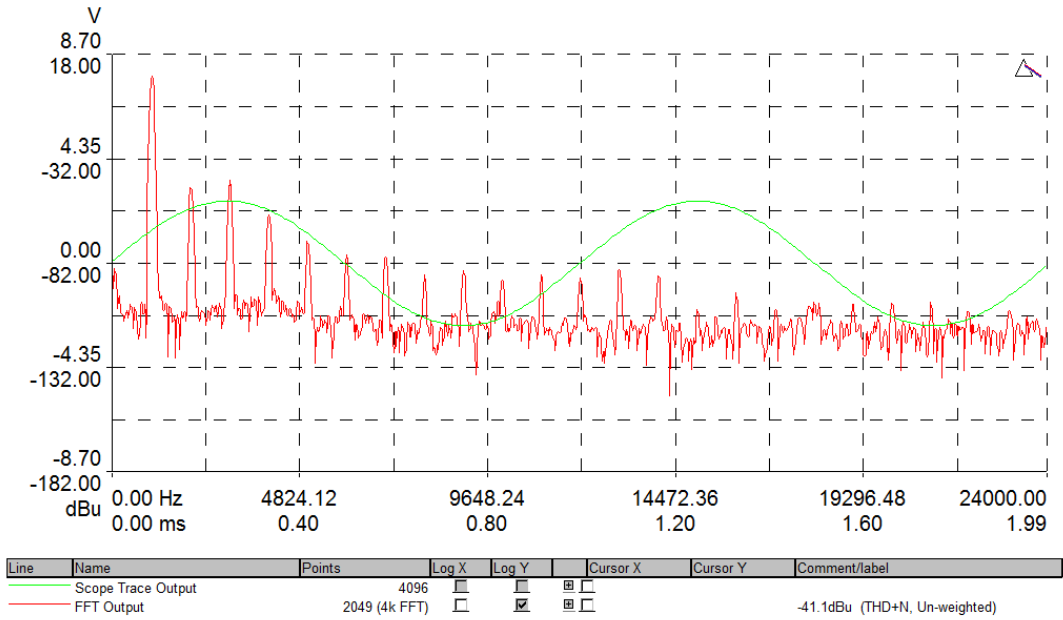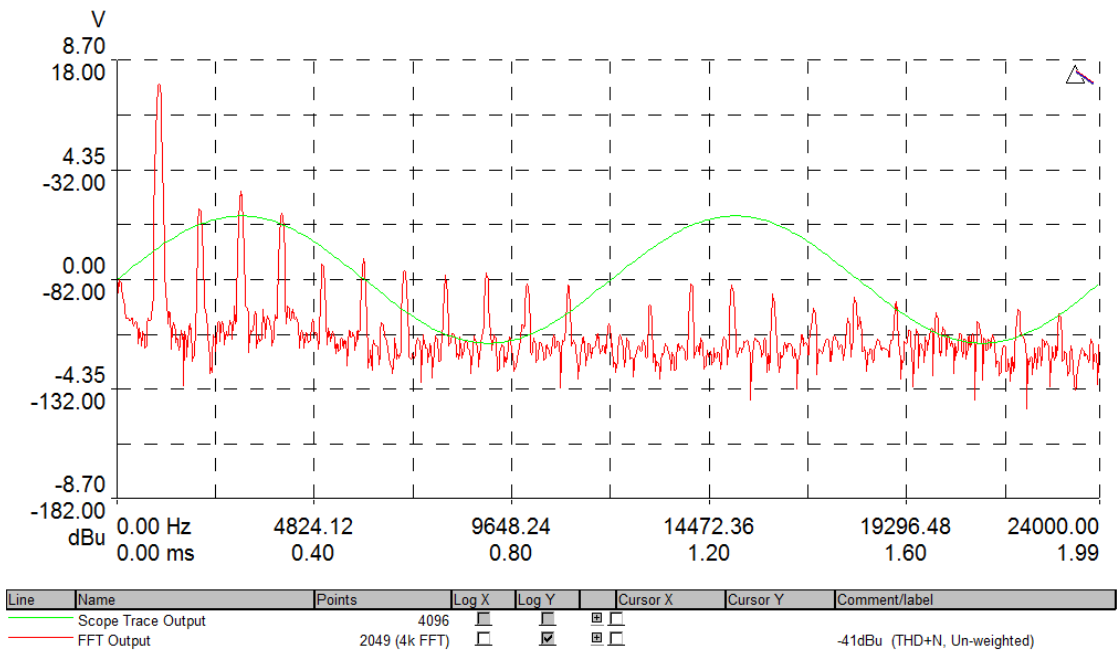


**CdS + Green El Panel FFT**
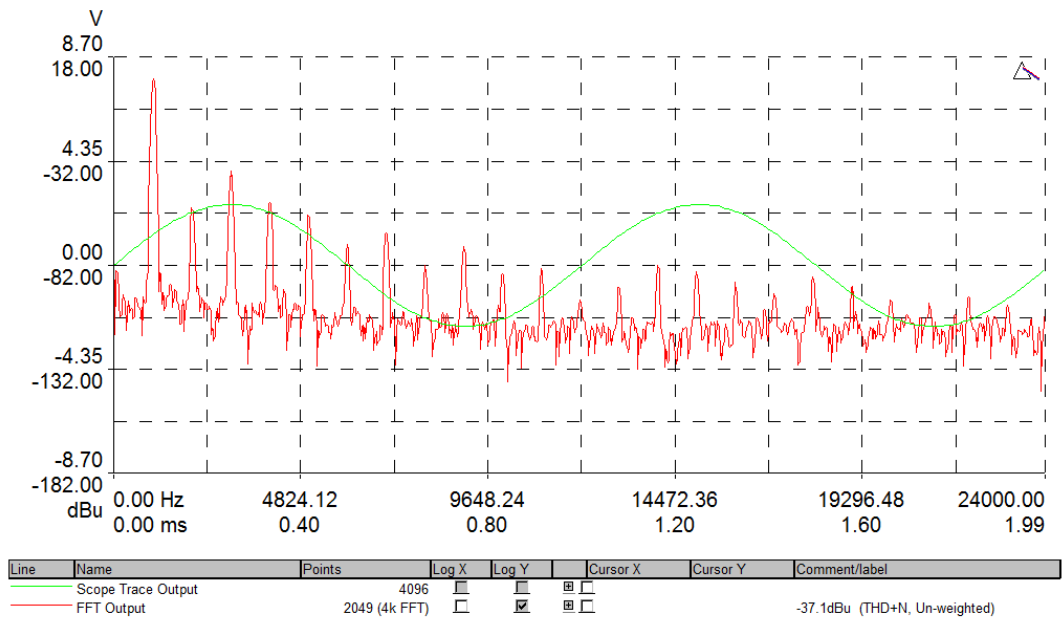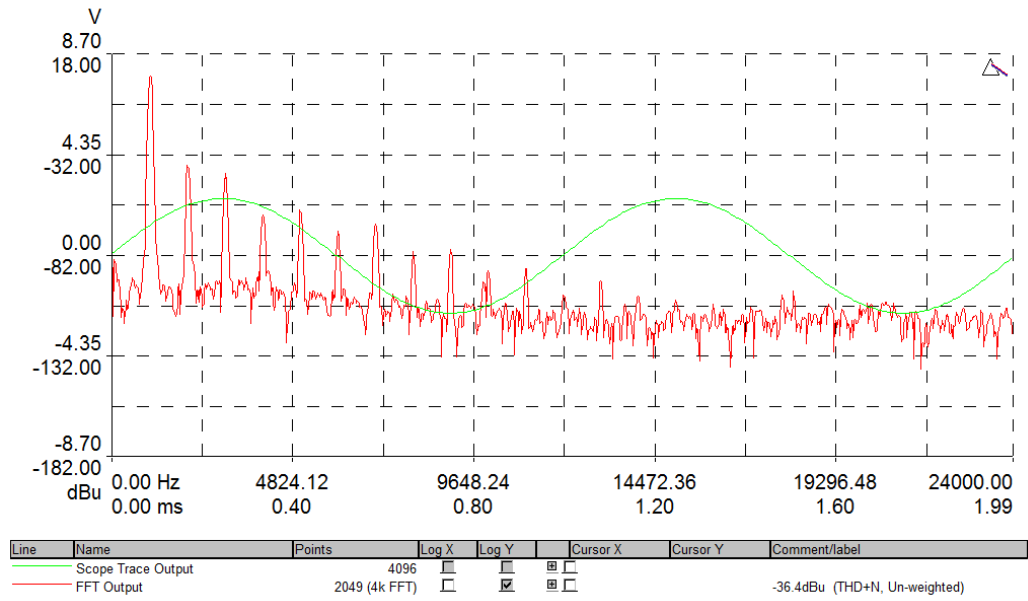


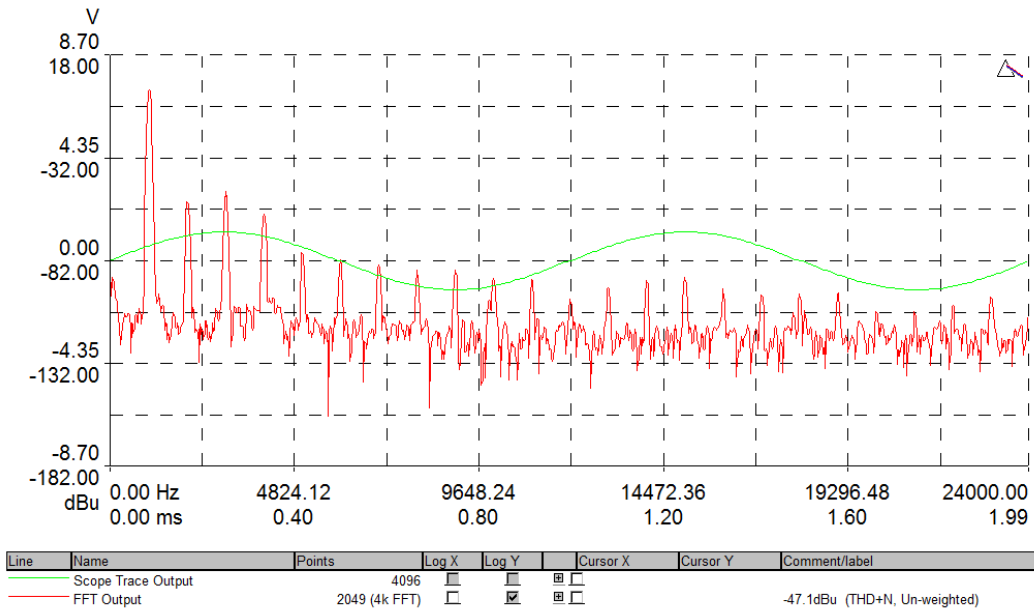**CdSe + Green EL Panel FFT**

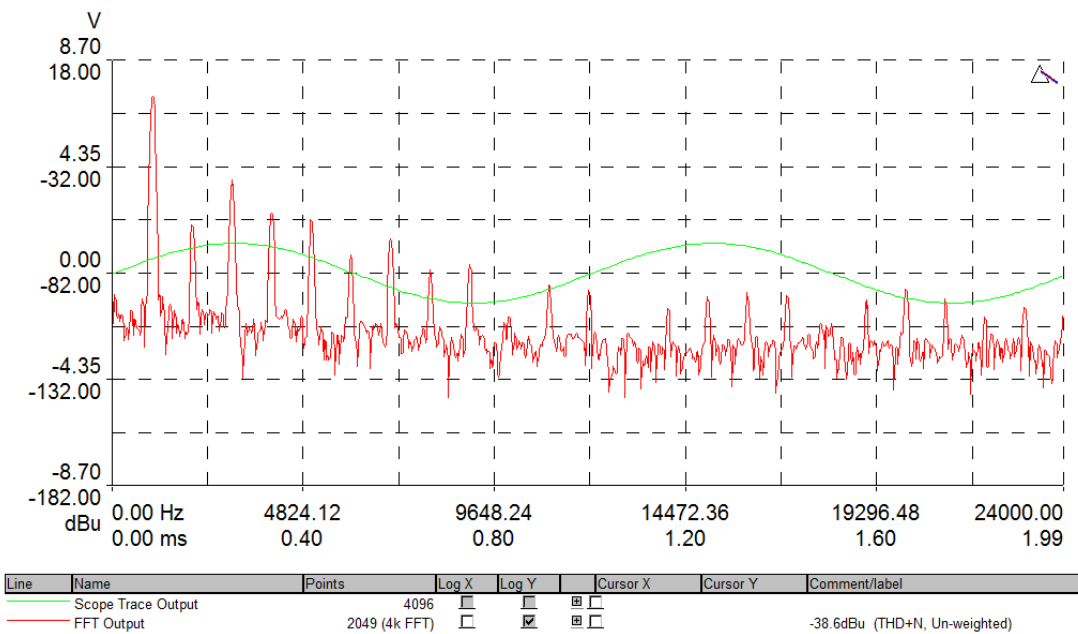**CdS + Red EL Panel FFT**



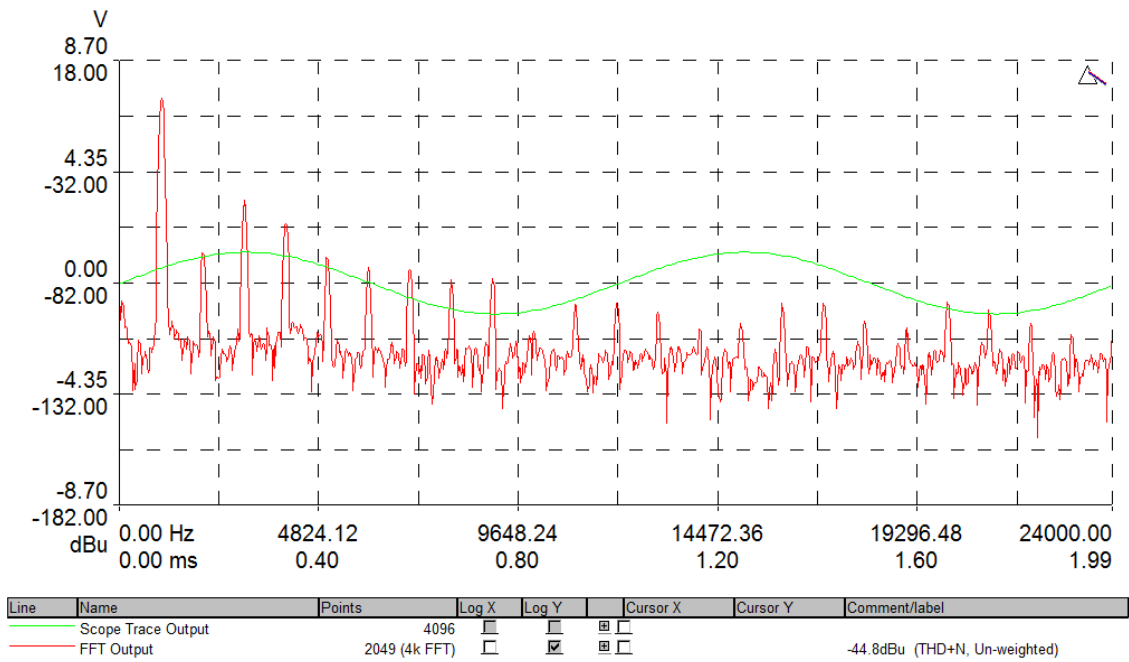**CdSe + Red EL Panel FFT**

**CdSe + Old Modelled EL Panel FFT**

## Section B: FFT at 12 dB Gain Reduction



**CdS + Green El Panel FFT**

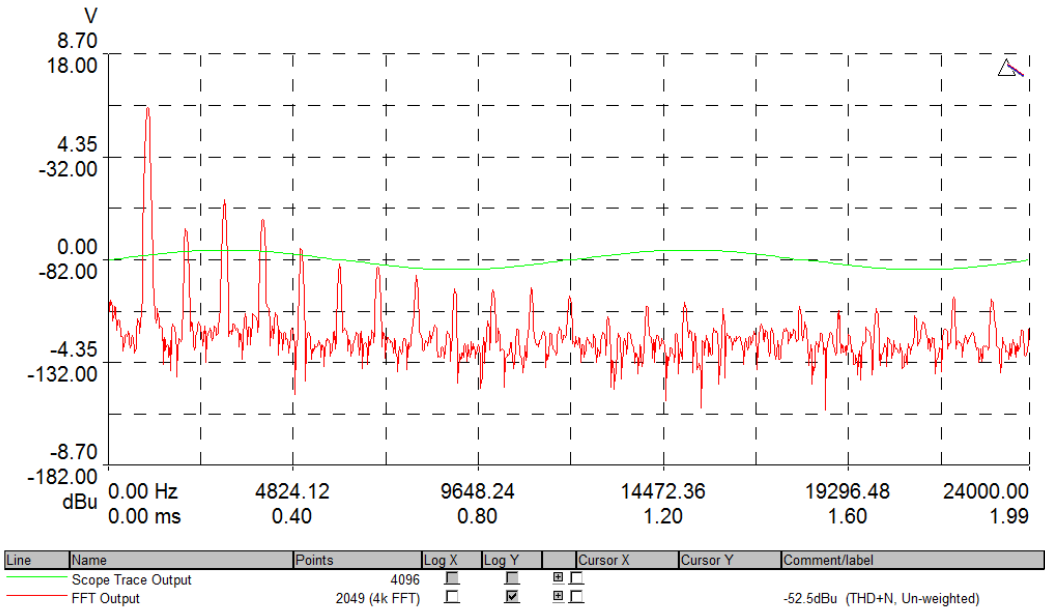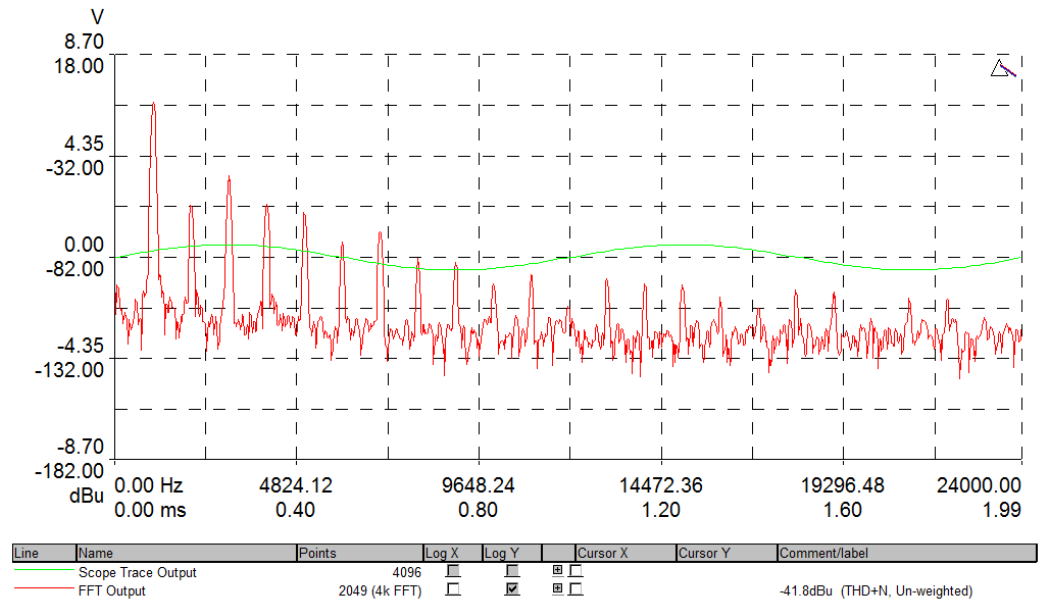**CdSe + Green EL Panel FFT**



**CdS + Red EL Panel FFT**

# Section C: FFT at 20 dB Gain Reduction



**CdS + green EL Panel FFT**



**CdSe + Green EL Panel FFT**